Compartmentalization of Formation Waters, Prince Colliery, Cape Breton, Nova Scotia

Angela Marie Kennedy

Submitted in Partial Fulfillment of the Requirements
for the Degree of Bachelor of Science, Honours
Department of Earth Sciences
Dalhousie University, Halifax, Nova Scotia
April 1997

Distribution License

DalSpace requires agreement to this non-exclusive distribution license before your item can appear on DalSpace.

NON-EXCLUSIVE DISTRIBUTION LICENSE

You (the author(s) or copyright owner) grant to Dalhousie University the non-exclusive right to reproduce and distribute your submission worldwide in any medium.

You agree that Dalhousie University may, without changing the content, reformat the submission for the purpose of preservation.

You also agree that Dalhousie University may keep more than one copy of this submission for purposes of security, back-up and preservation.

You agree that the submission is your original work, and that you have the right to grant the rights contained in this license. You also agree that your submission does not, to the best of your knowledge, infringe upon anyone's copyright.

If the submission contains material for which you do not hold copyright, you agree that you have obtained the unrestricted permission of the copyright owner to grant Dalhousie University the rights required by this license, and that such third-party owned material is clearly identified and acknowledged within the text or content of the submission.

If the submission is based upon work that has been sponsored or supported by an agency or organization other than Dalhousie University, you assert that you have fulfilled any right of review or other obligations required by such contract or agreement.

Dalhousie University will clearly identify your name(s) as the author(s) or owner(s) of the submission, and will not make any alteration to the content of the files that you have submitted.

If you have questions regarding this license please contact the repository manager at dalspace@dal.ca.

Grant the distribution license by signing and dating below.

_____ _____

Name of signatory Date

Dalhousie University

Department of Earth Sciences
Halifax, Nova Scotia
Canada B3H 3J5
(902) 494-2358
FAX (902) 494-6889

DATE April 15, 1997

AUTHOR Angela Marie Kennedy

TITLE COMPARTMENTALIZATION OF FORMATION WATERS, PRINCE COLLIERY, CAPE BRETON, NOVA SCOTIA.

Degree BSc Convocation May Year 1998

Permission is herewith granted to Dalhousie University to circulate and to have copied for non-commercial purposes, at its discretion, the above title upon the request of individuals or institutions.

Abstract

The Prince Colliery is located offshore of Point Aconi, Cape Breton , Nova Scotia. The colliery is presently extracting coal from the Hub seam of the Morien Group, part of the Carboniferous Sydney Basin. Directly overlying the Hub seam is a channel sandstone body which contains formation water. Water was sampled directly from the roof before mining as well as from collapsed areas (gob areas) after mining.

Two formation waters were identified, (1) a low salinity formation water with Na/Cl ratios between 0.87 and 0.72 and chloride concentrations up to 11 200 mg/L, (2) a high salinity formation water with Na/Cl ratios between 0.6 and 0.7 and chloride concentrations between 24 400 and 30 000 mg/L. Gob water samples have chemistries similar to the high salinity formation water even at sampling depths similar to the low salinity formation water. Gob water samples have Na/Cl ratios between 0.6 and 0.7 and chloride concentrations up to 28 000 mg/L. The high salinity formation water and the gob waters are enriched in Br.

A 24 cm mudstone divides the channel sandstone body overlying the Hub coal seam into two sandstone units. The upper sandstone (8.56 m thick) has vertical permeabilities up to 20.9 mD and the lower sandstone (1.56 m thick) has vertical permeabilities up to 1.33 mD. A vertical salinity profile constructed from geophysical data for drill hole P6 reveals the more saline formation water overlies the low salinity formation water.

The channel sandstone body or aquifer overlying the Hub coal seam is compartmentalized by an area of low permeability which separates two distinct formation waters.

The chemistry of the high salinity formation water suggests that it is related to lower basinal brines. The low salinity formation water is a mixture of the high salinity formation water and a dilute ocean water end member. Mixing probably took place during geologic time. The gob waters are shown to be a mixture of these two formation waters and not sourced by the overlying modern seawater. Mixing models completed for the gob water samples support this conclusion.

Key Words: Compartmentalized, Formation Waters, Brine, Aquifer, Permeability, Chloride, Bromide, Na/Cl ratio, Salinity, Colliery, Gob.

TABLE OF CONTENTS

CHAPTER 3 WATER CHEMISTRY DATA

CHAPTER 4 ROCK BODY

CHAPTER 5 CHEMICAL MODELING

Chapter 6 Interpretations

Appendix 2 Petrographic Descriptions

List of Tables

Chapter 3 Water Chemistry Data

Chapter 4 Rock Body

Acknowledgments

I would like to thank the following people for their help and support during this project:

Supervisors: **Dr. A. Thomas Martel**
Dr. Martin Gibling

For, the job which let me develop my thesis during the summer, the immense help in improving my writing skills, and the general support that you have given me all year. It was great being part of the CHYP team!

Cape Breton Development Corporation:

Brendan MacKenzie

Geological Survey of Canada:

John Shimald

ADI Nolan Davis:

Fred Baechler

Dalhousie University:

Don Fox for helping with my slides and lending me Drever
Gordon Brown (Thin Section Lab)
Bob MacKay (Microprobe Lab)

And last but certainly not least,

Brian Creaser

Thank-you for bringing me supper when I stayed late at school, proof reading countless drafts and supporting me throughout the whole process. I couldn't have done it without you!

Acknowledgments

I would like to thank the following people for their help and support during this project:

Supervisors: **Dr. A. Thomas Martel**
Dr. Martin Gibling

For, the job which let me develop my thesis during the summer, the immense help in improving my writing skills, and the general support that you have given me all year. It was great being part of the CHYP team!

Cape Breton Development Corporation:

Bredon MacKenzie

Geological Survey of Canada:

John Shimald

ADI Nolan Davis:

Fred Bechalor

Dalhousie University:

Don Fox for helping with my slides and lending me Drever
Gordon Brown (Thin Section Lab)
Bob MacKay (Microprobe Lab)

And last but certainly not least,

Brian Creaser

Thank-you for bringing me supper when I stayed late at school, proof reading countless drafts and supporting me throughout the whole process. I couldn't have done it without you!

CHAPTER 1 INTRODUCTION

1.0 Introduction

The purpose of this study is to assess the presence of compartmentalized formation waters above the Hub seam of the Sydney Coalfield. The Prince Colliery, owned and operated by the Cape Breton Development Corporation (CBDC), "makes" water. This project has bearing on determining the source of these waters entering the mine and specifically the source of the high salinity gob water. One concern with mining at shallow depths beneath the ocean is that ocean water could leak down into the mine and jeopardize mine safety resulting in the closure of the colliery.

The compartmentalization of formation waters is suggested by a vertical geophysical salinity profile (Shimeld 1997) calculated for Drill Hole P6. This technique has been used widely at a scale of ten's of metres in the petroleum industry and has had limited use in hydrogeology. The salinity profile used in Shimeld's study was constructed on a metre scale and the results are supported by water chemistry data presented in this thesis.

This study is unique because the salinity of the channel sandstone waters above the Hub seam are evaluated in 3 separate time periods:

1. Before mining, using geophysical methods,
2. During tunnel drivage and before coal extraction, by collecting roof drips from the base of the channel sandstone,
3. For the entire sandstone following coal extraction.

This project is part of a larger scale analysis of groundwater in the Prince and Phalen Collieries being conducted by the Carboniferous Hydrogeological Project (Dr. A.T. Martel and Dr. M.R. Gibling) under an NSERC Strategic Grant. This project also involves ADI Nolan Davis, Geological Survey of Canada, Nova Scotia Department of Natural Resources in cooperation with the Cape Breton Development Corporation (CBDC). A dataset and problem were selected from the body of materials available to be pursued as an honours project.

1.1 Geologic Setting

The study area of this thesis is the Prince Colliery, offshore Point Aconi, Cape Breton (Figure 1.1). This subsea coal mine is extracting coal from the Hub seam (Figure 1.2) which belongs to the Morien Group, located within the Carboniferous Sydney Basin. The Sydney Basin covers an estimated area of 36,300 km^2 and is exposed on land in Cape Breton (Hacquebard 1993). The rocks are relatively undeformed and dip gently towards the east, extending beneath the Laurentian Channel and Grand Banks towards Newfoundland (Gibling & Bird 1994).

The Morien Group is Westphalian B to Stephanian in age and is composed of three formations: the South Bar Formation, Wadden's Cove Formation and the Sydney Mines Formation (Figure 1.3). The rocks are separated from the underlying Canso Group by a major unconformity (Gibling *et al.* 1987).

The study area, located within the Sydney Mines Formation, contains coal of high volatile A bituminous rank high in sulphur, ranging from 2% to 8% (Hacquebard 1993). The formation is composed of repeated sequences or cyclothems of coal, limestone and shale;

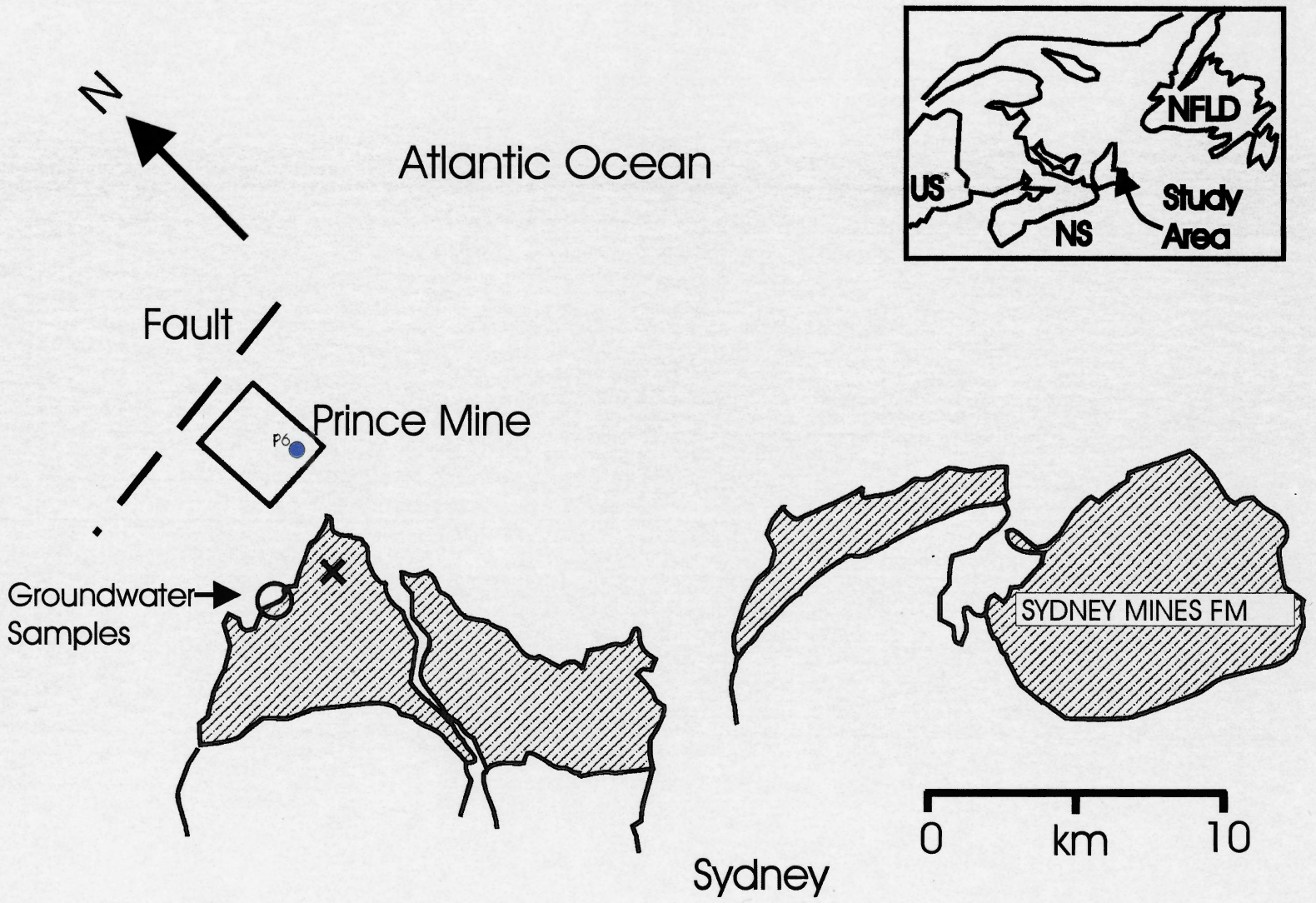

Figure 1.1 Generalized map of Study Area. Onshore location of Prince Colliery is indicated by an 'x'. The mine shaft extends to the north. The mine workings are located offshore to the north.

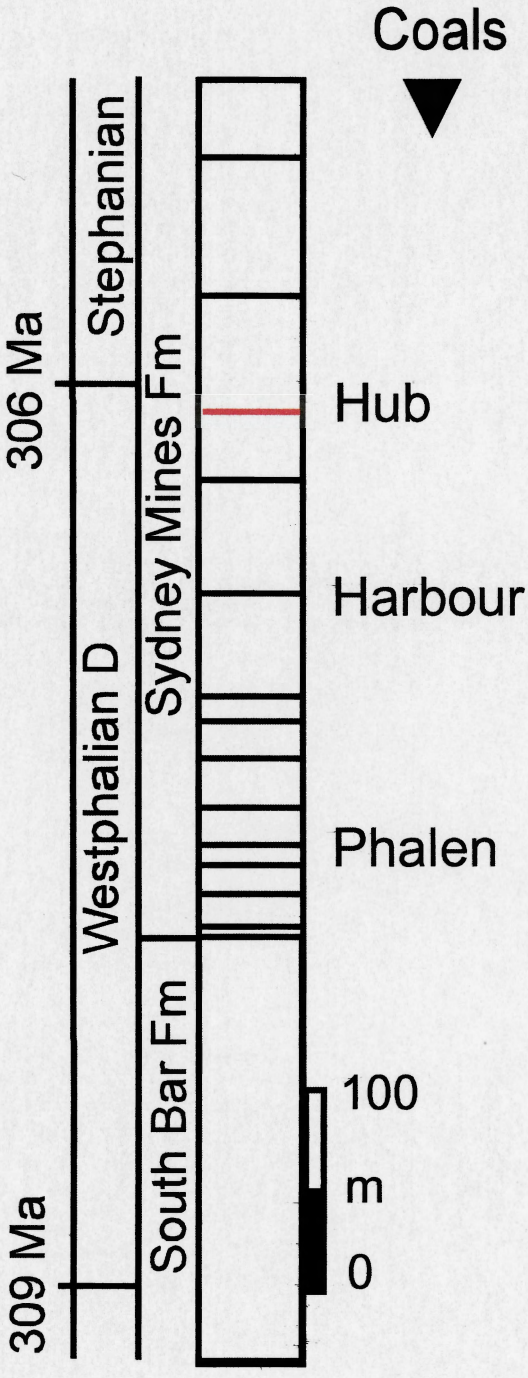

Figure 1.2 Stratigraphic location of the Hub Coal Seam

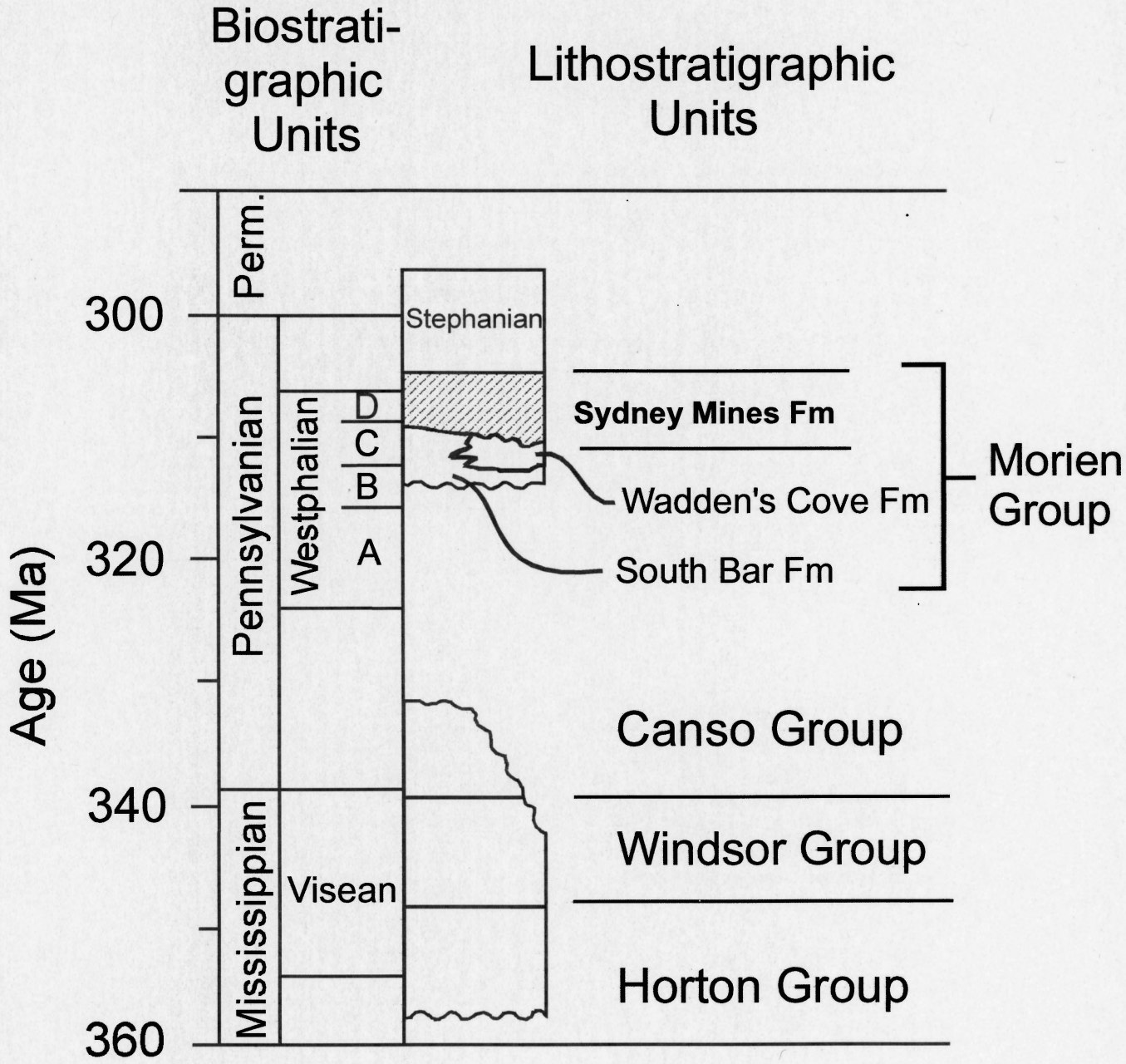

Figure 1.3 General stratigraphy of the study area.

interbedded with sandstone-dominated units (Gibling and Bird 1994). The sandstone-dominated units are fine- to coarse-grained and form channel-fill deposits between 2.5 m to 20 m thick (Gibling and Bird 1994). This study looks at the formation water contained within the sandstone aquifer overlying the Hub seam.

1.2 Previous Work

Previous work on the area has focused mainly on the stratigraphy and sedimentology of the Morien Group and specifically the Sydney Mines Formation. The Geological Survey of Canada used multibeam swath bathymetry and reflection seismic profiles to identify geologic structures in the area to aid in mine planning (Duggan 1995). A number of internal reports were produced by CBDC involving the Prince Colliery for the purpose of mine planning and safety. Calder (1987) produced a report discussing the stratigraphy and sedimentology of the Hub seam roof strata of the Prince Colliery. From this report it was determined that:

- Drill Holes H-12B and P-6 intersect a channel sandstone body overlying the Hub seam
- Holes H12, P5 and H12A do not intersect the large sandstone body
- the channel sandstone body trends northwest-southeast
- and both the Hub coal seam and the overlying channel sandstone body are terminated to the northwest by the Mountain Fault.

As mining progresses in the colliery, geologic data are continuously being acquired to evaluate the integrity of the roof rock.

A major project, of which this study is a part, is the first large scale analysis of the formation water chemistry above the Hub coal seam at Prince Colliery.

CHAPTER 2 METHODS

2.0 Introduction

Water analyses were completed by CBDC (1986-1995) and by Dr. A.T. Martel (1996). Samples were taken from water dripping from the roof of the mine and water flowing out of collapsed mined areas during various stages of mine development. Groundwater was sampled by ADI Nolan Davis between December 1994 and September 1995. All samples were analyzed for major ion chemistry. Water sampled by Martel (1996) was also analyzed for selected stable isotopes (^{34}S) and bromide. Six rock samples were collected from core P6 and petrographic analyses were completed for each. Information on the overlying sandstone was provided from Drill Core P6 as well as from roof boreholes drilled by CBDC within the Colliery.

2.1 Major Ion Chemistry

2.1.1 Water Sampling Procedures

Water could only be sampled where it was dripping from the overlying sandstone body. Water drips commonly stop a short time after the tunnel has been driven and because of this water sampling is restricted to specific areas. Water was sampled from drips from the sandstone roof or from boreholes drilled into the roof. Martel (1996) took one roof sample from a borehole and three samples from water flowing out of collapsed mined areas. Water was sampled in separate Nalgene bottles and immediately sent for

analysis. Filtered and non-filtered samples were taken at each location using a 0.45 μm filter with a cellulose nitrate membrane.

2.1.2 Water Analysis

Major ion chemistry analysis was completed at the University College of Cape Breton (UCCB). The Geological Survey of Canada (GSC) in Ottawa analyzed the water sampled by Martel for bromide and the University of Waterloo analyzed for a stable isotope (^{34}S). Appendix 1 contains the procedures for the analysis conducted by UCCB. Information was unavailable on the procedures used at the University of Waterloo and the GSC.

2.1.3 Method of Interpretation

Relationships between ionic species, ionic ratios, chloride, bromide and depth were used to recognize trends in the water samples. Models of water mixes were produced by the hydrochemical program Hydrowin (Calmbache). Plots of data were made in mmoles/L and ionic ratios are molar so as to eliminate any bias caused by differences in molecular weight. Data from core samples, various core logs (i.e. resistivity, descriptive), and borehole data were used to complement the chemical data.

2.2 Core Samples

Six rock samples were taken from a major sandstone body intersected by core P6 which was drilled by CBDC in 1979 (refer to Figure 1.1), and is now stored at the Stellarton core library. Thirteen rock samples had been selected previously for porosity

and permeability analyses by CBDC; and measurements were completed by Core Laboratory's Canada Ltd. in 1979.

2.2.1 Analysis of Core Samples

Blue epoxy was applied to the rock samples and they were then mounted on slides at Dalhousie University and cut to 0.03 mm thickness. Petrographic descriptions were completed for each thin section. Visual estimates were made to approximate maturity, sorting, mineral percentages, pore abundance and percentage of pores filled with kaolinite. Average grain and pore size were calculated by measuring the longest dimension of a minimum of 20 random grains/pores throughout the thin section and averaging these measurements. Sorting and roundness (maturity) were estimated using charts from Tucker (1981) based on Pettijohn *et al.* (1973).

Microprobe analyses were completed at Dalhousie University for samples P6-2 and P6-6 on carbonate grains to identify their composition.

CHAPTER 3 WATER CHEMISTRY DATA

3.0 Introduction

In this study, two types of waters were sampled within the Prince Colliery: formation water and gob water (Figure 3.1). Formation water, as defined by Drever (1988), is water found in the pores of a deeply buried sedimentary rock. Formation water was sampled after tunnel drivage, but before mining commenced at the sample location (and therefore before significant fracturing in the overlying rock). As mining progresses, the main shaft is extended to greater depths. Water is sampled either directly from the sandstone roof or from roof boreholes. Therefore, this water is thought to have been derived from the base of the channel sandstone overlying the Hub seam.

CBDC extracts coal using retreat longwall mining, this consists of drilling two drivage tunnels which are then connected. The coal is extracted back from this connection, towards the main shaft. After coal extraction the tunnel is left to collapse and this collapsed area is the gob (Figure 3.2). Roof collapse creates fractures in the overlying rock which provide additional pathways for water to flow from the entire sandstone body. Water from the overlying sandstone travels through the collapsed area or gob and exits at the tunnel entrance where it is sampled. As a result, gob water samples are a mixture from different stratigraphic levels within the sandstone body.

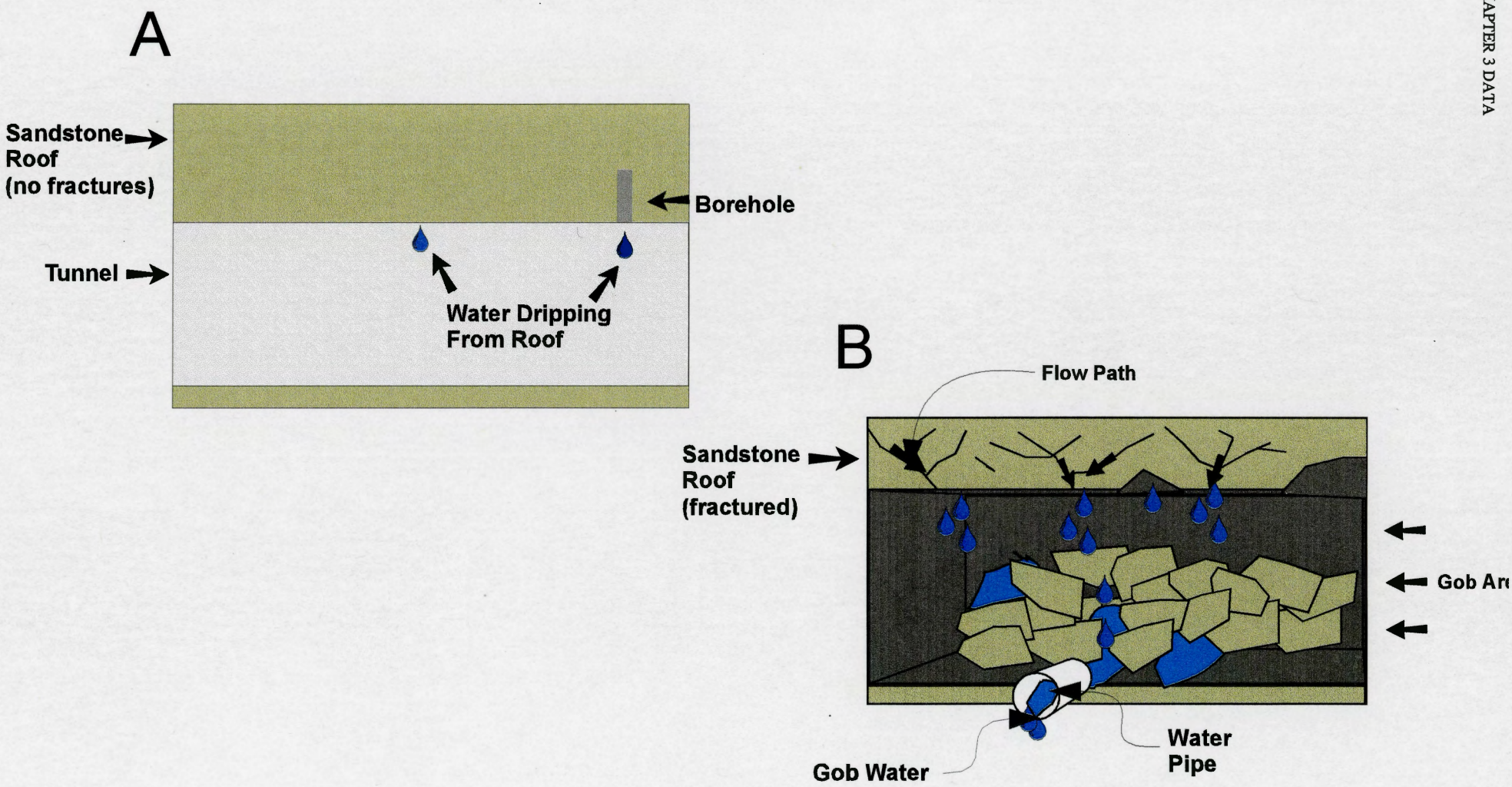

Figure 3.1 Diagram illustrating two types of water sampled in the Prince Colliery.
A- Formation water, B- Gob water.

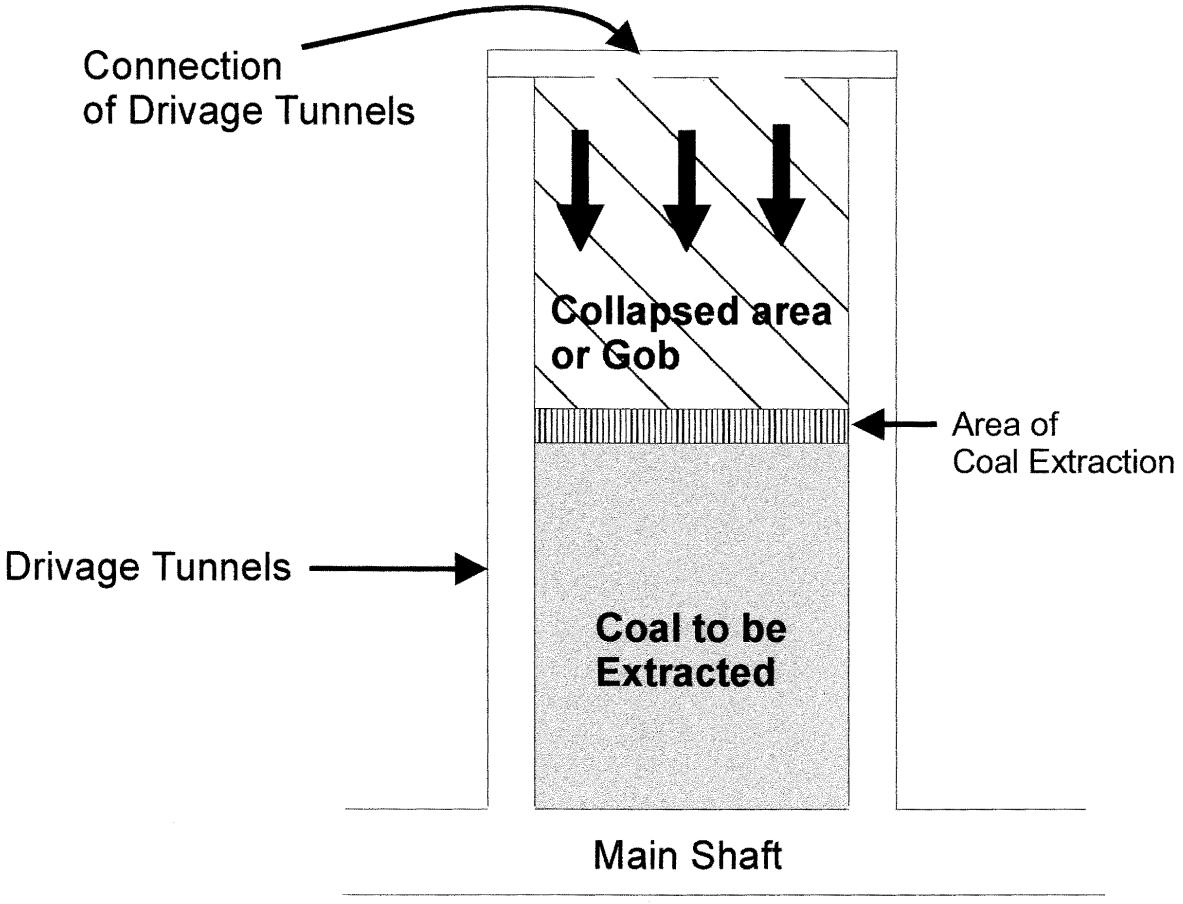

Figure 3.2 Diagramatic explanation of Retreat Longwall Mining (plan view).

3.1 Surficial Groundwaters

Surficial groundwater samples (Table 3.1) were collected by ADI Nolan Davis are used here as a "baseline" for surficial groundwaters in the Sydney Coalfield area. Water was sampled from Quaternary sediments and bedrock at the Point Aconi Power Plant, Cape Breton (Figure 1.3). The groundwater samples consist of two populations, a more calcic population and a more sodic population which is also more saline. This relationship is clearly seen on a piper plot. The more sodic water was sampled from Forebay well and plot in close proximity to the Prince Formation waters (Figure 3.3). Forebay well shows a more ocean-like character than the other groundwater samples and plots near ocean water on the HCO_3 , Cl, SO_4 and central rectangular fields.

3.2 Major Ion Chemistry

3.2.1 Geophysical Logs

Gamma ray, neutron porosity, density and resistivity logs were used to calculate a salinity profile of drill hole P6. Calculations were completed on the computer program NLS (Figure 3.4; Shimeld 1997). To calculate the resistivity of the water (R_w), data points in non-shaley units had to be identified and the porosity of the rock had to be calculated. Porosity calculations were completed using an equation (Schlumberger 1991) which relates neutron porosity and density logs to the porosity of the rock. The gamma ray and neutron porosity logs were used to identify non-shaley intervals in core P6. The

Well #	Date	Na	K	Ca	Mg	Alkalinity	SO4	Cl	SiO2	Fe	Cond (umhos/cm)	pH (pH units)	Hardness (as CaCO3)	Ion Sum
PA1	13-Dec-94	30.9	1.9	56.2	16	23	120	79.7	7	<0.02	641	6.1	206	335.57
PA1	07-Mar-95	26	1.6	40.5	12.4	26	94	51.9	6.4	<0.02	469	6.4	152	259.11
PA1	16-Jun-95	30	1.6	51.2	15.6	32	130	69.5	7	<0.02	625	7.3	192	337.44
PA1	12-Sep-95	22.9	1.6	33.7	10.8	30	96	32.1	6.6	<0.02	416	6.5	129	233.79
PA4	22-Dec-94	20.3	1.7	74.3	7.9	133	25	57.1	7.3	0.05	498	7.4	218	326.81
PA4	17-Mar-95	20.8	1.8	67.4	7.7	135	23	56.1	7.9	0.13	510	7.8	200	320
PA4	21-Jun-95	15.6	1.7	67.6	7.3	158	22	53.2	8.1	0.12	520	8.2	199	333.78
PA4	18-Sep-95	19.9	1.8	67.2	7.6	137	25	52.7	7.6	0.03	529	7.7	199	318.99
PA5	22-Dec-94	7.7	0.4	6.02	1.9	17	4	13.6	6.8	<0.02	101	6.2	22.9	57.44
PA5	16-Mar-95	8.8	0.7	6.21	2	16	3	15.8	6.5	<0.02	96.7	6.9	24	59.63
PA5	21-Jun-95	7.5	0.6	5.78	2	16	4	15.9	6.9	<0.02	95.6	6.7	22.7	58.7
PA5	22-Sep-95	9.1	0.7	8.21	2	22	5	15.6	7	<0.02	110	6.5	28.7	69.63
PA6	19-Dec-94	105	7	6.08	4.1	128	N/A	96.6	0.6	<0.02	601	8.4	32.1	347.39
PA6	Frozen													0
PA6	22-Jun-95	122	7.9	21.4	6.4	200	N/A	133	1.9	<0.02	794	8.4	79.8	492.63
PA6	18-Sep-95	122.00	8.20	25.30	6.70	191	N/A	106.00	3.00	<0.02	769	8.2	90.8	462.25
PA7	22-Dec-94	19.60	5.80	25.20	7.50	134	N/A	10.50	3.70	<0.02	303	7.6	93.8	206.44
PA7	17-Mar-95	20.80	5.90	34.10	8.70	128	9.00	10.90	4.10	<0.02	297	8.1	121	221.66
PA7	15-Jun-95	17.30	6.10	36.30	8.40	160	7.00	10.80	4.20	<0.02	318	8.3	125	250.26
PA7	07-Sep-95	15.90	5.80	33.40	8.10	133	5.00	12.20	3.00	<0.02	296	8.0	117	216.51
PA11	22-Dec-94	14.90	3.20	44.20	7.90	134	5.00	15.50	10.10	<0.02	314	7.7	143	234.95
PA11	15-Mar-95	16.00	4.00	39.70	8.70	127	4.00	17.00	12.10	<0.02	299	8.2	135	228.6
PA11	20-Jun-95	14.10	4.00	37.40	8.30	130	4.00	17.50	13.00	0.06	306	8.3	128	228.47
PA11	19-Sep-95	14.80	4.10	36.60	8.20	131	5.00	16.80	12.10	0.02	338	7.8	125	228.72
PA9	19-Dec-94	118.00	13.80	264.00	50.70	196	613.00	206.00	4.50	<0.02	2580	7.2	868	1466.48
PA9	16-Mar-95	91.30	12.40	258.00	54.60	180	589.00	171.00	4.00	<0.02	2150	7.9	869	1360.92
PA9	21-Jun-95	372.00	14.40	305.00	67.90	422	874.00	348.00	4.40	<0.02	4140	8.1	1040	2407.92
PA9	19-Sep-95	158.00	15.10	290.00	62.30	249	754.00	198.00	5.10	<0.02	3020	7.4	981	1731.77
PA12	22-Dec-94	13.90	2.50	73.80	13.70	128	65.00	68.70	11.40	<0.02	632	7.1	241	378
PA12	14-Mar-95	17.80	2.60	66.20	24.50	82	150.00	38.70	10.70	<0.02	652	7.6	266	393.74
PA12	15-Jun-95	14.10	2.30	60.60	12.00	103	32.00	61.90	11.10	<0.02	522	7.6	201	297.8
PA12	14-Sep-95	11.20	3.30	48.50	9.60	135	16.00	24.60	10.80	0.04	407	7.8	161	259.36
PA13	19-Dec-95	38.40	2.50	48.20	7.10	158	28.00	40.40	8.10	<0.02	446	7.5	150	330.84
PA13	07-Mar-95	32.60	2.40	45.70	6.70	140	18.00	30.00	8.10	<0.02	419	8.1	142	283.55
PA13	16-Jun-95	36.20	2.30	47.40	6.70	149	16.00	39.70	8.60	<0.02	471	8.2	146	305.99
PA13	12-Sep-95	31.70	2.60	47.80	6.80	151	21.00	30.10	8.20	<0.02	462	7.7	147	299.29
PA14	13-Dec-94	44.80	1.30	72.30	9.60	75	91.00	90.70	7.40	0.73	678	6.5	220	394.45
PA14	07-Mar-95	46.50	1.20	58.00	10.10	67	92.00	83.50	6.90	0.50	632	7.4	186	367.41
PA14	16-Jun-95	48.80	1.80	54.20	10.90	63	93.00	100.00	7.40	0.84	698	7.6	180	381.66
PA14	07-Sep-95	53.00	1.80	63.10	9.90	101	110.00	77.20	7.70	0.07	711	7.1	198	424.96
PA15	13-Dec-94	29.30	0.80	48.20	5.20	110	8.00	45.10	13.20	<0.02	399	7.1	142	261.06
PA15	07-Mar-95	28.20	0.90	43.70	5.30	105	9.00	44.30	13.40	<0.02	377	7.7	131	251.33
PA15	16-Jun-95	26.50	0.80	41.80	5.00	114	9.00	49.60	13.00	0.12	396	8.1	125	261.31
PA15	07-Sep-95	27.80	0.90	42.80	4.60	110	10.00	48.50	13.50	<0.02	423	7.3	126	259.64
ForeBay	19-Dec-94	1510.00	35.70	126.00	88.40	24	19.00	2780.00	0.60	2.58	9920	6.6	678	4587.94
ForeBay	14-Mar-95	1560.00	34.00	124.00	91.50	5	7.00	2850.00	<0.5	1.99	10100	6.6	686	4675.91
ForeBay	21-Jun-95	1640.00	33.40	124.00	78.20	4	N/A	2990.00	<0.5	19.20	10500	5.5	631	4891.75
ForeBay	18-Sep-95	1550.00	36.50	164.00	88.50	123	42.00	2780.00	2.80	0.06	10200	7.5	744	4788.24

Table 3.1 Species measurements are in mg/L unless otherwise indicated.

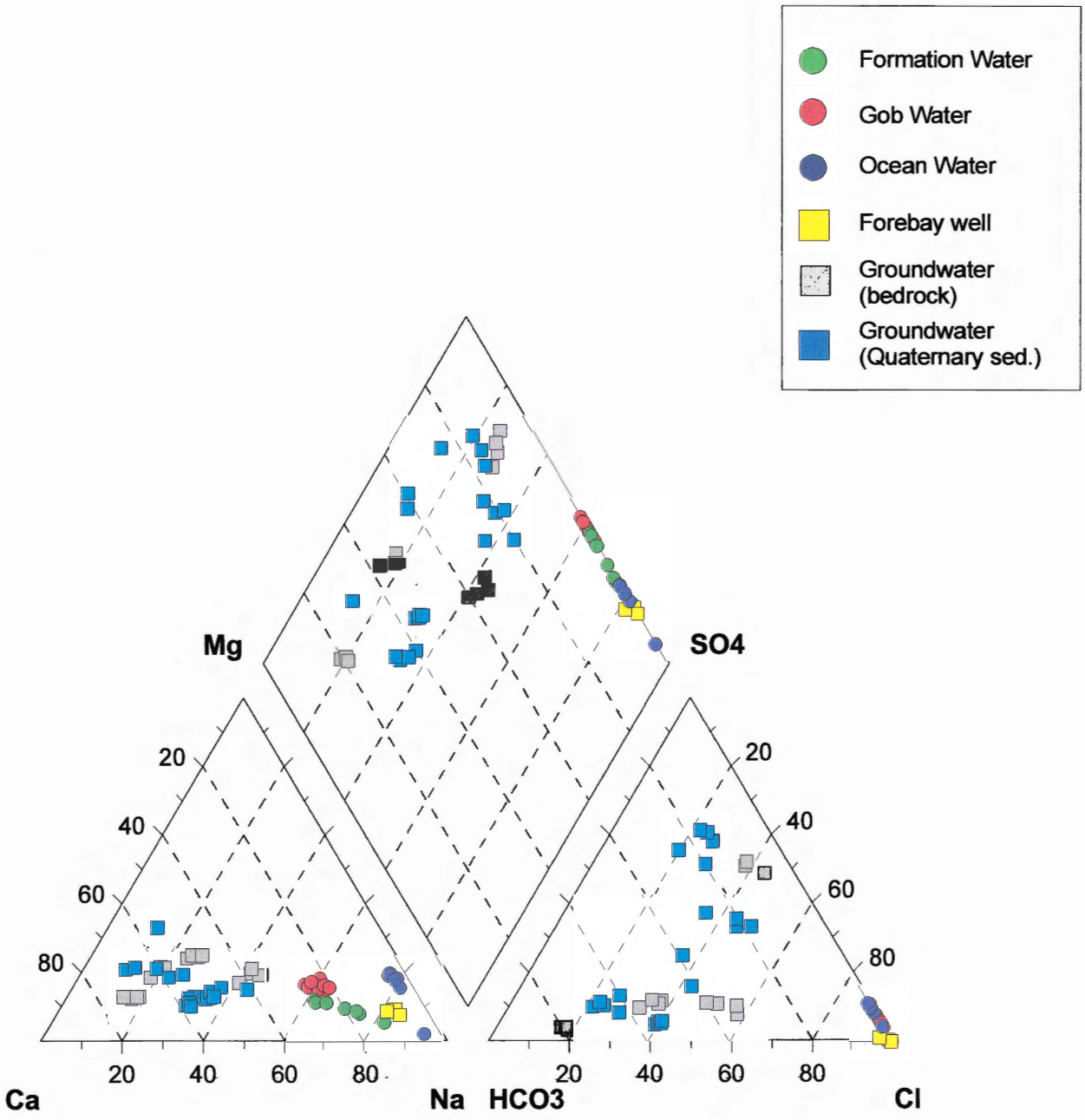

Figure 3.3 Piper plot of groundwater, formation water, gob water ocean water and Forebay well.

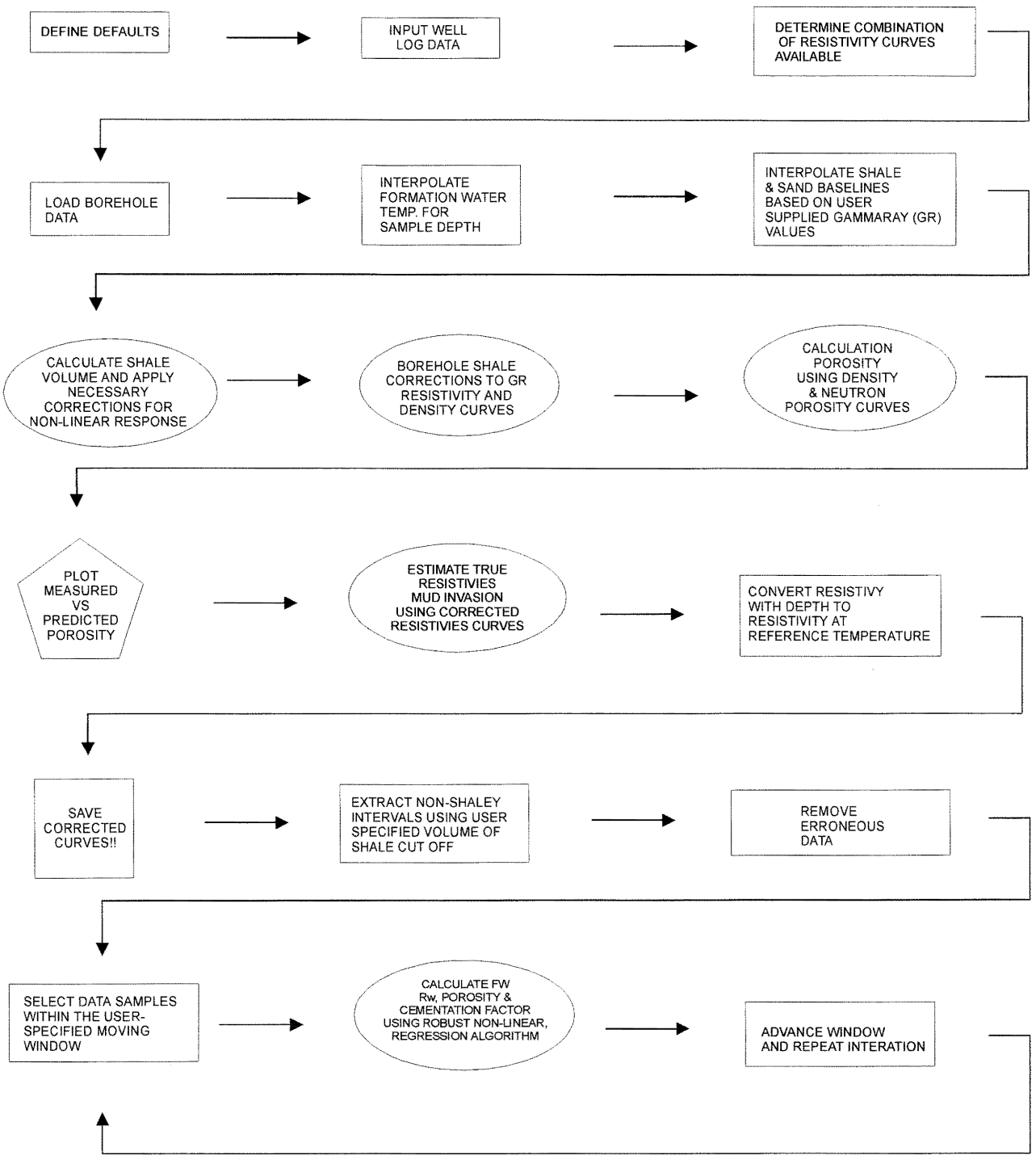

Figure 3.4 Flow diagram illustrating steps involved in the program NLS (Shimeld 1997) used to generate water resistivity values.

data points within these non-shaley intervals were used to calculate R_w and m in Archie's Law which can be rearranged into the following equation:

$$f = ((\frac{R_w}{R_t})^{\frac{1}{m}} - \phi) \quad (3.1)$$

Where R_t is the resistivity of the rock, m is the cementation factor and ϕ, is the porosity. f is the difference between the porosity calculated from the geophysical logs (ϕ) and the porosity calculated using Archie's Law. Values of R_w and m are optimal when f is at a minimum. Minimization of the function was completed using a robust nonlinear regression technique from Entyre (1992). Hydraulic conductivity was then calculated using R_w. Salinity was calculated using an empirical equation from Bateman and Konen (1977). The equation was developed for calculating the salinity of Na-Cl waters. Although the formation waters at Prince Colliery are predominatly Na-Cl waters, the calculated salinities should still only be used as an approximation of the actual salinity values.

The results show two populations of total dissolved solids, averaging 65 ppt and 12 ppt (Figure 3.5). With increasing depth the salinity of the formation water decreases. The change in salinity occurs over a short depth interval at approximately 230 m depth.

3.2.2 Major Ion Chemistry of Deep Groundwaters

The chemistry of the water sampled (Table 3.2) in the Prince Colliery also shows a salinity variation. Chloride increases sharply between water sampled from 266 m and 281 m depth below sealevel (11 700 mg/L to 24 405 mg/L) (Figure 3.6). In this 15 m interval the chloride concentration increase is 861 mg/L per metre. Formation waters

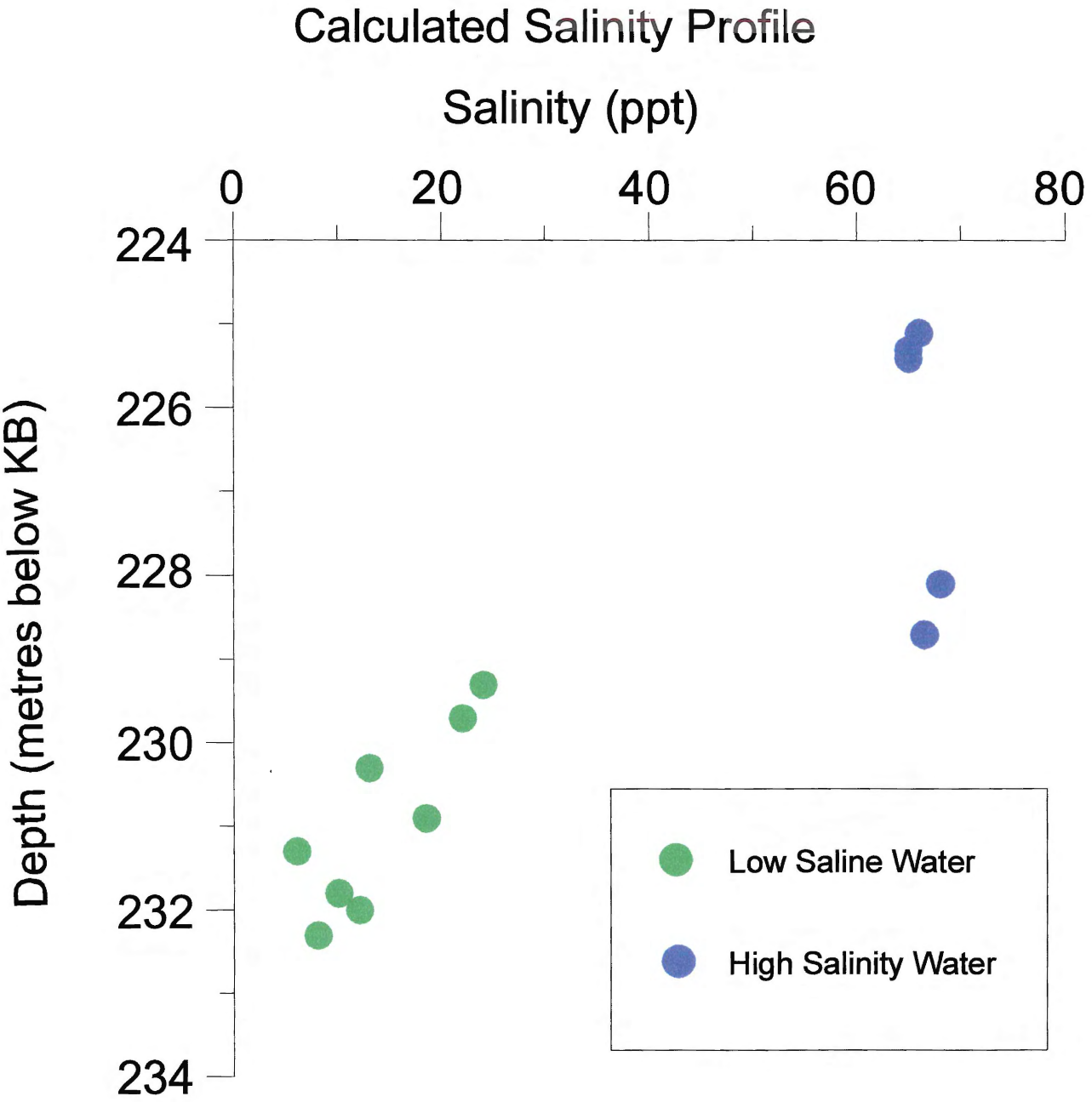

Figure 3.5 Calculated salinity profile produced by Shimeld (1997).

SAMPLE #	DATE	MINE	SECTION	SITE DISCRIPTION	SOURCE	Na	K	Ca	Mg	ALKALINITY
CBDC-43	12/20/88	PRINCE	8 W T	ROOF	formation	3200	64	463	175	210
CBDC-518	15-Jan-86	PRINCE	4 W W F	Drip from SS roof	formation	2650.0	52.0	345.0	93.0	177.0
CBDC-559	07-Feb-90	PRINCE	4 Decline	Drip from SS roof	formation	5200.0	81.0	1030.0	294.0	160.0
CBDC-594	30-Apr-91	PRINCE	9W	Drip from SS roof	formation	5590	90	1370	402	76.0
CBDC-570	25-Apr-90	PRINCE	6 WWF		gob	7230.0	112.0	1900.0	830.0	1.0
CBDC-571	25-Apr-90	PRINCE	5 WB		gob	6770.0	104.0	1900.0	660.0	1.0
CBDC-602	16-Aug-91	PRINCE	9 WWF	Drip from SS roof	formation	4830.0	72.0	991.0	302.0	140.0
CBDC-673	16-Jul-94	PRINCE	13 WT x-cut # 3		gob	9000.0	180.0	2800.0	1120.0	0.4
CBDC-674	19-Aug-94	PRINCE	13 WT x-cut # 3		gob	8640.0	163.0	2675.0	1060.0	3.5
CBDC-676	27-Oct-94	PRINCE	14 WB	Drip from borehole	formation	11100.0	93.0	4090.0	1135.0	44.9
CBDC-679	11-Jan-95	PRINCE	13 WT x-cut # 2		gob	10175.0	174.3	3470.0	1473.0	0.4
CBDC-680	23-Jan-95	PRINCE	13 WT x-cut # 3		gob	9000.0	159.0	3018.0	1163.0	23.1
CBDC-681	11-Apr-95	PRINCE	13 WT x-cut # 2		gob	9145.0	164.0	2760.0	1265.0	0.4
CBDC-684	18-Oct-95	PRINCE	14 WT x-cut #1		gob	11400.0	141.0	3210.0	1470.0	0.0
DAL Pr 7WB	26-Aug-95	PRINCE	7WB		gob	5615.0	66.9	2025.0	871.0	<0.4
)AL Pr 10WE	26-Aug-95	PRINCE	10WB		gob	8070.0	126.0	2535.0	1290.0	<0.4
)al Pr 12 WE	26-Aug-95	PRINCE	12 WB		gob	10700.0	153.0	4280.0	1625.0	<0.4
Dal Pr 4D	26-Aug-95	PRINCE	4Decline	Drip from borehole	formation	11900.0	108.0	4345.0	1145.0	31.5
Pr-3	01-Jul-97	PRINCE	15 W	Drip from SS roof	formation	10580.0		3320.0	958.0	105.0

Table 3.2 Species measurements are in mg/L unless otherwise indicated.

SAMPLE #	HCO3	CO3	SO4	Cl	NH3	Mn	Fe	Conductivity (umhos/cm)	pH (pH units)	Ion Sum	Na/Cl	Depth (m)
CBDC-43			2	6100	1.9	0.43	6.8	22350	7.7	178.4404	0.81	unknown
CBDC-518	1.3	175.6	2.4	4700.0	1.4	0.2	0.0	13356.0	7.9	7845.5	0.87	192.0
CBDC-559	158.0	1.9	12.0	11200.0	3.9	0.8	0.9	38400.0	8.1	17981.3	0.72	266.0
CBDC-594	75.8	0.23	3	11100	2.9		2.47	40000	7.5	18634	0.78	240.5
CBDC-570			1870.0	16700.0	3.7	32.0	197.0	63000.0	2.9	28877.4	0.67	219.8
CBDC-571			1420.0	15600.0	3.1	14.0	32.0	56100.0	2.7	26504.1	0.67	215.2
CBDC-602	139.0	0.5	2.0	10000.0	3.1	0.5	0.4	35400.0	7.6	16340.0	0.74	240.5
CBDC-673	0.0	0.0	1978.7	21330.0	3.8		19.8	47900.0	5.2	36478.9	0.65	260.5
CBDC-674	0.0	0.0	1983.5	21830.0	3.5	6.7	28.4	85000.0	5.6	36455.4	0.61	260.5
CBDC-676	44.9	0.0	3.6	27105.0	5.8	1.8	5.1	107200.0	6.7	43651.8	0.63	312.5
CBDC-679	0.4	0.0	2063.7	24318.0	5.4		95.4	98300.0	3.1	41865.0	0.65	269.5
CBDC-680	23.1	0.0	1678.8	21410.0	2.6		39.4	85700.0	5.9	36533.9	0.65	260.5
CBDC-681	0.0	0.0	1810.0	20815.0	2.2		79.4	85300.0	5.2	36081.7	0.68	269.5
CBDC-684	0.0	0.0	1914.8	25242.0	4.7		24.6	89600.0	4.9	43876.7	0.70	294.4
DAL Pr 7WB	0.4	0.0	2235.0	13440.0	3.0		187.0	35300.0	2.6	24253.1	0.64	223.7
)AL Pr 10WE	0.4	0.0	2313.0	20550.0	4.0		712.0	48800.0	4.0	34884.2	0.61	265.8
Dal Pr 12 WE	0.4	0.0	1633.0	27950.0	4.8		149.0	63500.0	4.4	46341.2	0.59	290.1
Dal Pr 4D	31.2	0.2	<1	30230.0	6.1		4.5	67700.0	7.9	47747.9	0.61	330.7
Pr-3	105.0		3.7	24405.0	0.7		7.5	52300.0	7.3	39433.8	0.67	280.9

Table 3.2 Species measurements are in mg/L unless otherwise indicated.

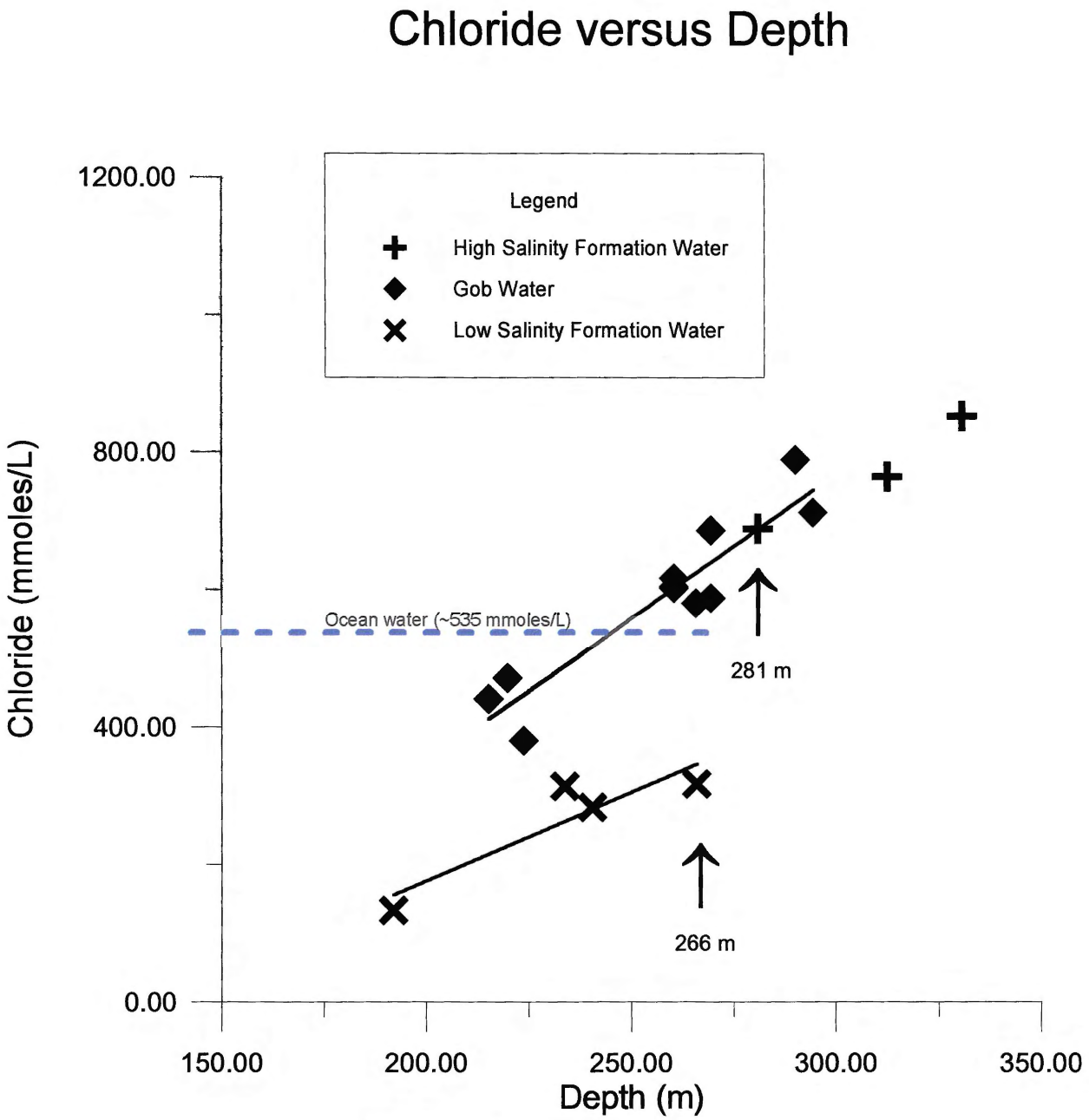

Figure 3.6 Chloride (mmoles/L) versus Depth (m). Formation water samples do not increase evenly with depth. There is a large increase between 266 m and 281 m (noted with arrows).

were separated on either side of this division into low salinity formation waters (LSFW) and high salinity formation waters (HSFW). The LSFW range between 4700 - 11 700 mg/L. Samples become more saline down dip over a vertical interval of 74 m at a rate of only 87.8 mg/L per metre. The gob waters increase by 164.8 mg/L per metre over a 75 m interval down dip, which is slightly greater than the increase shown by the HSFW (116 mg/L per metre). Gob waters sampled from the same depth as LSFW exhibit much higher chloride concentrations.

The Na/Cl ratio (Figure 3.7) of the LSFW decreases with depth and ranges between 0.87 and 0.72. The HSFW and gob waters have Na/Cl ratios between 0.6 - 0.7. Modern ocean water offshore Sydney and the Forebay well have Na/Cl ratios ranging between 0.96 - 0.81. The LSFW exhibits different Na/Cl ratios and chloride concentrations than gob waters at similar depths. The LSFW plot as an intermediate between Forebay well and the gob waters with respect to Cl (Figure 3.8)

The gob and high salinity formation water samples are enriched in bromide with respect to ocean water (Figure 3.9). Bromide and chloride are both conservative elements because there are limited sources and sinks for them in the hydrological cycle. They do not participate in water/rock reactions (Hanor 1994) so the main source and sink for these ions is evaporite deposits (Berner and Berner 1996).

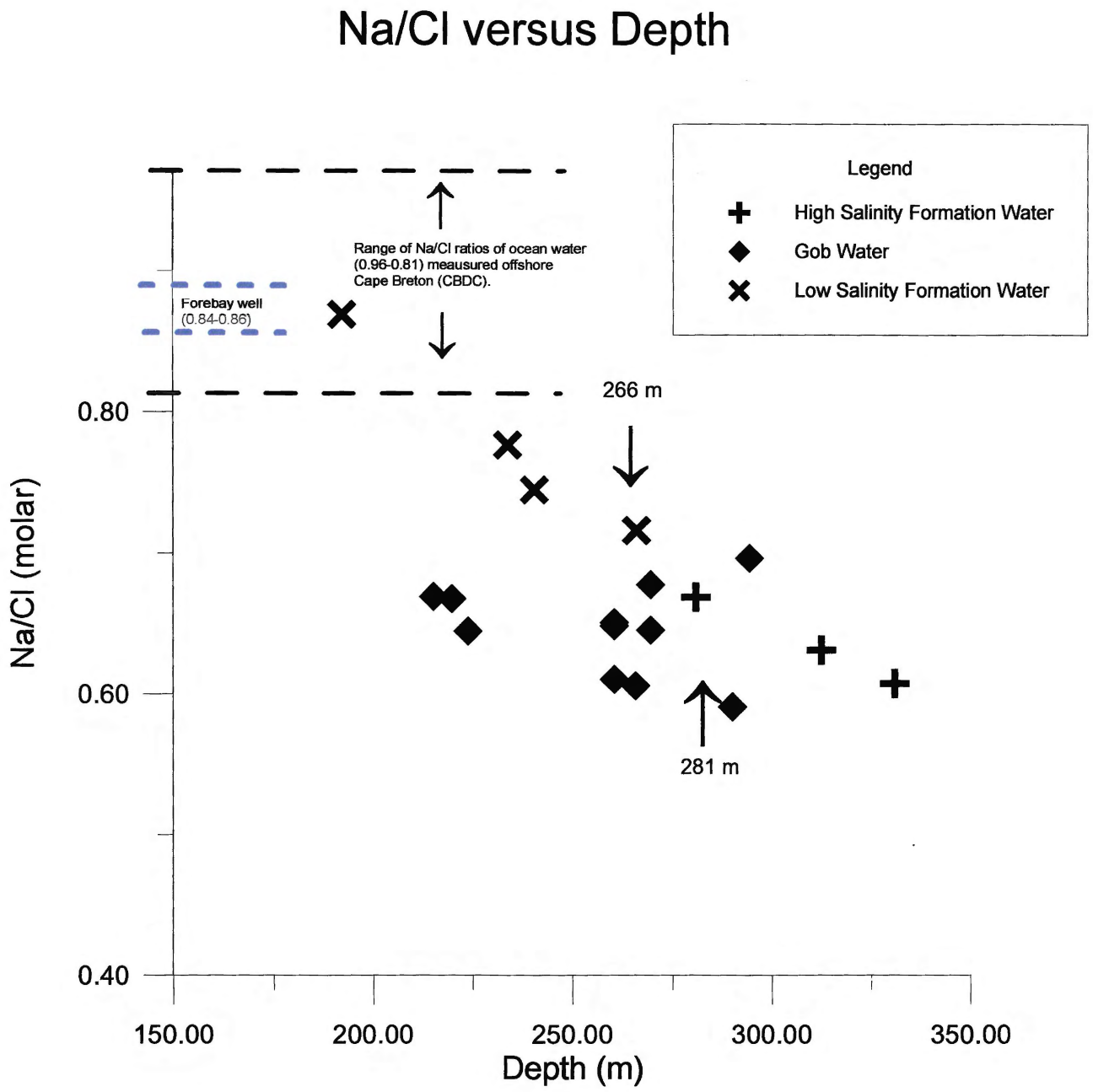

Figure 3.7 Na/Cl versus Depth (m). The Na/Cl ratio of the Formation water decreases with depth.

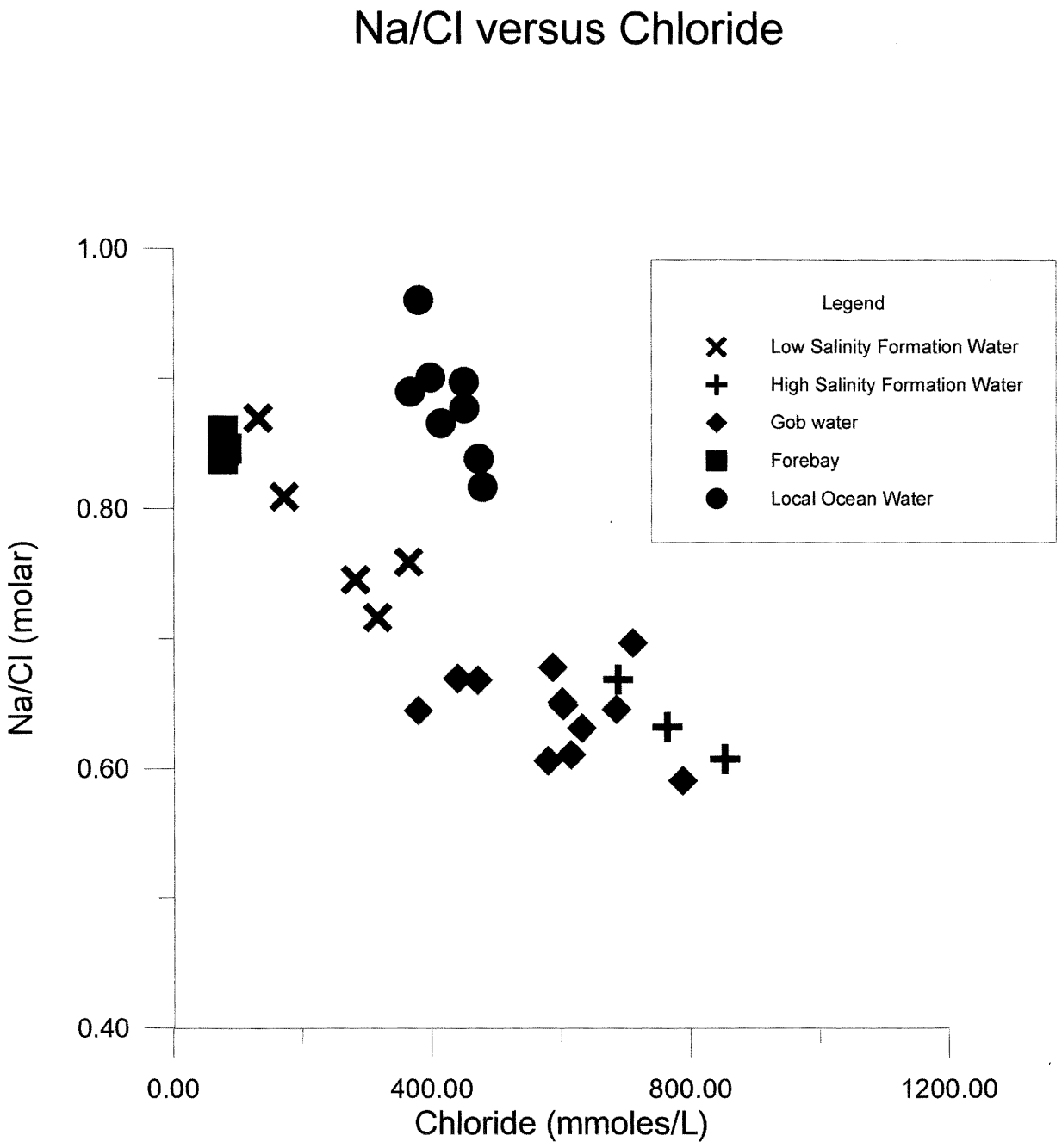

Figure 3.8 Na/Cl ratio versus Chloride (mmoles/L). The LSFW plot as an intermediate between Forebay well and the gob waters. Local ocean water was sampled by CBDC, offshore Cape Breton.

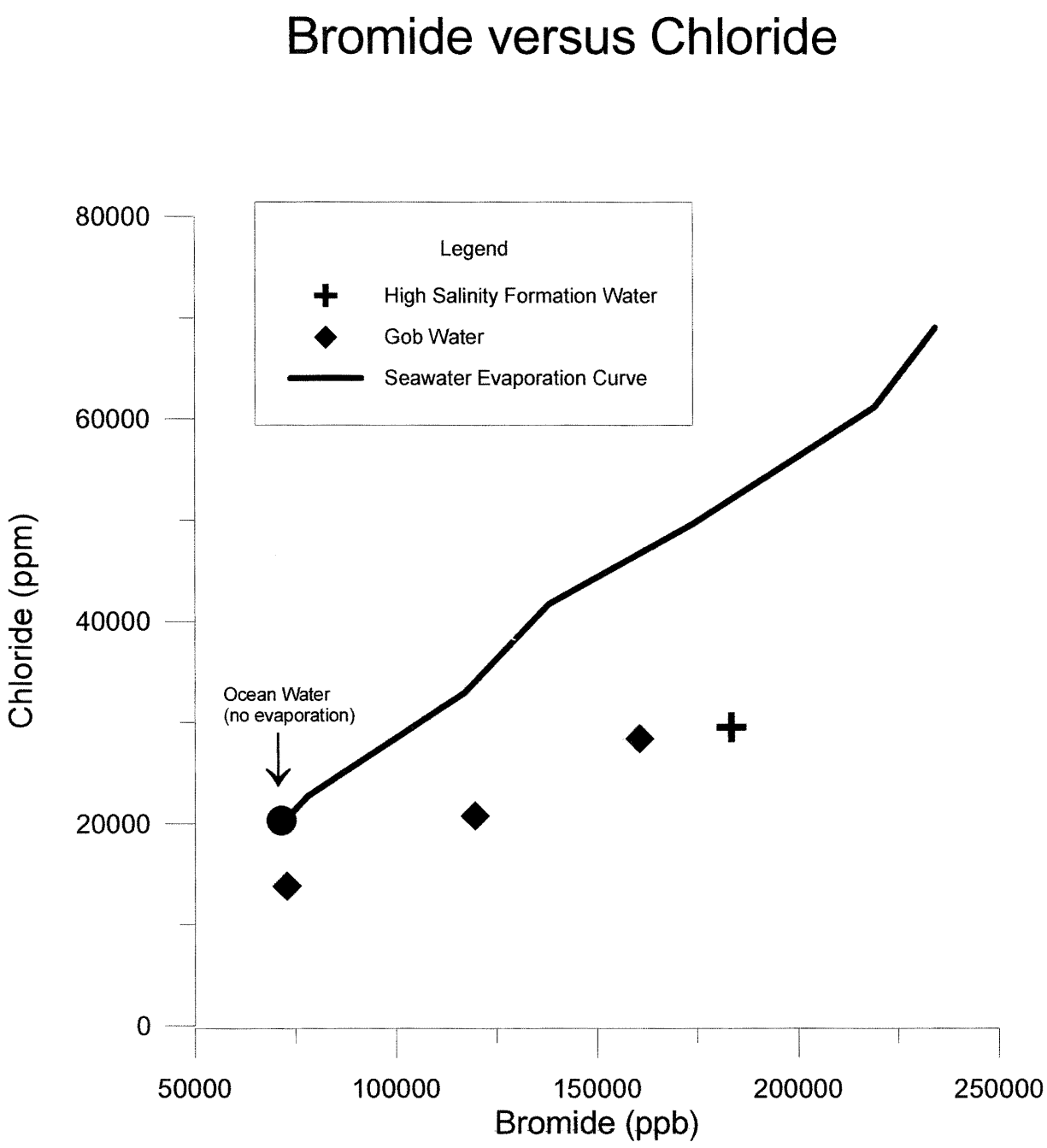

Figure 3.9 Bromide (ppb) versus Chloride (ppm).
Prince waters are enriched in bromide with respect to the seawater evaporation curve.
* Seawater evapration curve from McCaffrey et al. (1987).

On plots of Na and Ca ions versus Cl (Figure 3.10a & b), gob waters fall on a line intermediate between the high and low salinity formation waters. This relationship is also true for potassium. Alkalinity (Figure 3.11), sulphate (Figure 3.12) and to a lesser extent magnesium (Figure 3.13) do not follow this trend. The gob samples are enriched in sulphate, slightly enriched in magnesium and have below detectable carbonate alkalinity. Sulphate concentrations are as high as those measured in ocean water, but ^{34}S and ^{18}O in sulphate are more variable (Figure 3.14).

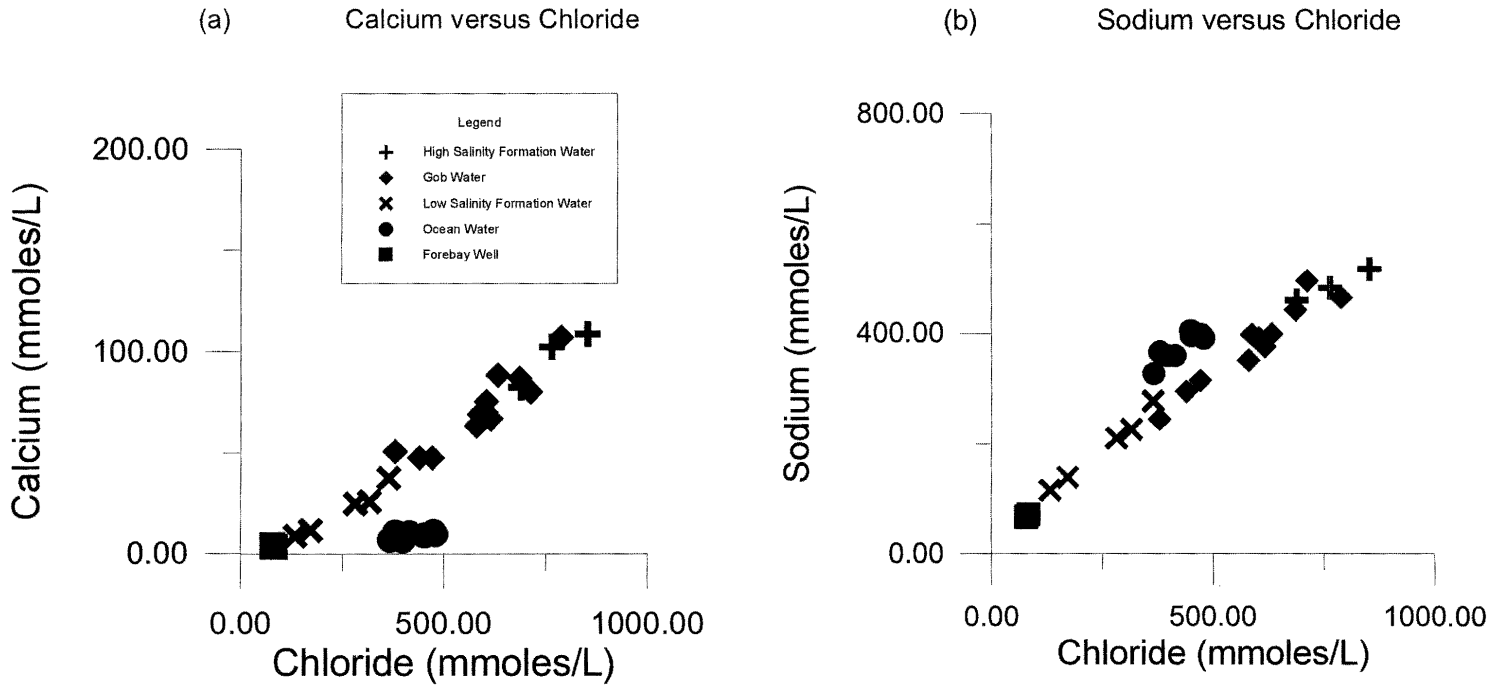

Figure 3.10 (a) Sodium versus Chloride, (b) Calcium versus Chloride.
LSFW intermediate between Forebay well and the HSFW in both (a) and (b).

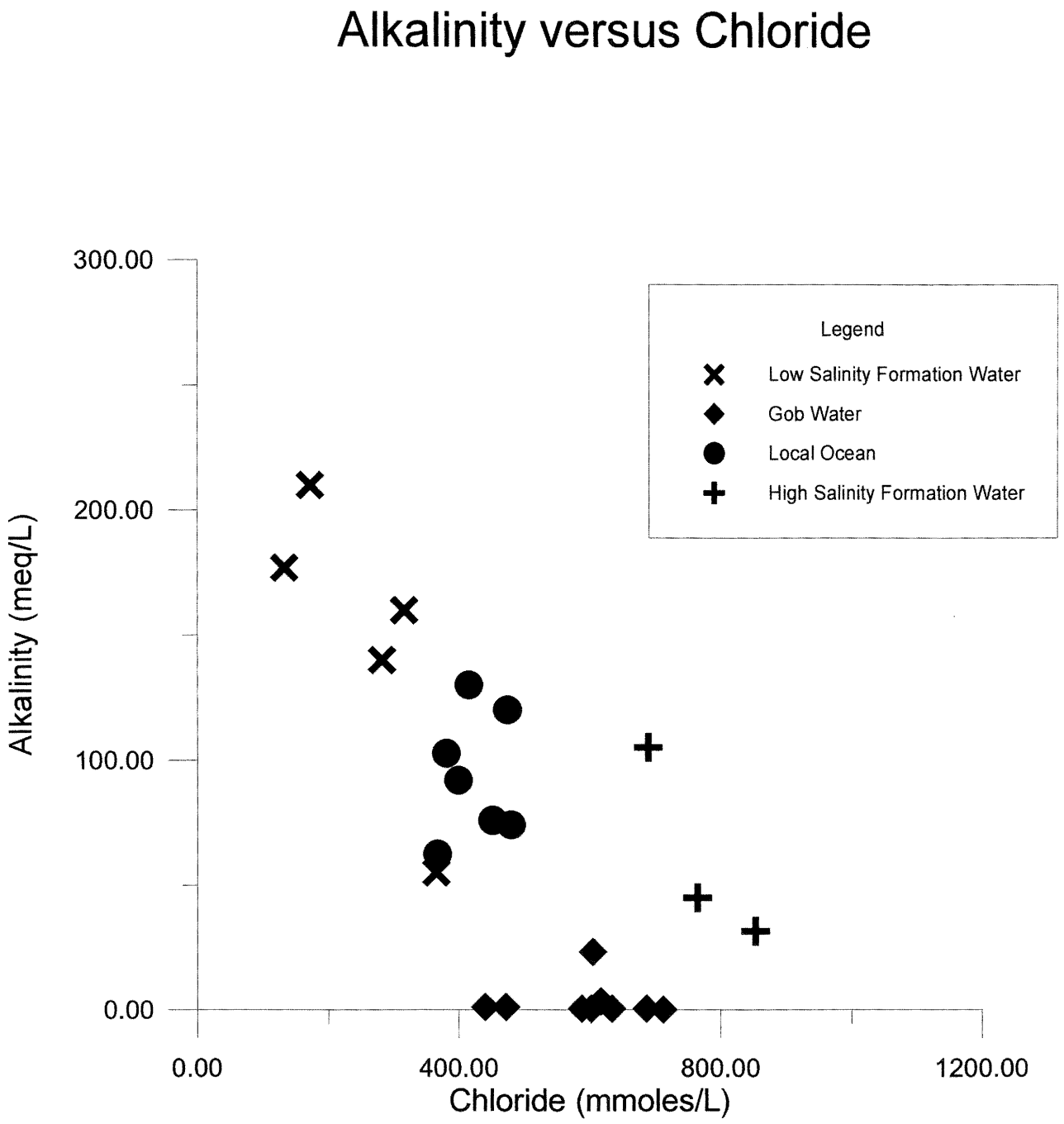

Figure 3.11 Alkalinity (carbonate) versus Chloride (mmoles/L).
Gob water samples have very little carbonate alkalinity.

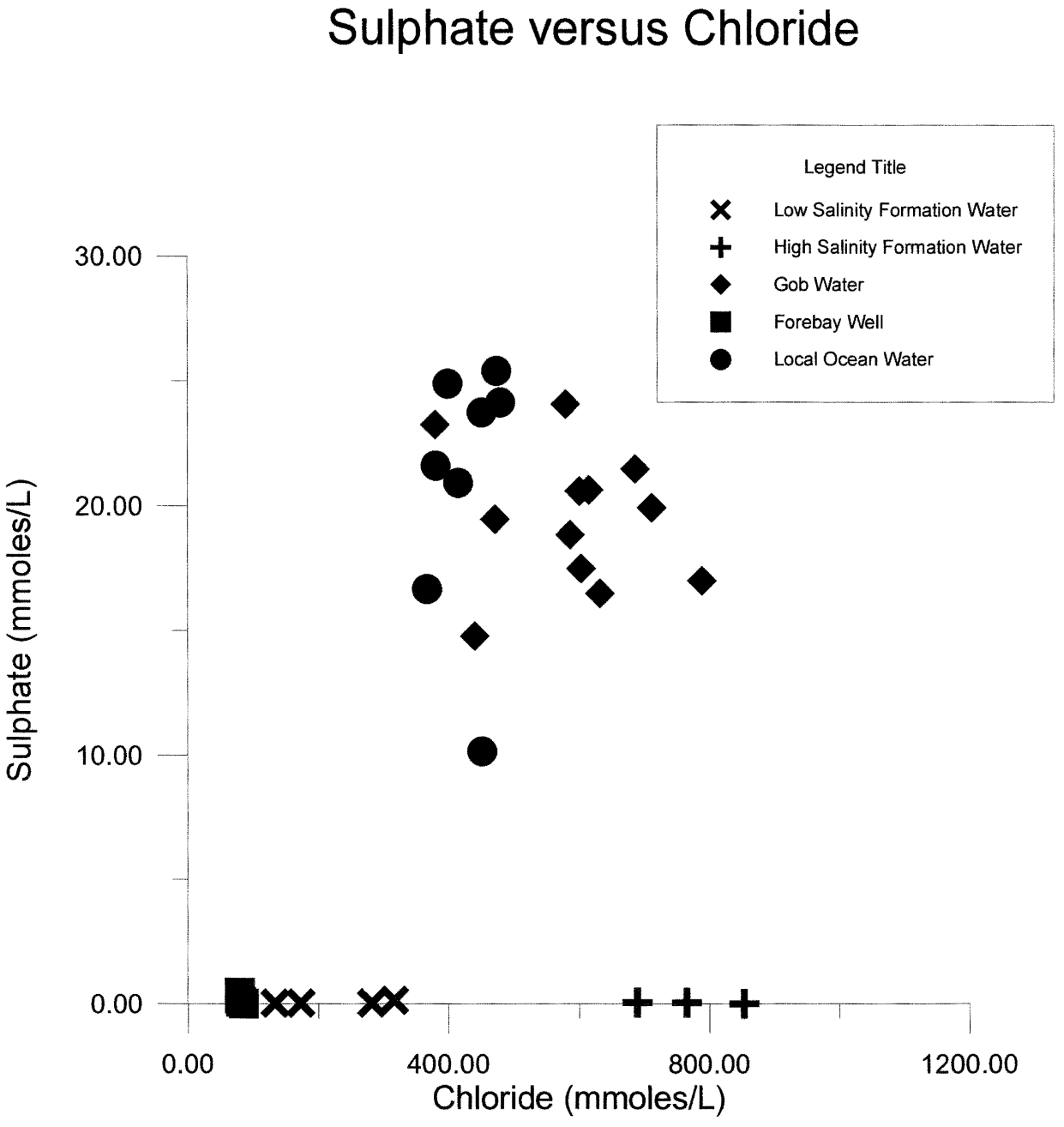

Figure 3.12 Sulphate (mmoles/L) versus Chloride (mmoles/L). Gob water samples are enriched in sulphate with respect to forebay well and formation water samples.

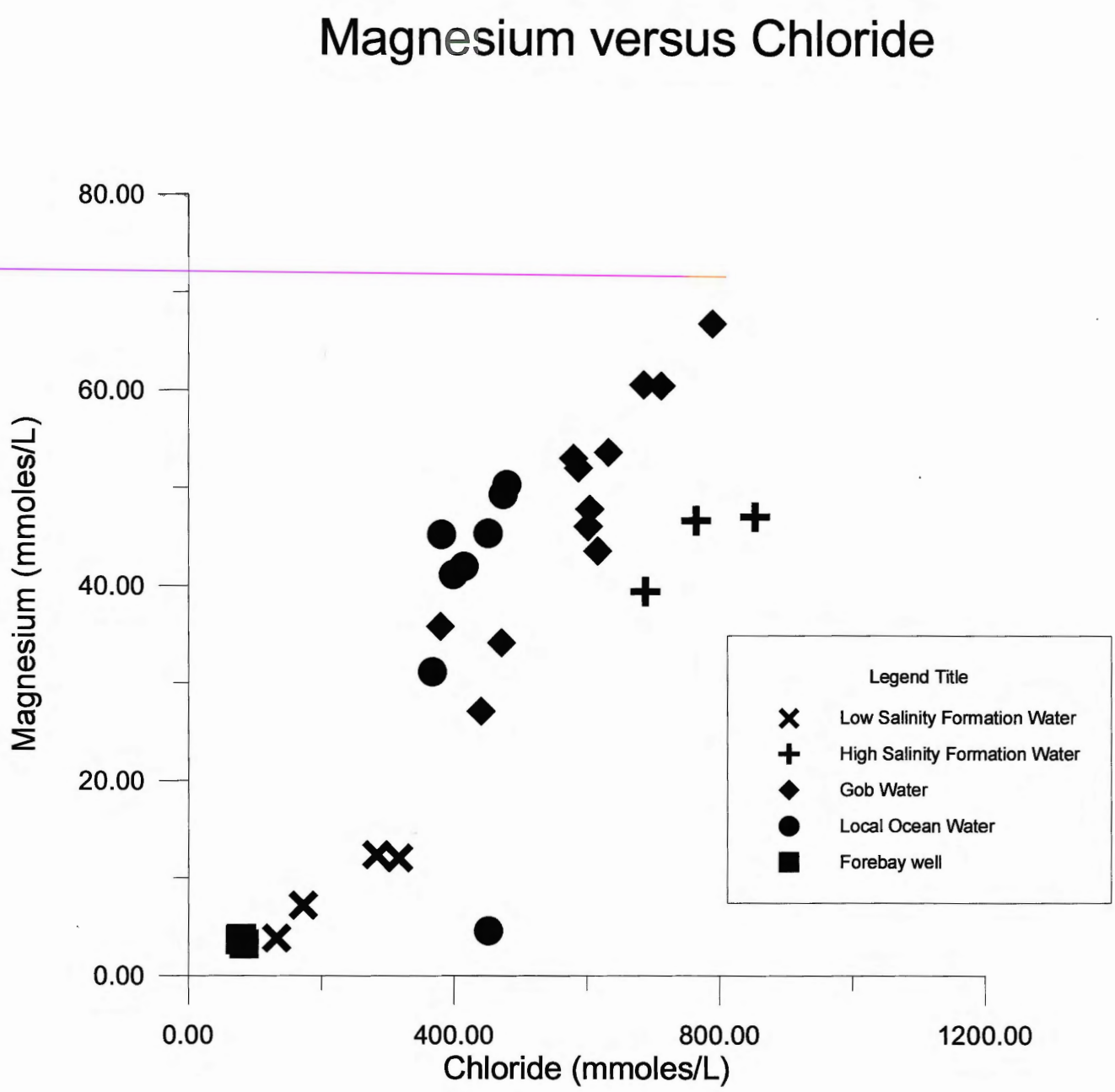

Figure 3.13 Magnesium (mmoles/L) versus Chloride (mmoles/L).
Gob samples surpass the magnesium concentrations of the high salinity formation water samples

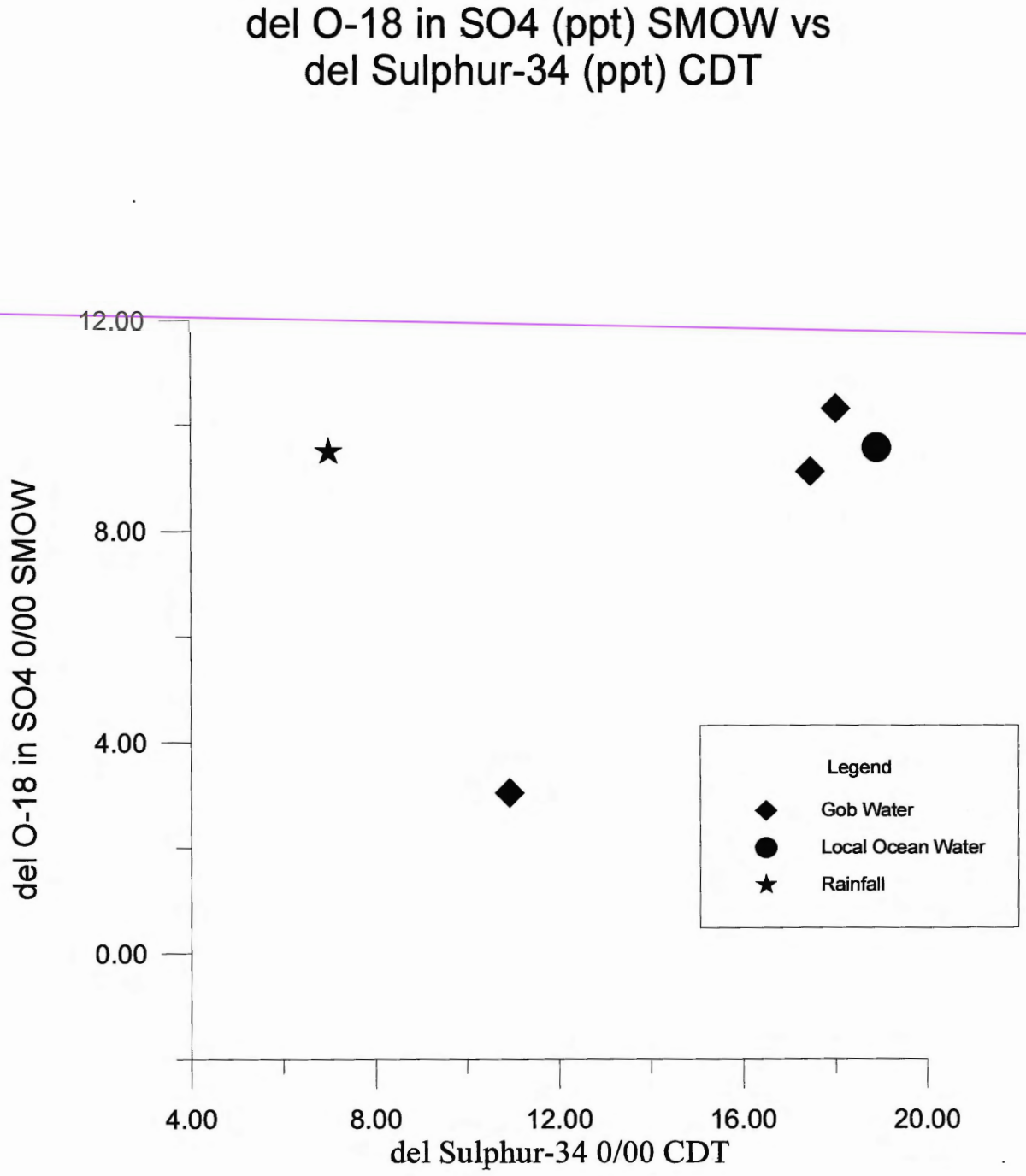

Figure 3.14 del O-18 in SO4 (ppt) versus del Sulpher-34 (ppt). Gob water samples show a range in del O-18 and del 34-S values. SMOW (Standard Mean Ocean Water), CDT (Canon Diablo Meteorite).
* Rainfall from CBDC Phalen Colliery Risk Assessment Report (1994).

CHAPTER 4 ROCK BODY

4.0 Introduction

Information on the geology of the rock body overlying the Hub coal seam was collected by the N.S. Department of Natural Resources (lithology logs for core P6), CBDC (roof boreholes) and the Geological Survey of Canada (gamma ray log, calculated salinity profile).

4.1 Drill Core Data

4.1.1 Drill Hole P6

Drill Hole P6 intersects the Point Aconi Seam (106.07 m), Lloyd Cove seam 1 (164.59 m), 2 (170.08 m) and 3 (173.74 m), the main Hub seam (233.17 m) and lower Hub seam (240.49 m) (Department of Natural Resources 1979). The cored interval of P6 (Figure 4.1) consists of two sandstone bodies separated by a mudstone. The upper sandstone is generally massive (minor cross laminae) and rich in carbonaceous material. There is an 0.18 m thick intraformational conglomerate at 220.83 m with 5 cm shale clasts, and a 0.37 m conglomerate at 228.63 m with a maximum clast size of 0.6 cm. The mudstone layer (0.24 cm thick) contains calcareous nodules and is cut by the overlying unit. The lower sandstone underlying the mudstone layer is 2.56 m thick, massive with minor cross laminations and contains a coaly shale (1.25 cm thick dipping 6° - 7°) near the base. The main Hub seam is intersected at 231.98 m and is generally homogeneous with minor streaks and bands of pyrite throughout. There is an irregular contact with the 0.55 m thick coaly mudstone below. Root traces are very common in this mudstone and

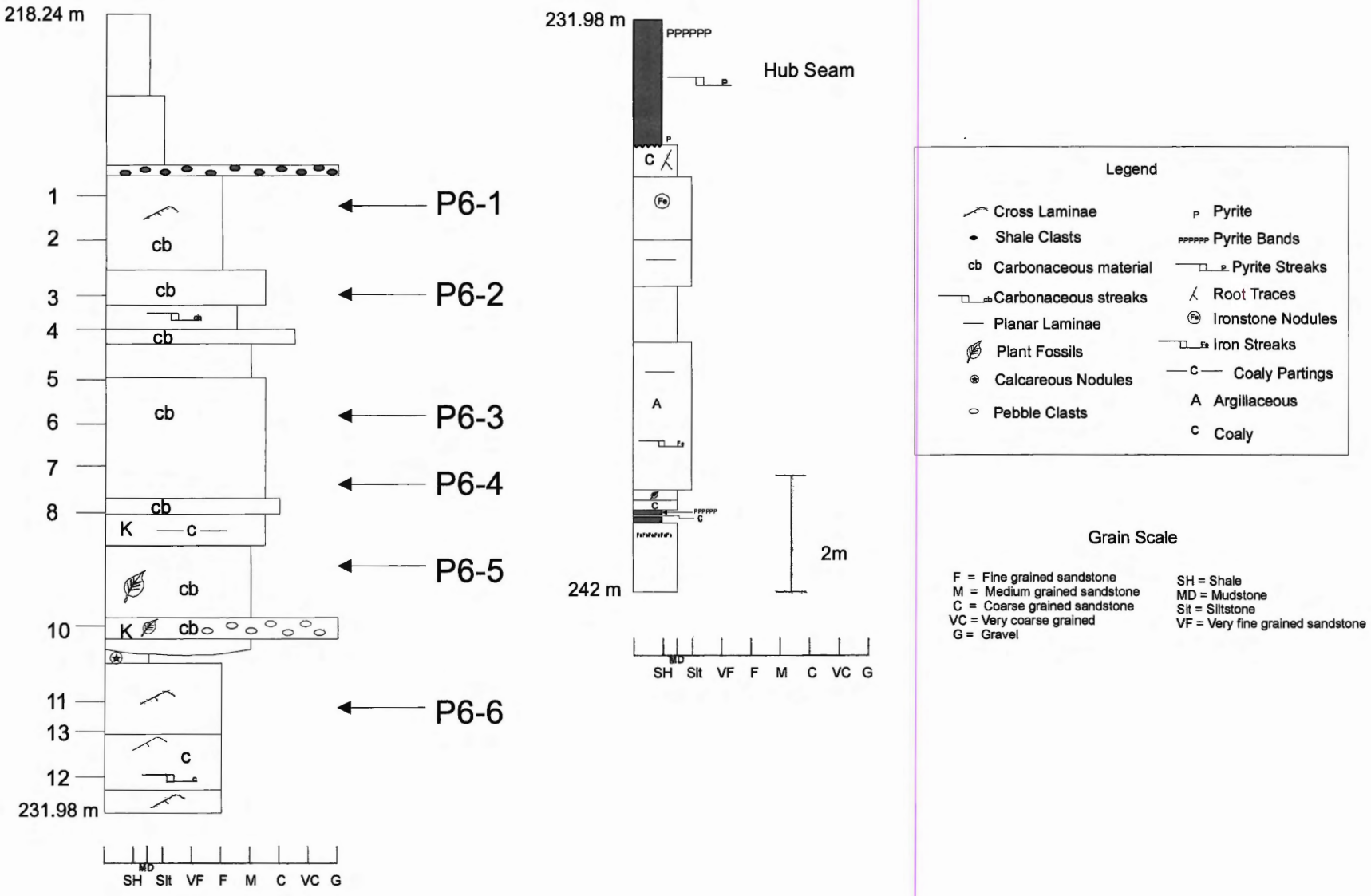

Figure 4.1 Lithology log of core P6 (N.S. Department of Natural Resources 1979). Thin section locations are indicated by labels P6-1 through to P6-6. Porosity and permeability measurements are indicated by the numbered tick marks on the left side.

the basal 0.30 m is a mixture of mudstone and siltstone. The lowest unit in the core is siltstone which contains small ironstone nodules.

A gamma ray log of P6 (Figure 4.2) shows a strong peak at approximately 230 mbkb that divides the sandstone into two distinct bodies that are marked by a mudstone visible in core P6 at approximately 230m. This depth also corresponds to the approximate division between the low and high salinity waters on the calculated salinity profile. There is a 1.3 m shift between the gamma ray log and the actual core (Schimeld 1997).

4.2 Roof Borehole Data

Boreholes between 6 and 18 m long were drilled into the roof above the coal at various locations within the Colliery. The purpose of the boreholes is to collect data on the roof quality. Twenty-nine of these boreholes have intersected a sandstone body. The borehole logs have been corrected for dip and the angle of the borehole. The stratigraphic sections indicate grain size (mudstone, shale, siltstone, sandstone - fine, medium, coarse) and the presence of plant fossils, rock fragments and/or ironstone nodules. No porosity or permeability data are available for the roof boreholes. A generalized cross section was constructed using boreholes 50, 42, 43, 40 and core P6 combined with knowledge of the overlying formation water chemistry (Figure 4.3a & b). The mudstone unit identified in core P6 can be correlated approximately 70 m in a direction roughly perpendicular to the paleoflow.

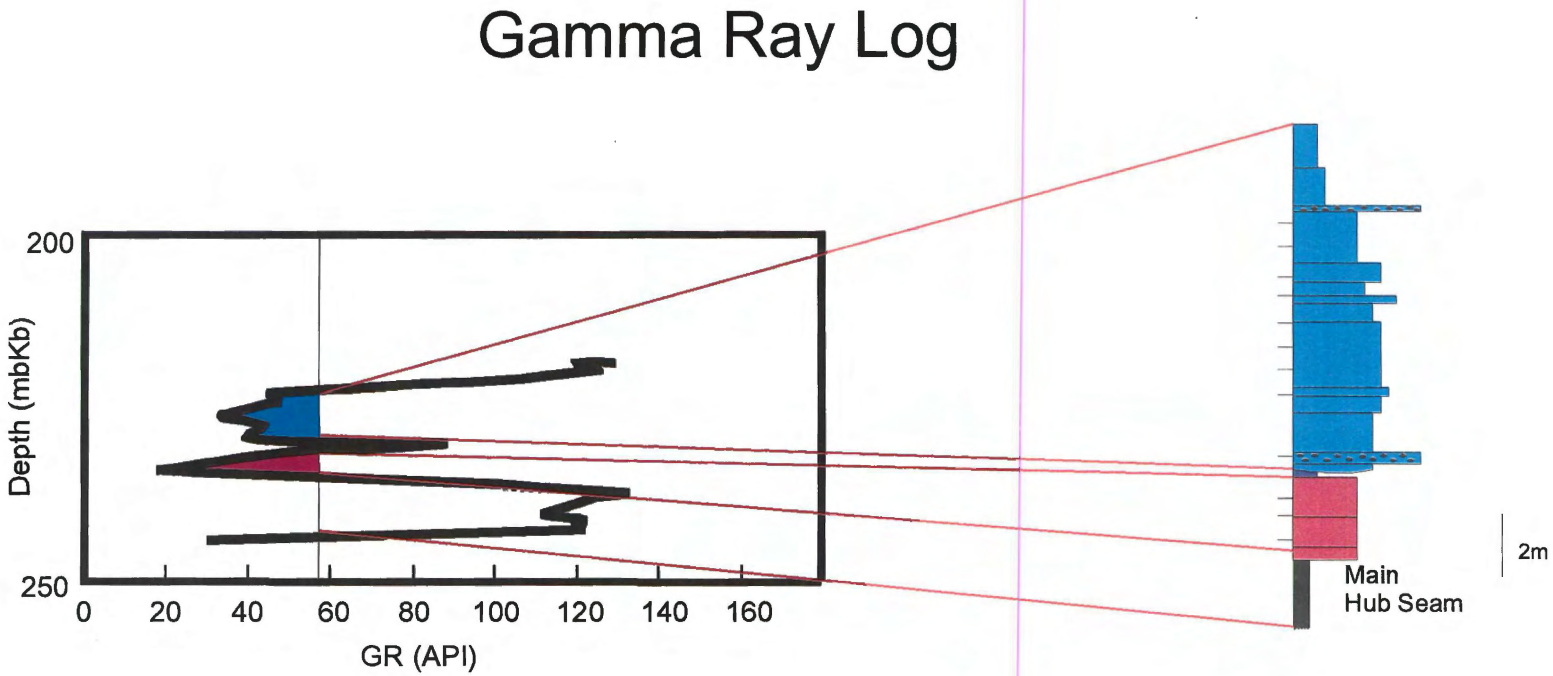

Figure 4.2 Gamma ray log for drill hole P6, correlations are shown in red. Note there is a 1.3 m shift between gamma ray log and core P6.

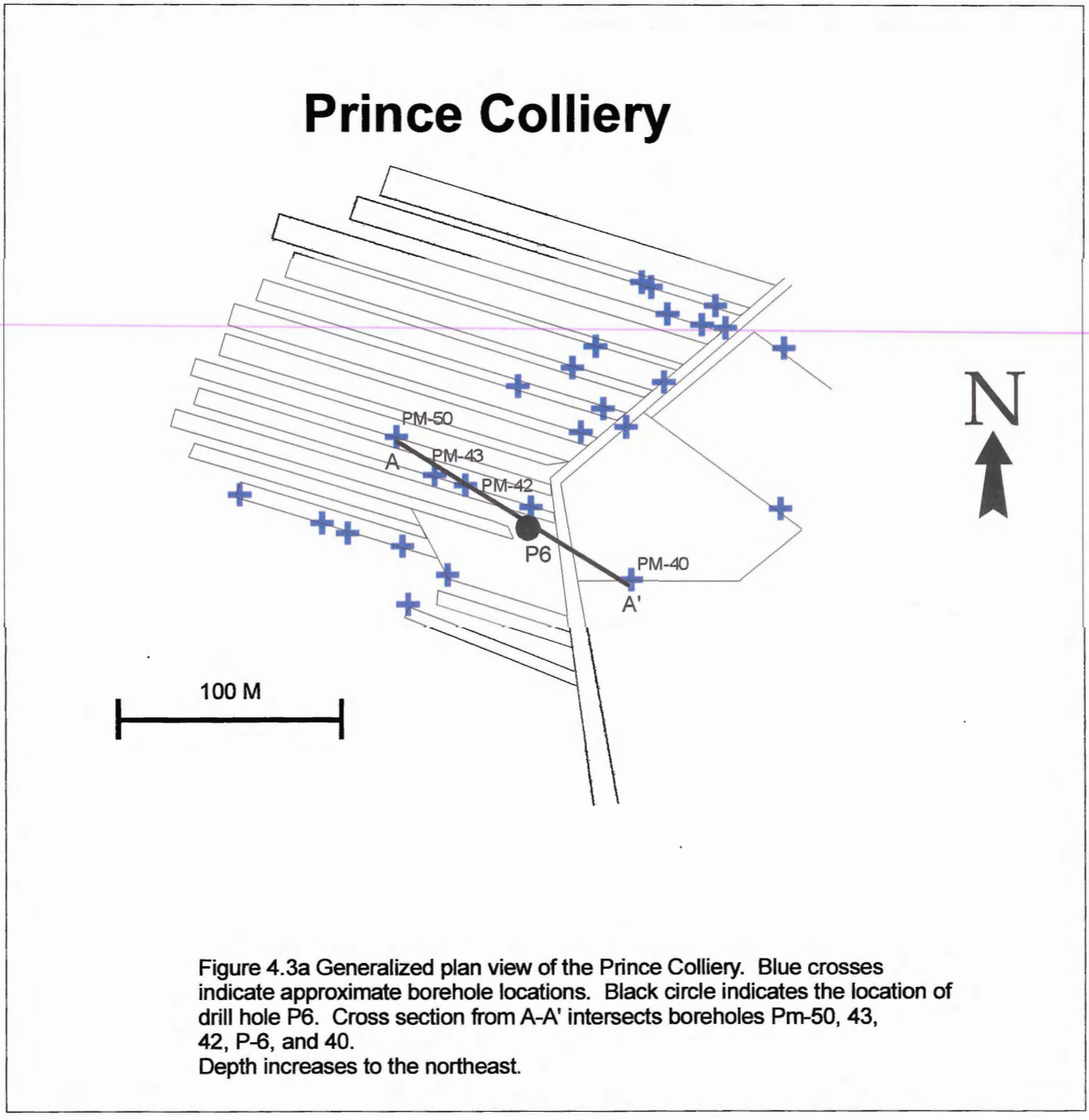

Figure 4.3a Generalized plan view of the Prince Colliery. Blue crosses indicate approximate borehole locations. Black circle indicates the location of drill hole P6. Cross section from A-A' intersects boreholes Pm-50, 43, 42, P-6, and 40.
Depth increases to the northeast.

4.3 Porosity and Permeability Data

Porosity and permeability measurements were completed for core P6 (Core Laboratory's Canada; Table 4.1). Porosity in P6 is fairly constant at about 13% but permeability is more variable (Figure 4.4). The upper sandstone has a distinctly higher permeability (up to 20.0 mD., vertical permeability) than the lower sandstone body.

4.4 Petrographic Data

Petrographic descriptions were completed for the six samples taken from drill core P6 (Figure 4.1)

4.4.1 Summary of Petrographic Data

The sandstone consists predominatly of quartz with common lithic grains (e.g. mica, metamorphic grains; average 15%). The grain size average ranges between 0.1 and 0.54 mm. Grains in thin section are sub-angular and sub-rounded with low apparent sphericity. Pore spaces average between 8 - 20 % in thin section. Pore shape is generally irregular but some pores are elongate and well formed. The inferred diagenetic history is similar for all thin sections (Figure 4.5).

There is a striking difference between two groups of thin sections. Thin sections P6-1 and -6 are well sorted with average grain sizes of 0.1 - 0.2 mm. Silica has been deposited as overgrowths on the boundaries of quartz grains (App. 2, Figure P6-1a).

Thin sections P6-2 to -5 have a more angular grain shape and larger average grain (0.5 - 0.54 mm) and pore sizes (as large as 1.5 mm). Good connectivity between pores

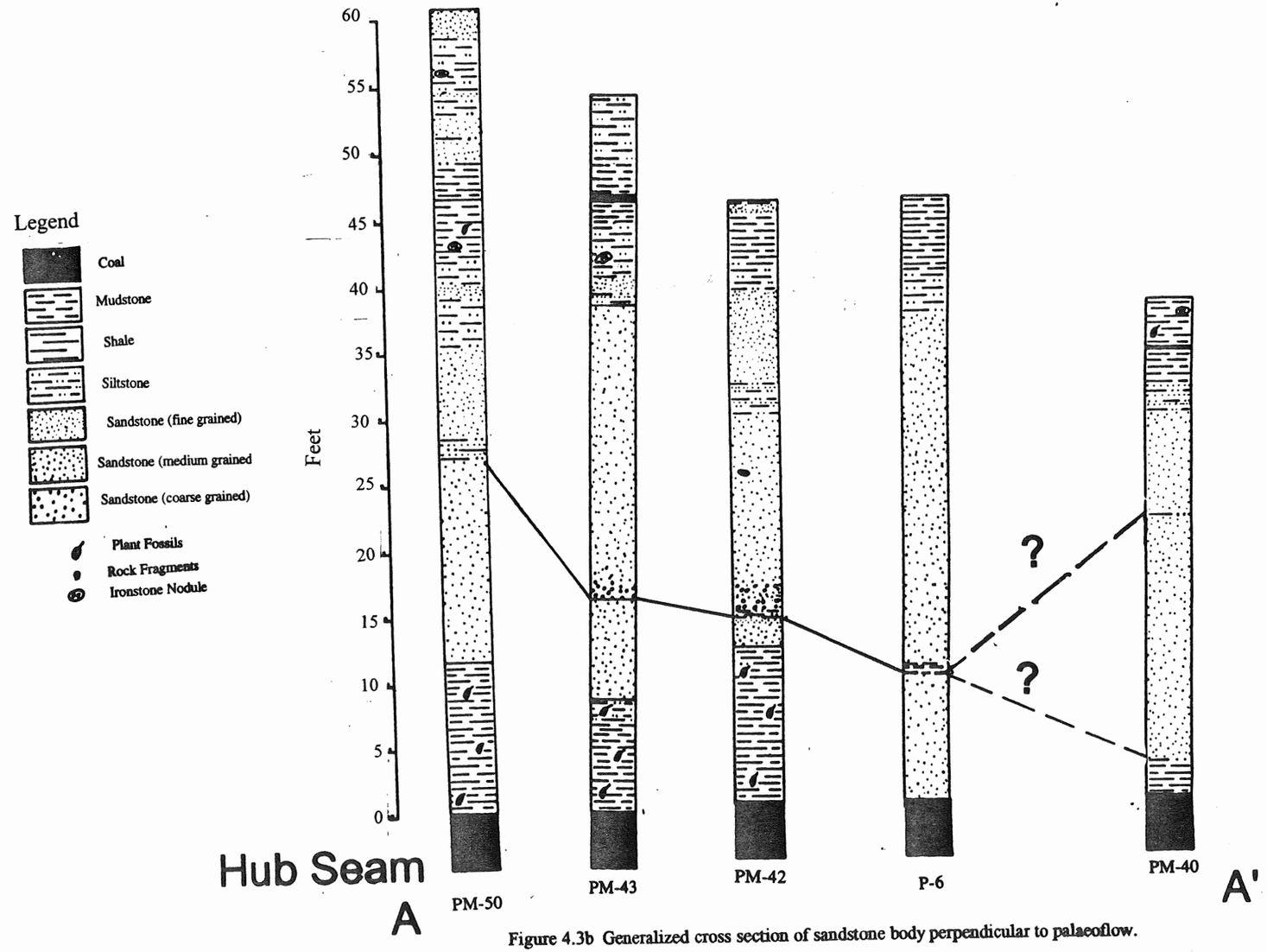

Figure 4.3b Generalized cross section of sandstone body perpendicular to palaeoflow.

Sample	Porosity (%)	Vertical Permeability (mD.)
1	14.9	3.8
2	13.5	0.41
3	13.9	2.11
4	14.1	20.9
5	16.9	18.7
6	14.9	14.9
7	14.8	4.08
8	15.8	7.43
9	15.5	no data
10	12.3	10.6
11	11.4	0.2
12	13.9	0.67
13	11.8	1.33

Table 4.1 Porosity and vertical permeability measurments completed for core P6.

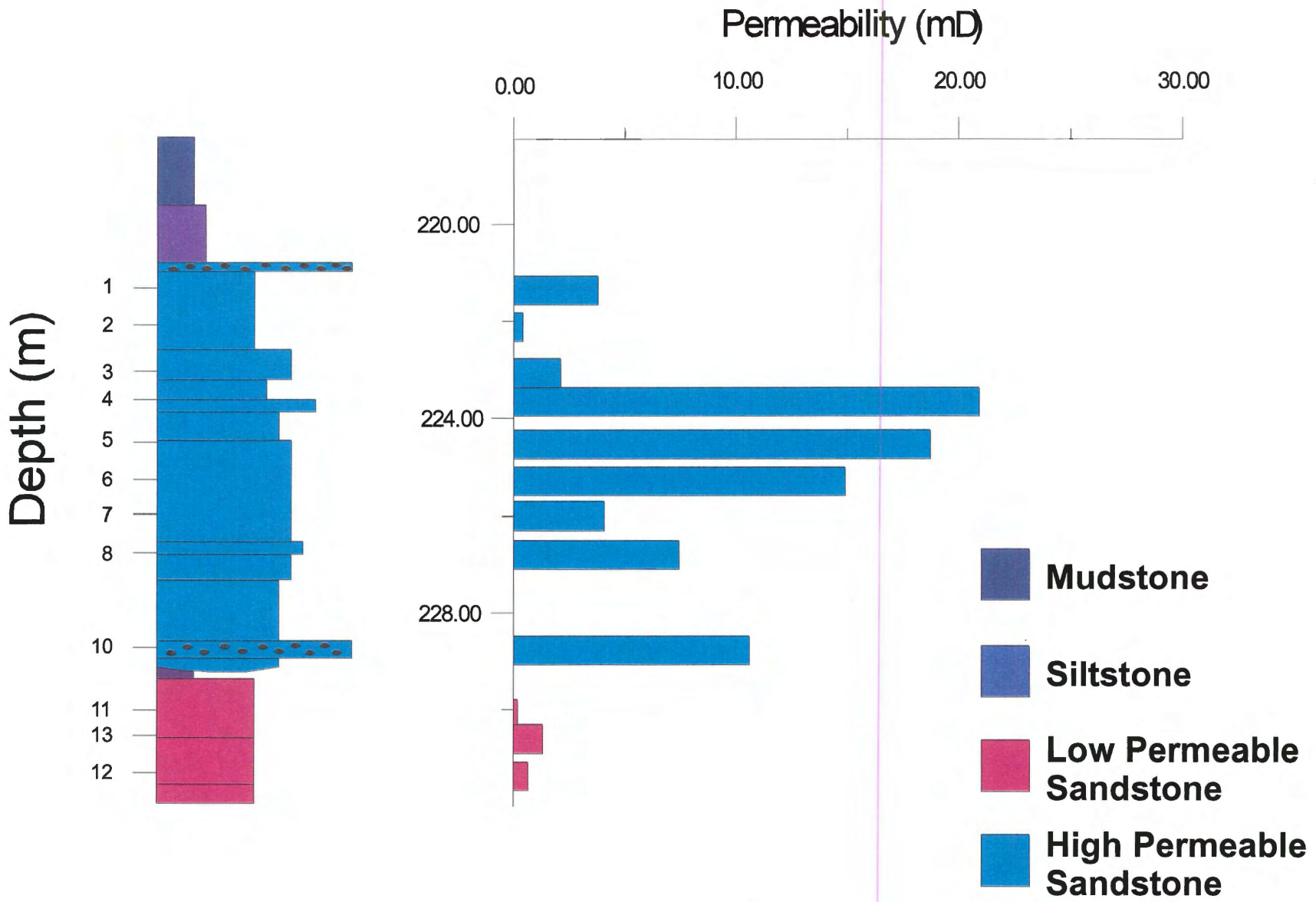

Figure 4.4 Permeability variation within core P6. Tick marks on lithology log indicate locations of permeability measurements.

Diagenetic History

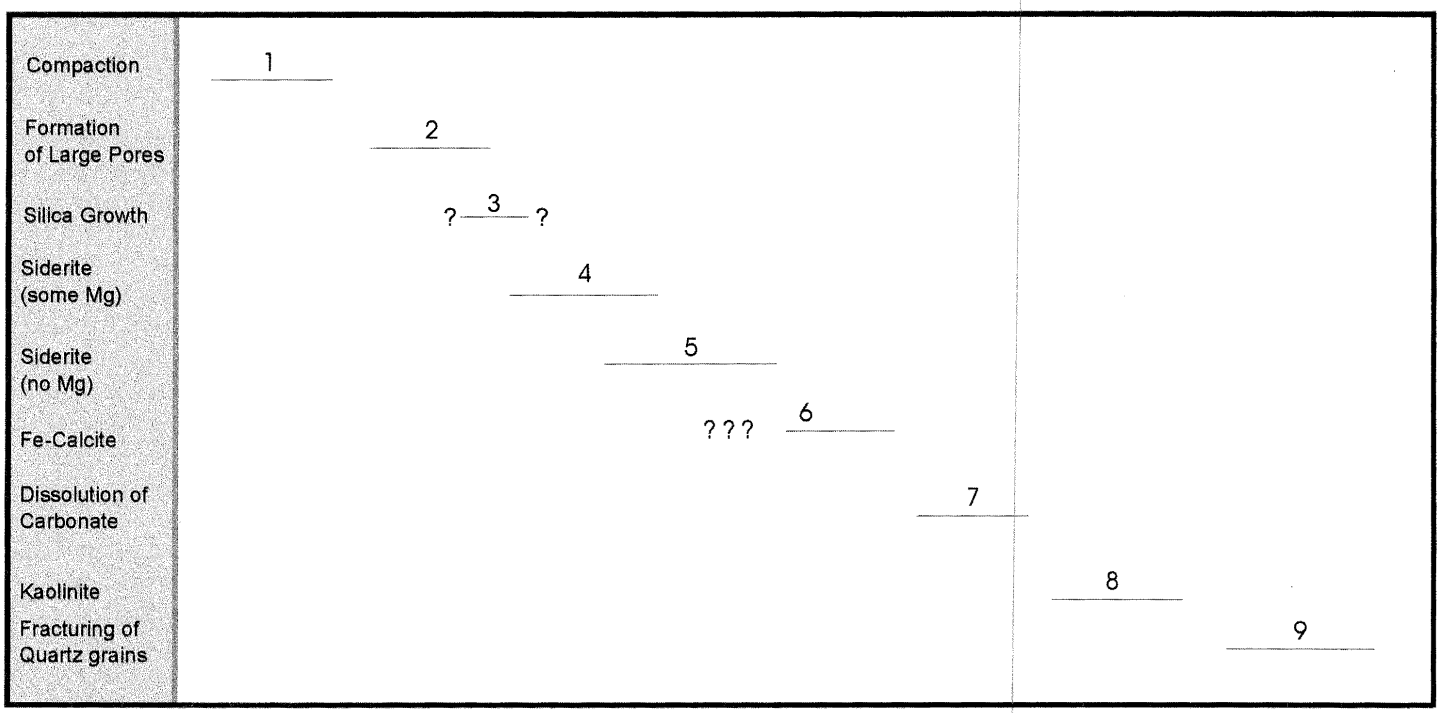

Figure 4.5 Diagenic history of thin sections from core P6.

can be recognized in thin section (App. 2, Figure P6-4a). Thin sections P6-2 to -5 contain siderite (App. 2, Figure P6-2a) varying in size between small clusters (< 0.1 mm) and euhedral grains (0.4 mm). The siderite fills some pores but generally is present around pore boundaries as individual crystals. Thin section P6-6 also contains this carbonate, but it is pore filling and more abundant and darker colored (App. 2, Figure P6-6a) than in other thin sections. In thin section P6-6 the siderite contains very little Mg as compared with P6-2. The more euhedral siderites are compositionally zoned with varying amount of Mg (App. 2, P6-2b).

4.5 General Conclusions

A 24 cm mudstone divides the channel sandstone body, overlying the Hub coal seam, into two units, a large upper sandstone (8.56 m) and a smaller lower sandstone (2.56 m). The lower sandstone can be correlated approximately 70 m from core P6 to borehole PM-50 (Figure 4.3b). The lithology logs were not detailed enough to correlate with units down dip.

The sandstone units are mineralogically very similar in core P6, the main differences between them are the amount of permeability and their size. The upper sandstone is larger and more permeable than the lower sandstone (Figure 4.4). This difference in permeability can be seen in thin sections P6-1 and P6-6. Both thin sections are from the topmost portion of the upper and lower sandstone units respectively. Although these two thin sections are similar in grain size, degree of sorting, and maturity, the permeability of P6-1 is up to 19 times greater than the permeability measured for P6-6 (up to 3.8 and 0.2 mD vertical permeability respectively).

CHAPTER 5 MODELING

5.0 Introduction

Two hypotheses were tested using the hydrochemical program Hydrowin: (1) that the gob waters are a mixture of high and low salinity waters from the overlying strata, and (2) that the LSFW are the mixing product of high (HSFW) and low (Forebay well) salinity end-members. To test hypothesis (1), I mixed selected high and low salinity formation waters to approximate specific gob waters using Hydrowin. Water samples were mixed from similar depths (Figure 5.1). I also attempted to quantify this mixture using a Piper plot.

To test hypothesis (2), two modeling steps were completed:

(a) Groundwater and ocean water were mixed to confirm a groundwater/ocean composition for Forebay well and

(b) Forebay well and the most saline HSFW sample were mixed to approximate all (4) LSFW samples.

I also attempted to quantify a mixture between the HSFW and Forebay well using a Piper plot.

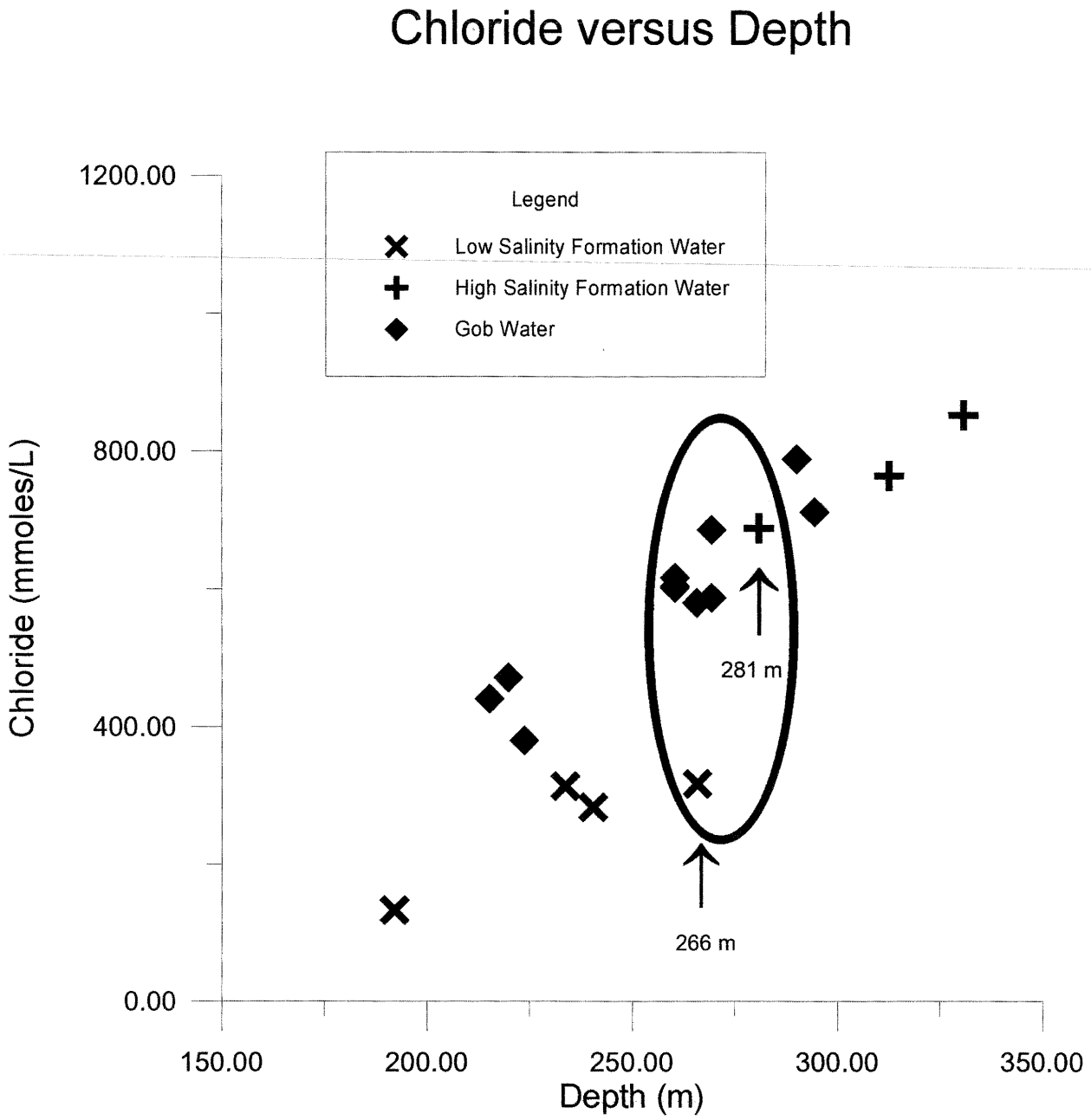

Figure 5.1 Chloride (mmoles/L) versus Depth (m). Water samples within the circle were used to test hypothesis (2).

5.1 Hydrowin

5.1.1 Method

Hydrowin mixes two selected waters (i & j) in 2% increments until the best possible match is made using the specified ions. The closest match is indicated by the smallest Euclidean distance according to the following equation:

$$d_{ij} := \left[\frac{\left[\sum_{k=1}^{n} \left(x_{ik} - x_{ij} \right) \right]}{n} \right]$$

where x_{ik} is the kth variable measured on sample i, x_{jk} is the kth variable measured on sample j, and n denotes the total number of specified parameters (e.g. species, ions). The optimum sample concentration is reached when d_{ij} (the distance between samples i and j) is at a minimum.

This model is limited. Because mixing is done in 2% increments, the equation puts more weight on species with high concentrations and the thermodynamic and solubility relations of the two solutions are not considered. The consequences of these limitations are that if a better match can be made at 81.6% instead of 82%, it will not be recognized, species in small concentrations (with respect to the others selected as parameters) may not match well, and any two solutions can be mixed and provide a solution even if the answer is not chemically reasonable.

Three series of mixes were completed:

LSFW + HSFW → Gob water

Groundwater + Ocean → Forebay

HSFW + Forebay → LSFW

5.2 Gob Waters

LSFW sample CBDC 559 and HSFW sample Pr-3 were mixed using Hydrowin in an attempt to reproduce five gob water chemistries (CBDC 673, 679, 680, 681 and Dal12WB) (Figure 5.2). Ideally the end-member waters should have been sampled from similar locations. The chemistry of the low and high salinity formation water varies down dip and the chemistry of the gob waters is a function of the area they drain. The end-members selected are within 15 m depth, but their spatial locations within the mine are more varied (up to ~150 m). Therefore, the selected end-member samples are only approximate.

Mixtures were optimized using Na, Cl, Mg, and Ca as parameters. Four out of the five models most closely approximated the gob waters (Figure 5.3A, B, C & D). The Na/Cl ratios of these optimized samples were within 0.03 of the actual samples. Sample Dal-10WB was also closely approximated, but the difference in Na/Cl ratio was greater (0.07) than the other four. All samples were a good fit considering the limitations of Hydrowin.

Gob samples CBDC 673, 679, 680 and 681 are from the same tunnel (#13) but, they drain different locations (Figure 5.2), and were sampled at different times during

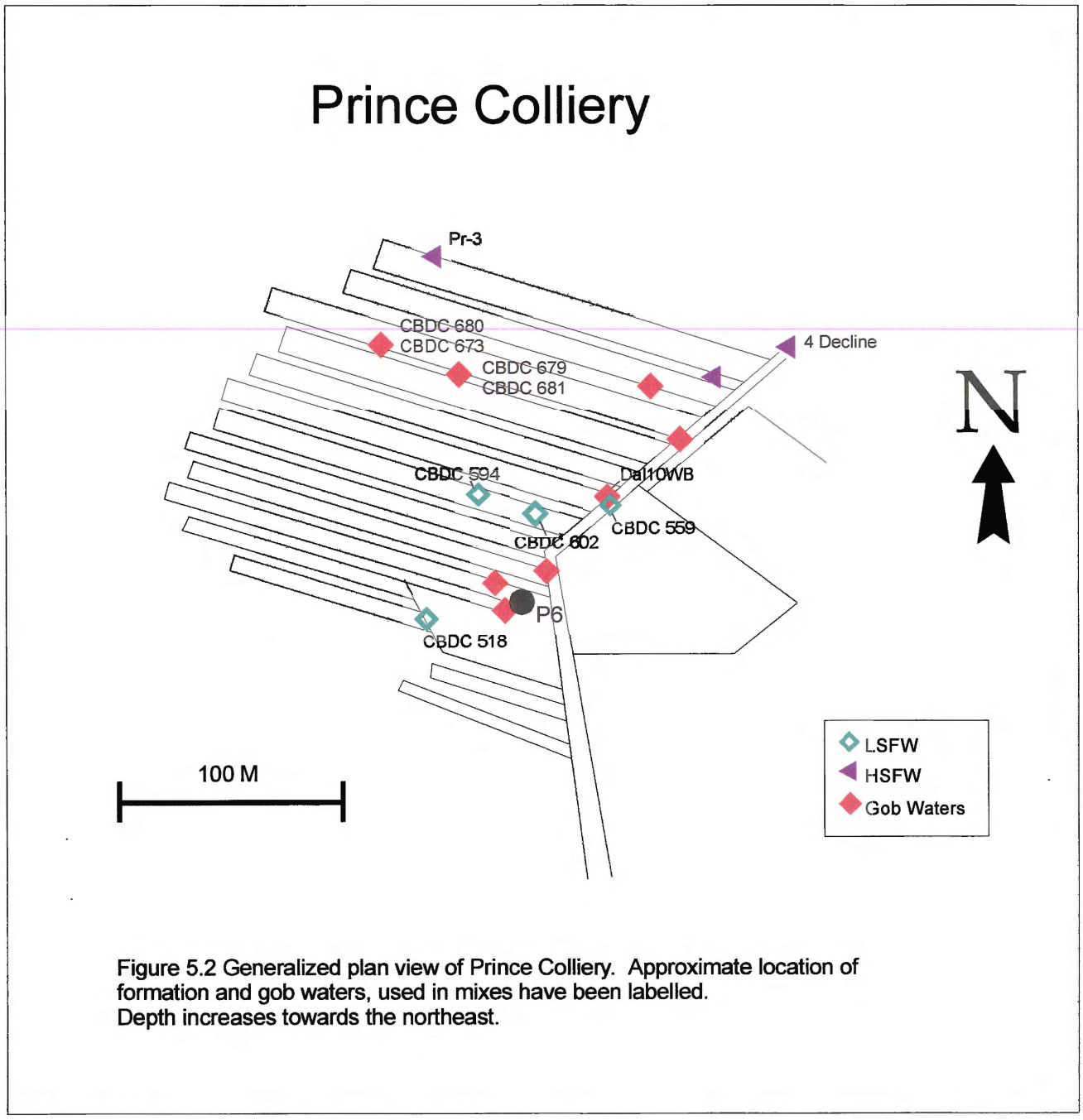

Figure 5.2 Generalized plan view of Prince Colliery. Approximate location of formation and gob waters, used in mixes have been labelled. Depth increases towards the northeast.

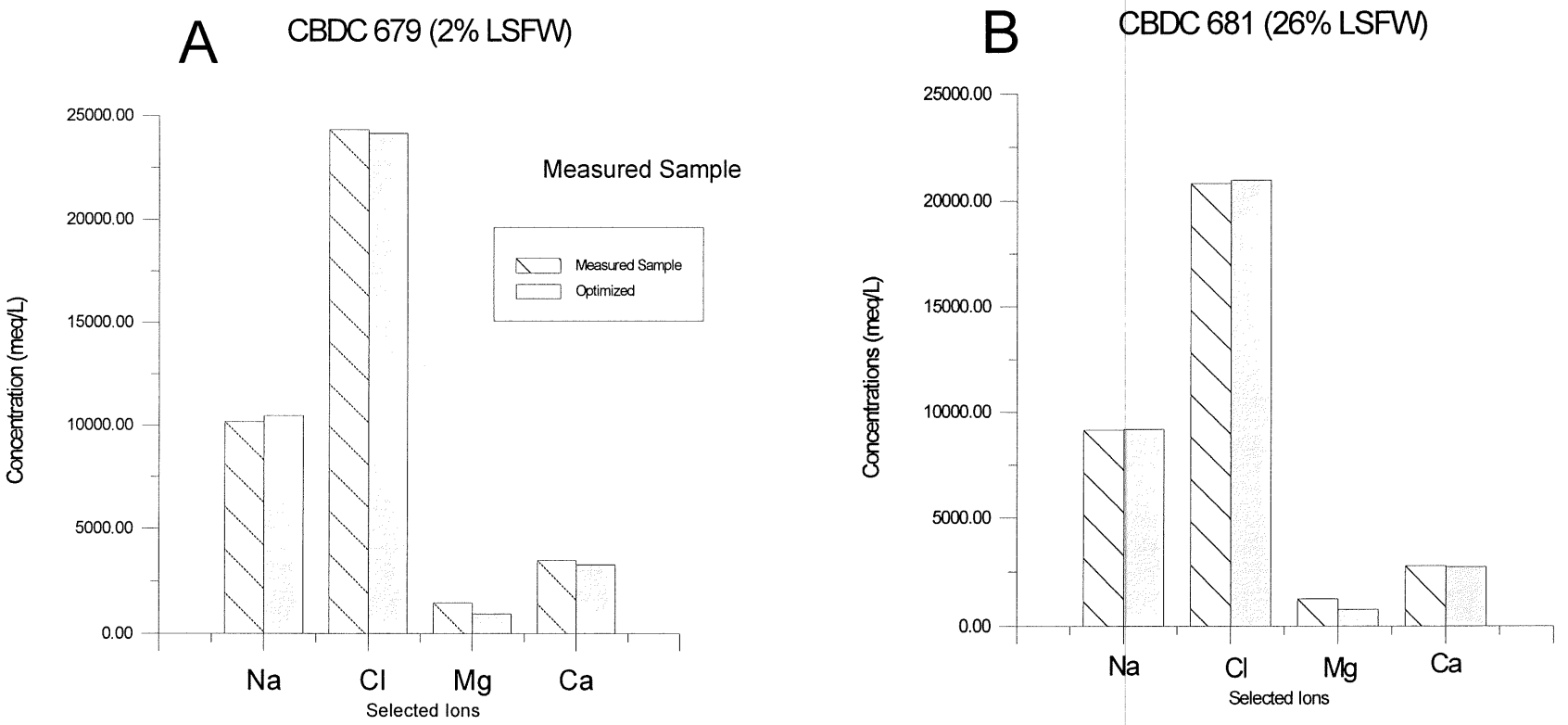

Figure 5.3 Bar charts A - E illustrate mixing results from Hydrowin. All mixes were completed using HSFW sample Pr-3 and LSFW sample CBDC 559. Five gob samples were mixed: CBDC 673, 679, 680 & 681, and Dal10WB. Refer to Table 3.2 for chemistries. Titles refer to the gob samples optimized and the percentage of LSFW is shown in brackets.

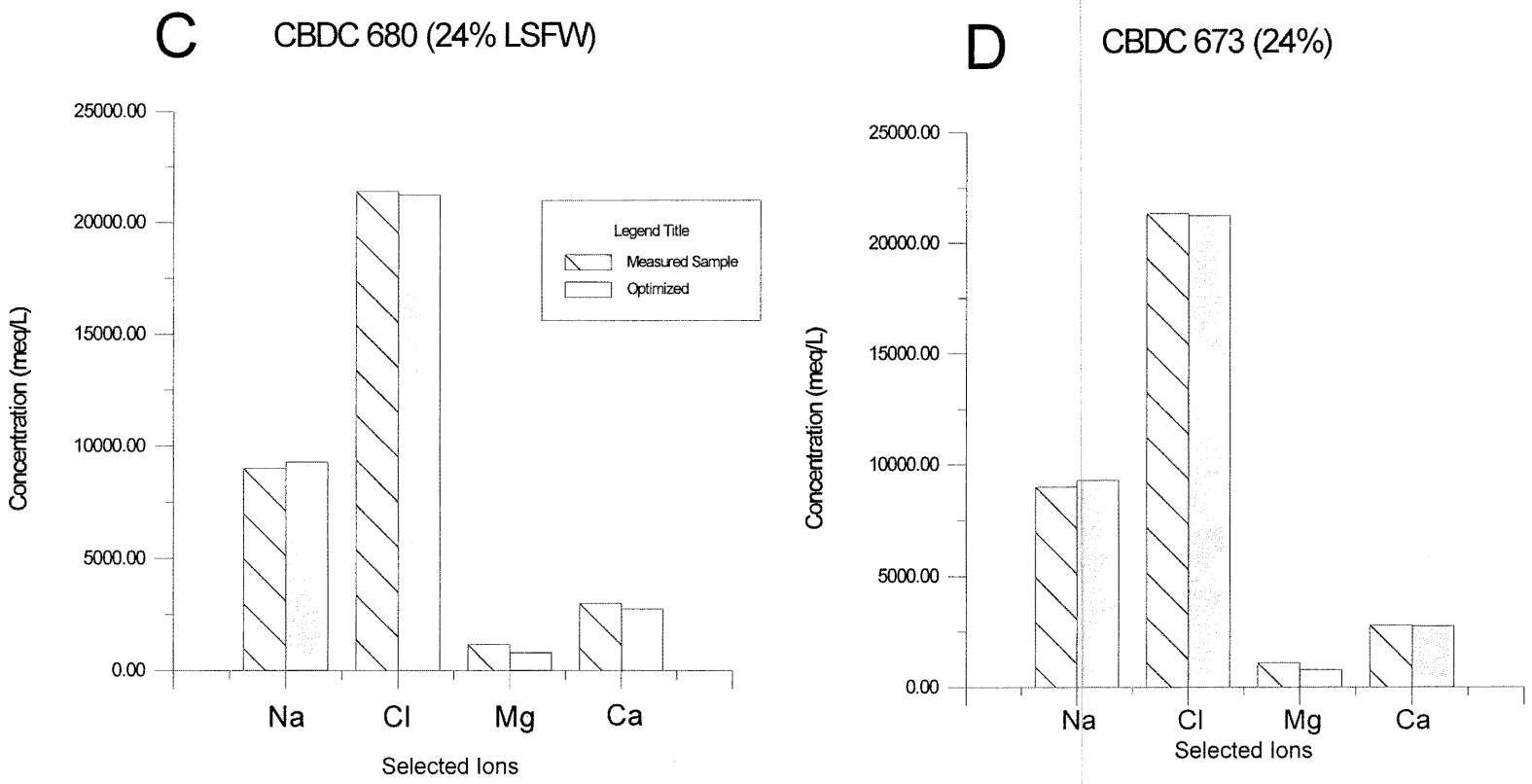
C
CBDC 680 (24% LSFW)
25000.00
20000.00
15000.00
10000.00
5000.00
0.00
Concentration (meq/L)
Legend Title
Measured Sample
Optimized
Na
Cl
Mg
Ca
Selected Ions
D
CBDC 673 (24%)
25000.00
20000.00
15000.00
10000.00
5000.00
0.00
Concentration (meq/L)
Na
Cl
Mg
Ca
Selected Ions

Figure 5.3 C & D

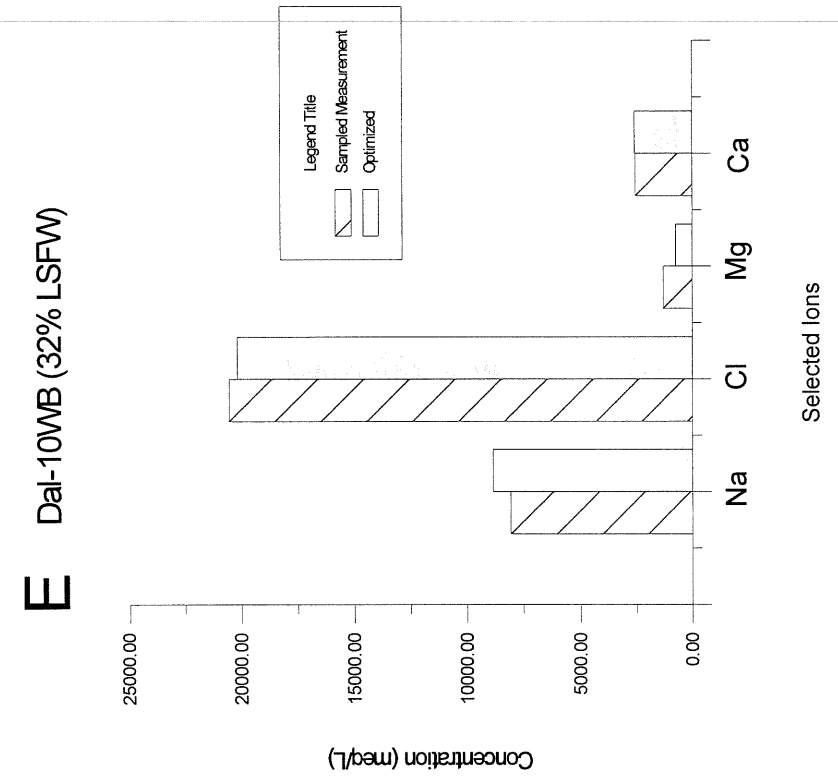
E
Dal-10WB (32% LSFW)
Legend Title
Sampled Measurement
Optimized
25000.00
20000.00
15000.00
10000.00
5000.00
0.00
Concentration (meq/L)
Na
Cl
Mg
Ca
Selected Ions

Figure 5.3E

mine development (Table 3.1). The different models for samples CBDC 679 and 681 are a result of their different chemistries. The chemistry variation between these two sample may be the result of mining in the area but without more information the cause cannot be confirmed.

For all models, the Na, Cl, and Ca concentrations were most closely approximated by Hydrowin and in each case Mg was under-calculated. These results indicate that, for the area tested, the mixture of end-members is consistent with the gob chemistry (Figure 5.3). The elevated magnesium in the actual samples supports the hypothesis that gob waters are gaining magnesium within the gob.

5.3 LSFW

The Na/Cl ratio of the least saline LSFW sample issimilar to ocean water, but is not as saline (Figure 3.7 and 3.8). Therefore, dilution of the HSFW with seawater alone would not have produced the LSFW concentrations that were present in the lower sandstone body. Most surficial groundwater is not saline enough to affect the ionic ratios of the brine, therefore, I have interpreted the dilute end-member as a dilute ocean water.

The Forebay well is located very near the seacoast and has experienced increased seawater invasion with time (Baechler 1996 pers. comm.). The Na/Cl ratio of the water is within the range measured for ocean water by CBDC offshore Cape Breton. The Forebay well is thus taken as having the approximate chemical fingerprint of the original dilute ocean-meteoric end-member. The Forebay well was modeled using a mix between 14

surficial groundwater samples, collected at Point Aconi Power Station within a square kilometre, and the ocean water sample CBDC 614. The Na/Cl ratio of this ocean water sample was closest to the Forebay well ratio and was sampled at Point Aconi.

5.3.1 Forebay well

K, Mg, Ca, Na and Cl (mg/L) were the ions selected as parameters. Only one Forebay sample (Dec 19, 1994; refer Table 3.1) was used because the concentrations of the data that were available for this study, are very similar. Hydrowin produced optimized concentrations of Forebay well which were 84% surficial groundwater and 16% ocean water (Figure 5.4). Na, Cl and Ca were the best approximated ions. Mg and K were assigned values by the program greater than the sampled concentrations.

The reason for the discrepancy is probably that the original end-members can only been approximated. These mixtures still provide a rough approximation of Forebay well composition.

5.3.2 LSFW

The most saline HSFW (4 Decline) was mixed with one sample from Forebay well (Dec 19, 1995; refer to Table 3.1) in an attempt to approximate the compositions for four LSFW samples (Figure 5.5). Na and Cl optimized concentrations most closely approximate the actual samples, but Na concentrations were consistently under-estimated (as much as 581.6 mg/L) and Cl concentrations were over- and underestimated (as much as +340.4 and -36 mg/L). The optimized concentrations for K were less than the

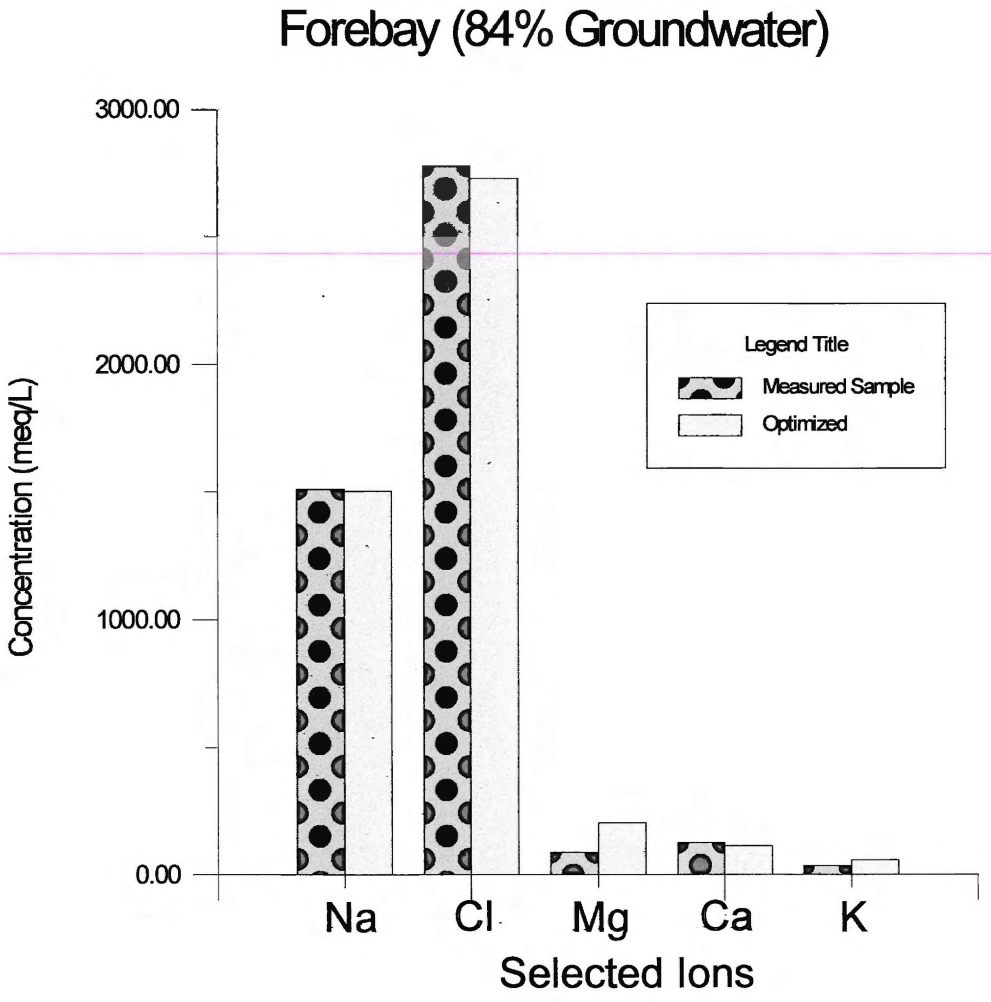

Figure 5.4 Bar chart illustrating result of Forebay mix.
Mean (harmonic) of Optimized and measured samples of Forebay well samples is shown. Mixtures were completed using various groundwater samples taken by ADI Nolan Davis and Ocean water Sample CBDC 658.

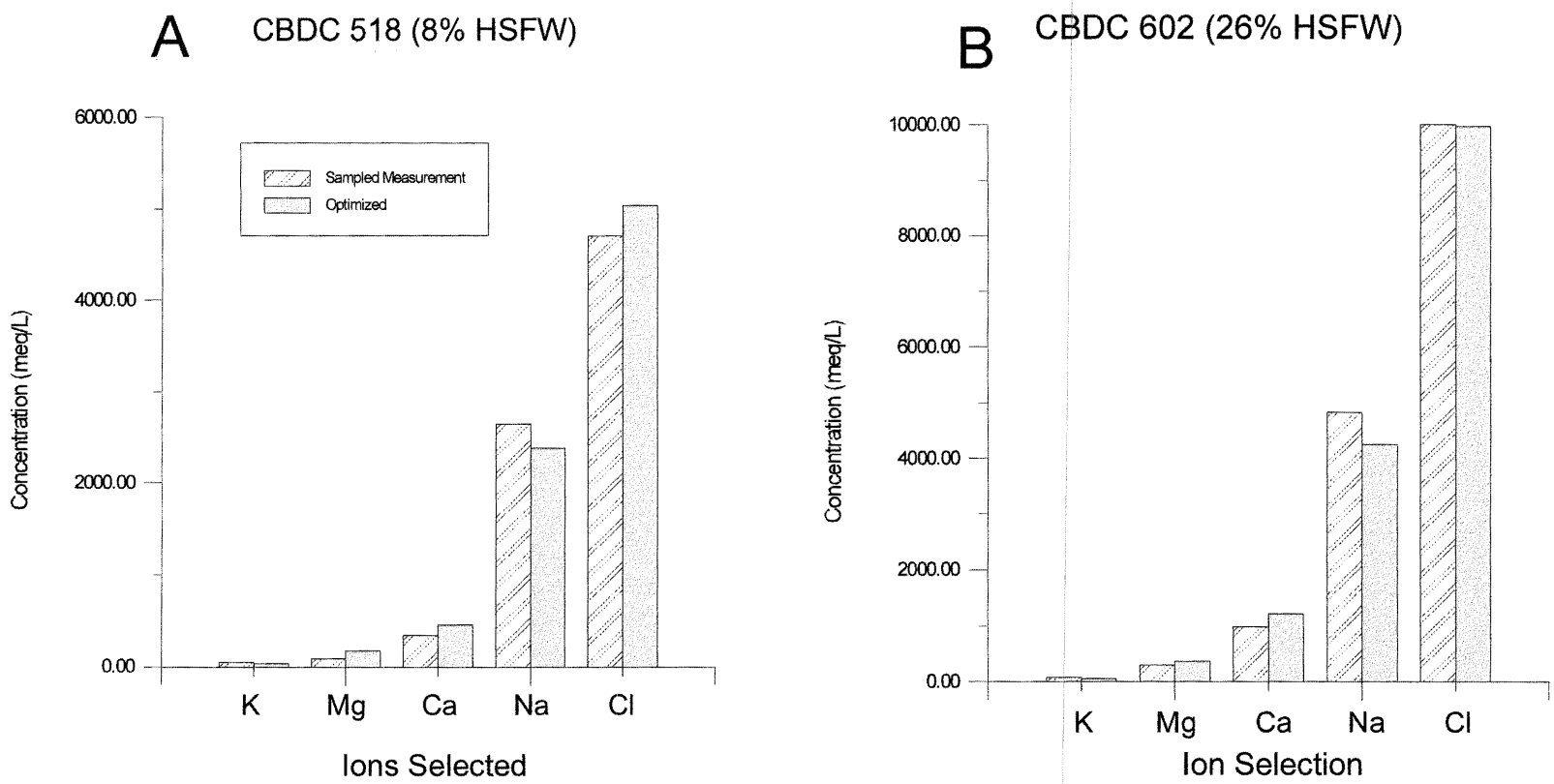

Figure 5.5 Bar charts A - D illustrate results of the LSFW mix. HSFW (Dal-Pr4D) was mixed with Forebay well to optimize the LSFW composition. Percentage of HSFW is indicated in brackets.

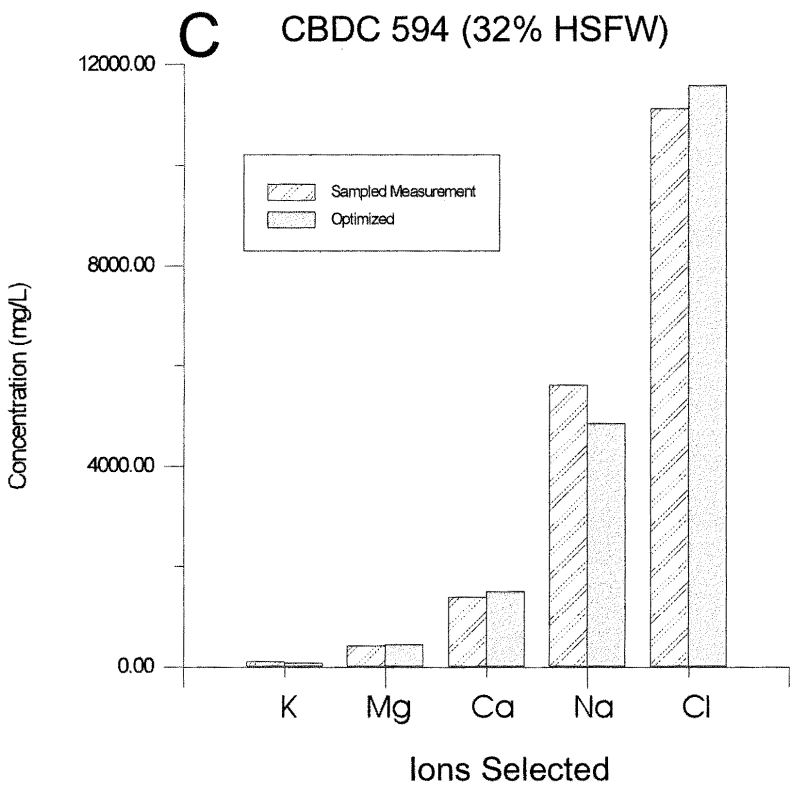
C
CBDC 594 (32% HSFW)
12000.00
8000.00
4000.00
0.00
Concentration (mg/L)
Sampled Measurement
Optimized
K
Mg
Ca
Na
Cl
Ions Selected

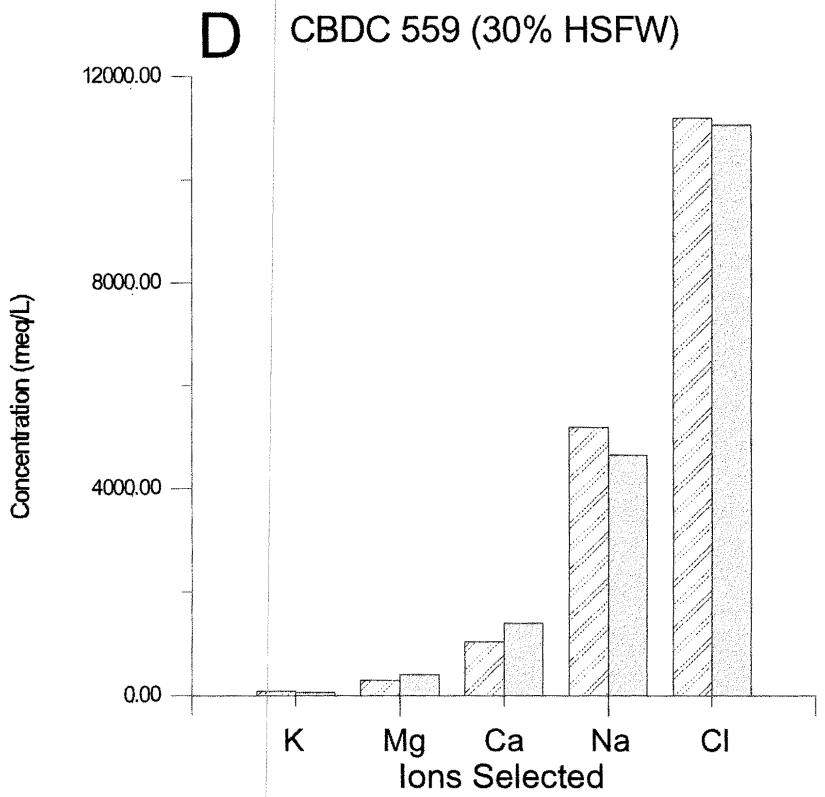
D
CBDC 559 (30% HSFW)
12000.00
8000.00
4000.00
0.00
Concentration (meq/L)
K
Mg
Ca
Na
Cl
Ions Selected

Figure 5.5 C & D

measured sample and Mg and Ca were greater than the measured sample. The variations are most likely due to the fact that the original end-members can only be approximated.

5.3 Quantitative Mixture (Piper 1944)

I attempted to quantify the mixtures of LSFW and gob waters discussed above using a Piper diagram (refer Piper 1944 for procedures). This technique is meant for "simple" mixtures between two waters (i.e. no water rock reactions). The mixtures did not satisfy the necessary criteria. This indicates that gob waters may have participated in water rock reactions while traveling through the gob (e.g. pyrite oxidation) and are therefore not "simple" mixtures. The most obvious reason for the discrepancy between the modeled and measured values for the Forebay well and HSFW mixture, is because they are only approximations of the original end-members for the LSFW.

CHAPTER 6 INTERPRETATIONS

6.0 Introduction

This study has identified two formation waters within the aquifer above the Hub coal seam, a HSFW and a LSFW. Two models are suggested for the origin of the LSFW (1) mixture with a dilute ocean (ocean-meteoric) water end-member and (2) hyperfiltration. Martel *et al.* (1997) have proposed that the HSFW (brine) is an evaporative residue. Compartmentalization of the aquifer above the Hub coal seam is evident in geophysical and chemical data. A 24 cm mudstone in combination with a 1 m thick low permeable sandstone are suggested as the barrier which separates the channel sandstone body above the Hub coal seam, and compartmentalizes the formation water (Figure 6.1).

6.1 Water Types

Waters were characterized using Br, Cl, Na and Na/Cl ratios. Na/Cl ratios have been used in other studies to characterized brines. Fontes and Matray (1993) used Na/Cl relationships to identify primary brines (formed from an evaporative residue) and secondary brines (formed by dissolution of evaporites). Bromide and chloride do not participate in water-rock reactions and can therefore be considered conservative (Hanor 1994).

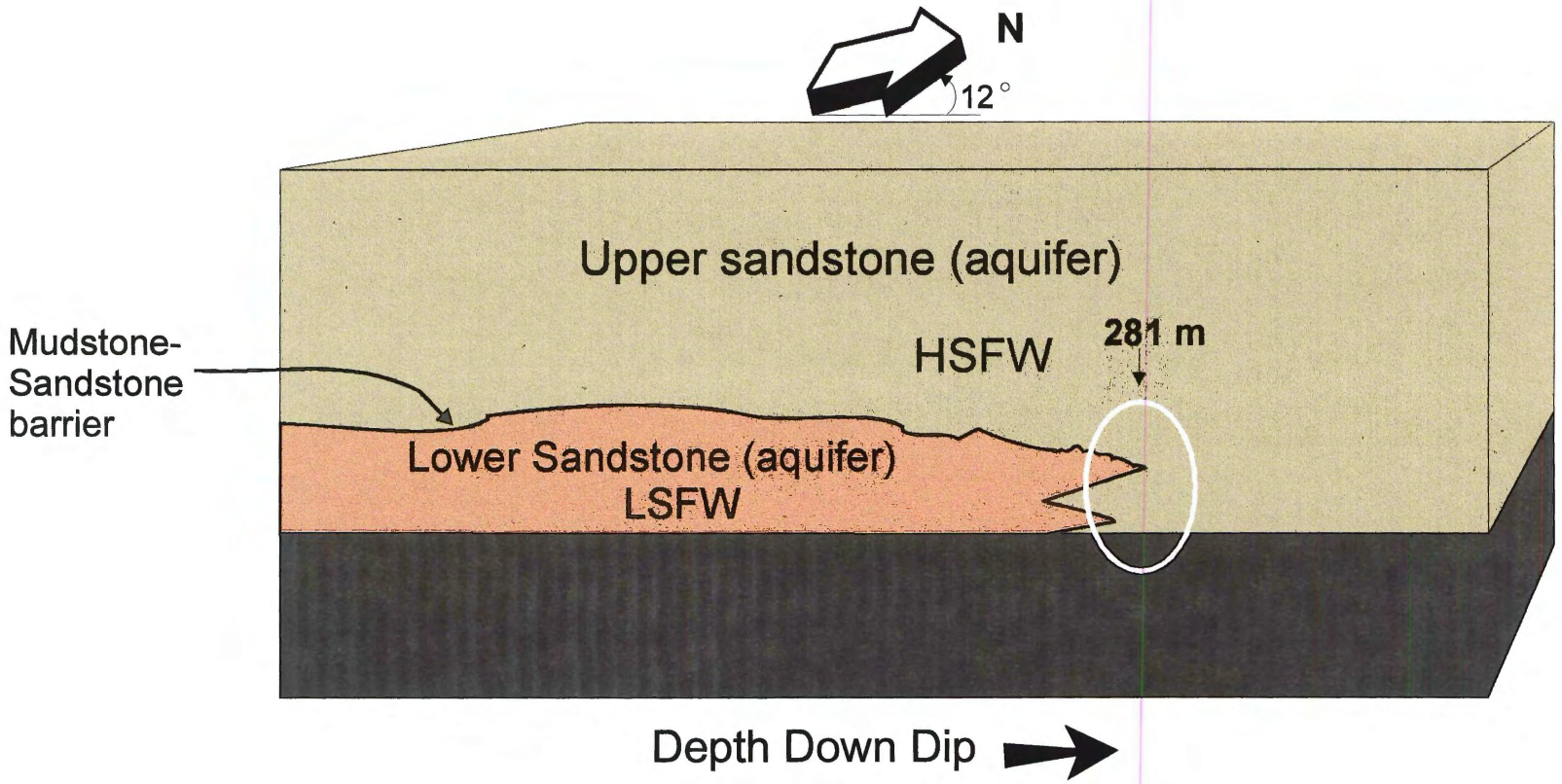

Figure 6.1 Drawing is not to scale, coal seam is inclined approximately 12 degrees from the horizontal. Cross sectional view of aquifer relationships above the Hub coal seam. The LSFW is located within the lower sandstone (aquifer) unit, directly above the Hub coal seam. The HSFW is located within a larger aquifer which partially surrounds the lower aquifer. Below 281 m depth down dip the aquifer which contians the HSFW directly overlies the Hub coal seam.

6.1.1 High Salinity Formation Water

The HSFW is enriched in bromide relative to the seawater evaporation curve, TDS is greater than ocean water and Na/Cl ratios range between 0.6 and 0.7. These characteristics strongly suggest that the HSFW is not ocean water. Martel *et al.* (1996, 1997) have proposed that the brines at Prince and Phalen Collieries are related. Both brines have similar chemistries, but the Phalen formation waters are more saline (~170 000 mg/L, as opposed to ~48 000 mg/L at Prince). The Na and Cl concentrations are linear with respect to Br and intersect the seawater evaporation curve at ~30 times the concentration of ocean water (Martel *et al.* 1997). The Na/Cl ratios of both brines are also similar and consistent with 30 times evaporation of seawater (Figure 6.2). From this information Martel *et al.* (1997) concluded that the high salinity brines at both the Prince and Phalen Collieries originated as an evaporative residue. The seawater was concentrated to 30 times its original salinity (beyond halite saturation), and then diluted to its present concentration.

6.1.2 Low Salinity Formation Water

The LSFW exhibits TDS less than ocean water (~35 000 mg/L) and Na/Cl ratios between 0.87 and 0.72 (Figure 3.7). The Na/Cl ratios of the LSFW decrease with depth, implying that the rate at which Na and Cl concentrations are increasing is not the same rate. This trend is also true for Ca/Cl and Mg/Cl.

Two possible origins for the LSFW are, mixture of brine with an ocean-meteoric or dilute ocean water end-member (as introduced in chapter 5), and hyperfiltration.

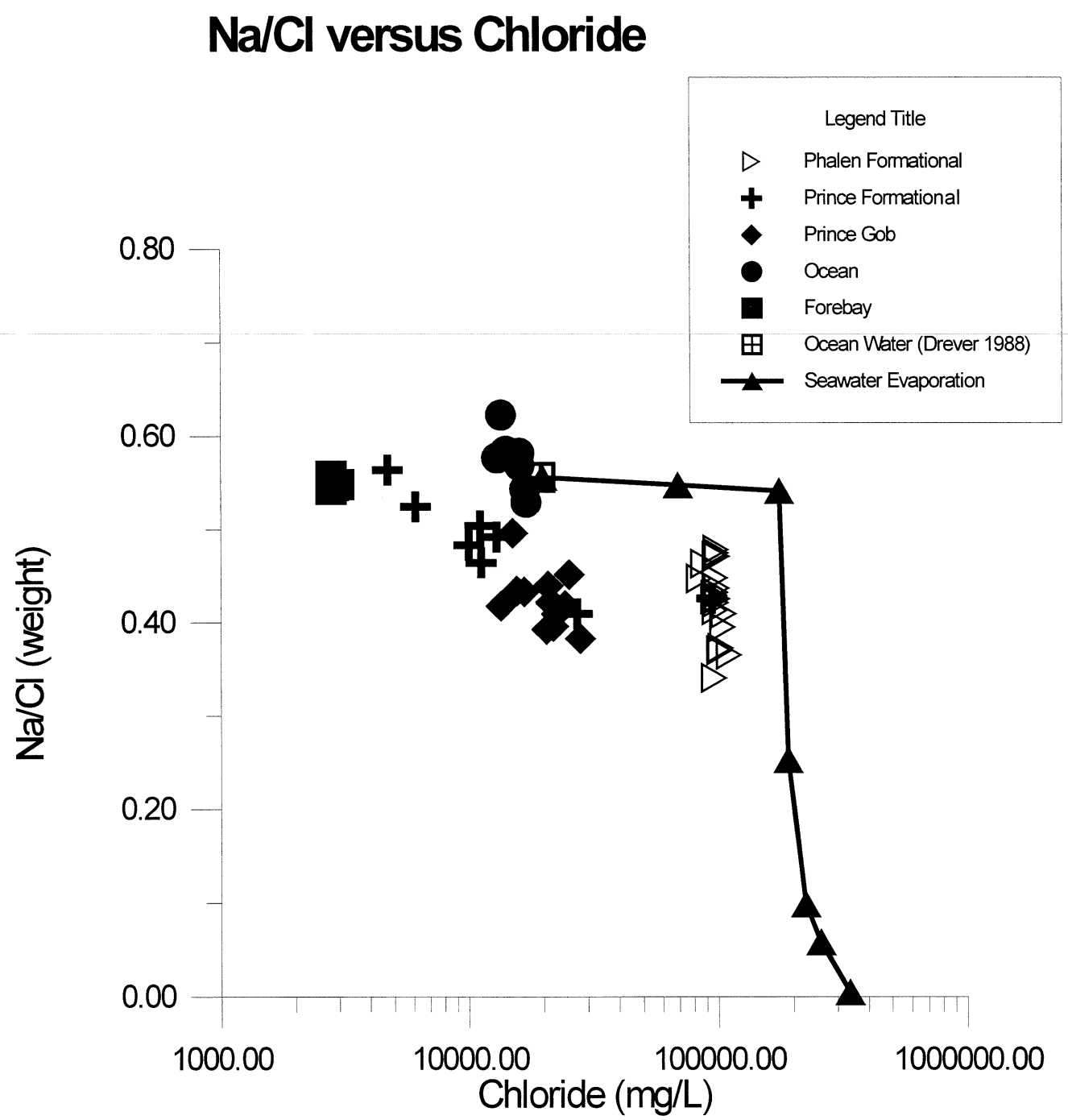

Figure 6.2 Na/Cl (weight) versus Chloride (mg/L). Prince, Phalen, Forebay well, ocean waters, and the seawater evaporation curve are plotted. (Modified from Martel et al. 1997). Gob water, Phalen formation waters and Prince HSFW have similar Na/Cl ratios.

Hyperfiltration has been suggested for the origin of formation waters at Prince Colliery because the vertical salinity change, illustrated in the geophysical salinity profile, is similar to the vertical salinity variation expected with hyperfiltration (see below).

Mixture with a dilute end-member

As discussed previously, the LSFW could be the result of a mixture between brine and dilute ocean water. In this hypothesis, it is assumed that the brine was emplaced first because it is old (Upper Mississippian; Martel *et al* 1997), originating with the Windsor salts. Mixture with a dilute end-member is supported by the low salinity of the LSFW and the high Na/Cl ratio with respect to the brine. The change in the Na/Cl ratio of the LSFW with depth down dip suggests that it is mixing with the brine.

The general low salinity of surficial groundwaters (as were sampled at Point Aconi Power Station) could not change the Na/Cl ratio of the brine at Prince Colliery, located above the Hub coal seam. The Forebay well was saline enough to change the Na/Cl ratio of the brine and roughly reproduce the LSFW compositions (Figure 5.5). An ocean water component is suggested for the dilute end-member because there is no other source of chloride in the area, but a seawater source cannot be confirmed without Br analyses. Forebay well was used for the dilute end-member because it is a groundwater well in the area that has experienced seawater invasion and chemical data was available for the well.

Variations in the above model could also have produced the LSFW composition. For example, ocean water could have mixed with the brine first, and then this mixture

could have been diluted with groundwater. It is apparent from the salinity of the LSFW that ocean water alone could not have produced its chemistry.

I choose to model the LSFW chemistry using Forebay well because (1) chemical data were available for a dilute ocean water end-member (Forebay well), (2) the LSFW plotted as an intermediate between the HSFW and this dilute ocean water end-member using several chemical parameters (Figure 3.9a & b) and (3) Hydrowin allowed me to optimize apparent mixtures of waters relatively easily. The mixing models support a dilute ocean water end-member for the LSFW. Whether ocean water was first mixed with the brine or with groundwater is a topic for future research. The question arises why the lower sandstone, and not the upper sandstone, was invaded with a dilute ocean water end-member. The stratigraphic relationships of the lower and upper sandstone bodies are not understood well enough at this time to hypothesize why the waters have different end-members.

Hyperfiltration

Hyperfiltration or reverse chemical osmosis refers to the retention of ions by a semi-permeable membrane or filter. The most common semi-permeable membranes in the geologic record are shales.

Clays are colloidal particles, i.e. when submerged in water that has a pH above its isoelectric point, a cation is released, resulting in a net negative charge. Cations will surround the clay forming two layers, a rigid stern layer and, a diffuse guouy layer. When the clay is compacted the pores will compress and at some point only the guouy

layers will occupy the pore spaces and no ions will be able to pass through the shale, assuming 100% efficiency (Drever 1988). This is rarely the case in nature, so that the efficiency of a membrane varies from shale to shale.

Many factors contribute to the shale's overall efficiency as a membrane including: the composition (i.e. minerals), the degree of compaction, and salinity of the water forced through the membrane. Hichon and Friedman (1969) estimated the membrane efficiency of shales in the western Canadian sedimentary basin at only 25% efficiency. On the USA Gulf coast shale efficiencies in the Chocolate Bayou Oil Field were estimated at 30% (Kharaka *et al.* 1977; Graf 1982). The result of this poor efficiency is that the shales can only retard selective ions and as salinity increases the shales ability to retard ions decreases (Fontes and Matray 1993).

During hyperfiltration the salinity increases directly below the shale membrane, whereas water on the upper side of the membrane will be more dilute (Figure 6.3). Species with a high surface charge will be preferentially retarded (i.e. Ca^{2+} will be retained at a greater rate than Na^{+}; Kharaka and Berry 1974). An increase in Ca/Na ratios with depth is often used as a red flag for indicating hyperfiltration. Ideally to prove hyperfiltration samples should be taken above and below shale units in order to monitor fractionation of ions.

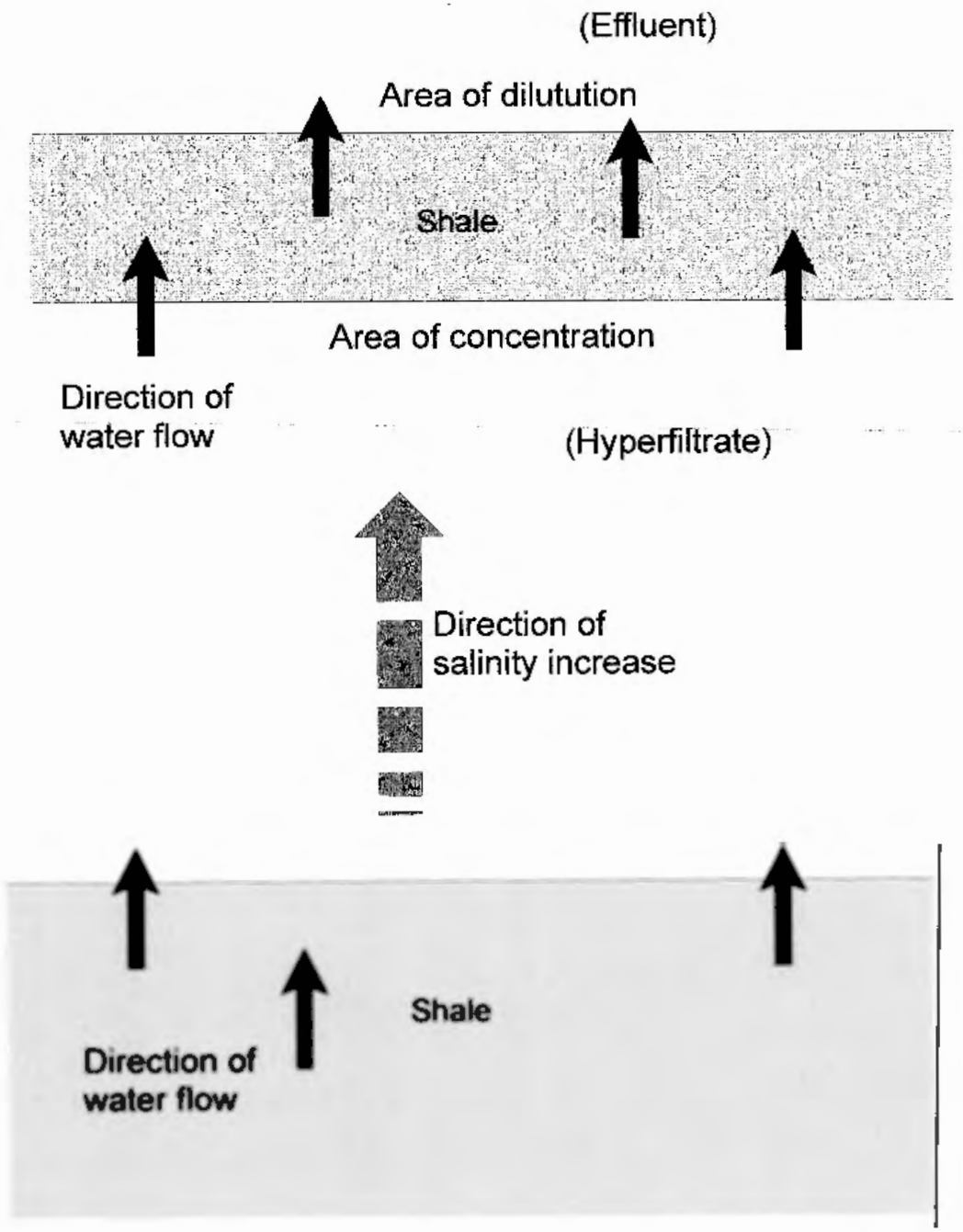

Figure 6.3 Diagramatic explanation of hyperfiltration.

Overpressuring is required in order to force the water up through the shale membrane. Sources of overpressure include:

1. Rapid sedimentation of fine grained materials
2. Lateral tectonic compression
3. Hydrothermal pressure
4. Dehydration of hydrous minerals (e.g. clay minerals, gypsum)

Lateral tectonic compression, rapid sedimentation and hydrothermal pressures are not occurring of the coast off Cape Breton at present (presently a passive margin). For dehydration reactions to have a significant effect there has to be a substantial amount of material present and the reaction rate has to be quick enough to maintain that pressure (Graf 1982).

The forces which produce overpressuring are not active in the study area. Elevated recharge areas have also been suggested as a source of overpressuring but it was concluded that elevation alone could not cause or maintain the necessary pressure gradient (Kharaka and Berry 1974).

To achieve concentrations similar to what is now present at the Prince Colliery, the average groundwater sample measured at the Point Aconi Power Plant would have to be concentrated ~460 times its original chloride concentration and standard ocean water (Drever 1988) would have to be concentrated 1.5 times its original chloride concentration to produce the most saline water sample at Prince (Dal4 Decline). Sea level has been at its present level only in the past few thousand years and ~120 ka (Figure 6.4; Piper and Asku 1992). Between this time, recharge in the area would have been from meteoric

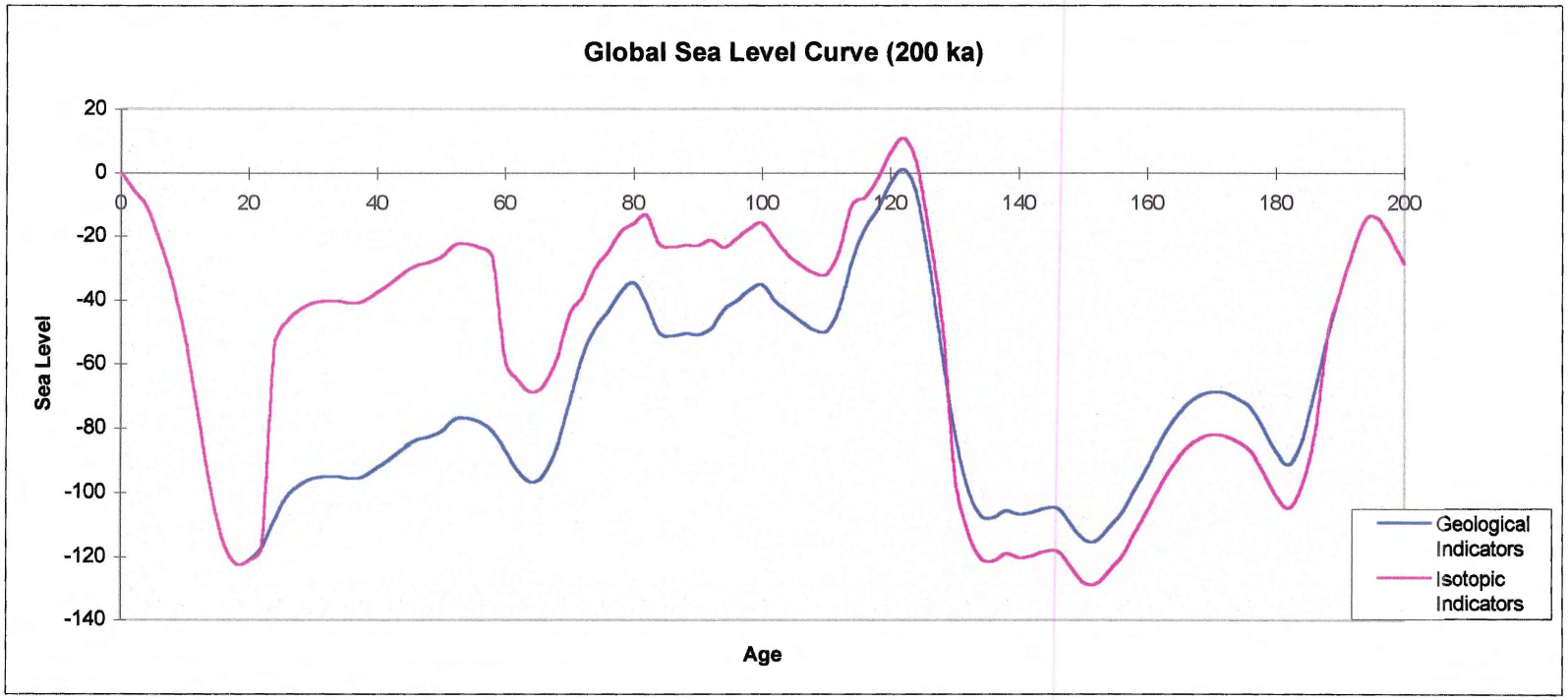

Figure 6.4 Global sea level curve calculated from del 18-O data as well as geologic indicators (Piper and Asku 1992).

water. The quantity of meteoric water needed, to produce the salinity of the formation water at Prince Colliery, would be substantial and depend on the membrane efficiency of the shale. Even if ocean water was recharging the aquifer the high salinity would compromise the efficiency of the membrane and a substantial amount of water would still be necessary.

The Ca/Na ratios at Prince do not increase with vertical depth between the HSFW and the LSFW. The Ca/Na ratios of the HSFW and gob water are higher than the LSFW, unlike what you would expect with hyperfiltration.

The lower formation water on the vertical salinity profile produced by Shimeld (1997) shows a slight increase proximal to the 24 cm shale identified in core P6 (Figure 3.5). The 24 cm shale which divides the channel sandstone is certainly not thick enough to be a suitable membrane. Even if the upper and lower formation water acted as one unit as depicted in Figure 6.2, the LSFW is not present at the base of the sandstone below 281m depth below sea level. There is no indication that there is a vertical salinity variation in the HSFW within the channel sandstone body. There is not a significant chloride difference between the HSFW and the gob waters which would indicate a vertical salinity variation (similar to that identified between the LSFW and the gob waters).

Although there are many problems with a membrane filtration model, the primary problems are a source of overpressuring and lack of chemical evidence. From this information I have concluded that the chemistry of the LSFW cannot be attributed to

hyperfiltration, and is most likely the result of mixing with a dilute ocean water end-member.

6.1.3 Gob Waters

The gob waters were originally suspected as being ocean water by the mine operators because they were more saline than formation water at similar depths. The fractures induced by retreat long wall mining were thought to have penetrated so close to the sea-floor that seawater was leaking into the mine. The geophysical salinity profile (Shimeld 1997) revealed HSFW above the LSFW. The mining induced fractures in the overlying sandstone channel provide excellent secondary porosity, allowing the HSFW to enter the gob. The vertical extent of these fractures is unknown but there is no indication from this study that they provide a conduit for seawater to enter the mine (e.g. elevated Na/Cl ratio).

Ocean water is not responsible for the high sulphate concentration in the gob waters (Figure 3.12). The $\delta^{34}S$ in the gob waters is quite variable and two data points plot near seawater in Figure 3.14. Since all the species concentrations in the water did not increase by the same magnitude as the SO_4 species, it is unlikely that the enriched sulphate in the gob samples is from addition of ocean water. The enrichment in SO_4 and variation in ^{34}S is probably the result of pyrite oxidation (equations 6.1 & 6.2). These equations also remove the carbonate alkalinity (equation 6.3) by adding H^+ ions to solution.

$$FeS_2 + 3.5O_2 + H_2O = Fe^{2+} + SO_4^{2-} + 2H^+ \quad (6.1)$$

$$Fe^{2+} + 0.25O_2 + 2.5\ H_2O = Fe(OH)_3 + 2H^+ \quad (6.2)$$

$$\text{Alkalinity}_{(\text{carbonate})} = HCO_3^- + 2CO_3^{2-} - H^+ \quad (6.3)$$

The variations in $\delta^{34}S$ measured in the gob samples is most likely due to a variation in $\delta^{34}S$ in the Hub coal seam. Coal from the Hub seam was sampled for ^{34}S analysis by Gibling *et al.* (1989). The concentration of $\delta^{34}S$ in that sample was 14.3 $^{0}/_{00}$. This value is between the concentrations of $\delta^{34}S$ measured from the gob waters and it is likely that the pyrite in the Hub coal seam varies in isotopic ($\delta^{34}S$) composition. The values of $\delta^{34}S$ measured from the gob waters are probably caused by this variation.

I have therefore, interpreted the gob waters to be a mixture of the two overlying formation waters. The mixing models produced in Hydrowin resulted in a very good overall approximation of the gob water chemistry (Figure 5.2A, B, C, & D).

6.2 Aquifer Compartmentalization

The compartmentalization of the aquifer, overlying the Hub coal seam, is supported by two independent sources of data, geophysical and chemical. The gob waters, which are sourced by the overlying formation water (previous section), exhibit different chemistries than formation waters shallower than 266 m (Figure 3.6). With depth, gob waters surpass the chloride concentration of the LSFW. If the gob waters are not sourced by the overlying ocean water then there must be a more saline water above the LSFW.

The 24 cm mudstone identified in core P6 (Figure 4.1) is located at the approximate depth as the salinity change in the geophysical salinity profile. Even though porosity in shales can be quite large (up to 70-80 %; Freeze and Cherry 1979), permeability at depth is normally restricted. The hydraulic conductivity of shales is commonly between 10^{-12} to 10^{-10} m/s and even with a large hydraulic head, it would take centuries for water to travel just a few centimeters (Freeze and Cherry 1979).
The mudstone unit is only 24 cm thick and may not be of sufficient size to compartmentalize the aquifer. But the mudstone, in combination with the first low permeable sandstone unit of the lower aquifer (1 m thick, vertical permeability 0.20 mD) should be enough to compartmentalize the formation waters.

Therefore, the mudstone (shale) layer in combination with the uppermost unit in the lower sandstone body, appear to be the barrier compartmentalizing the formation waters within the channel sandstone body, overlying the Hub coal seam. The lower sandstone aquifer contains the LSFW and is located directly above the Hub coal seam less than 281 m below sea level (depth of first HSFW sample). The upper sandstone, identified in core P6, overlies the lower sandstone (aquifer) at depths shallower than 281 m and the upper sandstone rests directly above the Hub coal seam where the lower aquifer is not present (Figure 6.1).

CHAPTER 7 CONCLUSIONS

7.0 Conclusions

The purpose of this study was to test the hypothesis of compartmentalization of the formation waters within the channel sandstone body above the Hub coal seam as well as to determine if ocean water was entering the mine through mine induced fracturing.

As a result of this study it can be concluded that:

1. The sandstone unit overlying the Hub coal seam is separated by an area of low permeability.
2. This area of low permeability compartmentalizes the formation water within this sandstone body. Two formation waters were identified: a low salinity formation water and a high salinity formation water.
3. The high salinity formation water is related to deeper basinal brines and can be correlated to the formation water in the Phalen Colliery in New Waterford, Cape Breton (Martel *et al.* 1997).
4. The low salinity formation water is the mixing product between the HSFW and a dilute ocean-meteoric water end-member.
5. The high salinity gob waters are not derived from the overlying ocean water but are a mixture of high and low salinity formation waters from the overlying aquifers.

6. This study also supports the geophysical conductivity (salinity) profile produced by Shimeld (1997) indicating that Archie's Law can be used to calculate R_w on the metre scale.

7.1 Further Research

Further research for this project should include:

•Detailed mapping and petrographic evaluation of the lower sandstone unit

•More analyses on the LSFW including, bromide and stable isotope analyses (deuterium and ^{18}O) in order to confirm an ocean component

•Construction of vertical geophysical salinity (conductivity) profiles for other drill holes in the area, for which the appropriate geophysical data is available, so as to better understand the vertical salinity variation

•Computer modeling with more advanced software would be useful in order to accurately document the history of the LSFW.

REFERENCES

Bateman R.M., and Konen, C.E., 1977. The log analyst and the programmable pocket calculator. *The Lob Analyst*, **September - October**: 3-11.

Berner K.E. and Berner, R.A., 1996. *Global Environment: Water, Air, and Geochemical Cycles (2nd edition)*. Prentice Hall.

Calmbach L., Hydrowin, version 3.0 Institut de Minéralogie BFSH2, 1015 Lausanne, E-mail: *Lukas.Calmbach@imp.unil.ch.*

Calder J., 1987, Stratigraphy and Sedimentary of the Hub Seam Roof Strata Prince Mine Block, Sydney Coalfield. Preliminary Report based upon offshore drill holes, Nova Scotia Department of Mines & Energy Coal Section.

Cape Breton Development Corporation, Phalen Colliery, Risk Assessment, 1994. Volume 2.

Drever J.I.,1988 The Geochemistry of Natural Waters 2nd edition, Prentice Hall, Inc. p. 12.

Duggan J. P., 1995. Structure of bedrock offshore from Point Aconi, Cape Breton Island, Nova Scotia. Unpublished B.Sc. Honours thesis, Earth Sciences Department, Dalhousie University.

Entyre L.M., 1992. Estimation of petrophysical parameters using a robust Levenburg-Marquardt procedure. *The Log Analyst*, July-August, pp. 373-389.

Fontes J.Ch., and Matray J.M., 1993. Geochemistry and origin of formation brines from the Paris Basin, France: 1. Brines associated with Triassic salts. *Chemical Geology*, **109**: 149-175.

Freeze R.A., and Cherry J.A., 1979. Groundwater, Prentice-Hall, Inc., p. 157-158, 279-286.

Graf D.L., 1982. Chemical osmosis, reverse chemical osmosis, and the origin of subsurface brines. *Geochimica et Cosmochimica Acta*, **46**: 1431-1448.

Gibling M.R., Zentilli M., and McCready R.G.L., 1988. Sulphur in Pennsylvanian coals of Atlantic Canada: geologic and isotopic evidence for a bedrock evaporite source, *International Journal of Coal Geology,* **11**: 81-104.

Gibling M. R. & Bird D. J., 1994. Late Carboniferous cyclothems and alluvial paleovalleys in the Sydney Basin, Nova Scotia. *Geological Society of America Bulletin*, **106**: 105-117.

Gibling, M.R., Boehner R.C., & Rust B.R., 1987. The Sydney Basin of Atlantic Canada: an upper Paleozoic strike-slip basin in a collisional setting. In: *Sedimentary Basins and Basin -Forming Mechanisms.* Edited by C. Beaumont, and Tankard. Canadian Journal of Petroleum Geologists Memoir 12 :269-285.

Hacquebard P.A., 1993. The Sydney Coalfield of Nova Scotia, Canada. *International Journal of Coal Geology,* **23**: 29-42.

Hanor J.S., 1994. Origin of saline fluids in sedimentary basins. In: Parnell, J. (ed.) Geofluids: In: *Origin, Migration and Evolution of Fluids in Sedimentary Basins, Geological*. Society Special Publication No. 78: 151-174.

Hitchen B., and Friedman I., 1969. Geochemistry and origin of formation waters in the western Canada sedimentary basin III: Factors controlling chemical composition. *Geochimica et Cosmochimica Acta*, **35**: 455-481.

Kharaka Y.K., and Berry F.A.F., 1974. The Influence of Geological Membranes on the Geochemistry of Subsurface Waters From Miocene Sediments at Kettleman North Dome in California. *Water Resources Research*, **10**: 313-327.

Martel A.T., Gibling M.R., Kennedy A., MacLeod G., and Baechler F., 1996. Spatial trends in brine chemistry from the shallow subsea area of the Carboniferous Sydney Basin, Nova Scotia, Canada. Geological Society of America 1996 Annual Meeting - Abstracts with Programs.

Martel A.T., Kennedy A., Gibling, M.R., 1997. Saline brines of the Sydney Basin: origin as evaporative Windsor residues? Atlantic GeoScience Society 25th Anniversary Colloquium and Annual General Meeting - Programs and Abstracts.

McCaffrey M.A., Lazar B., Holland H.D., 1987. The evaporation path of seawater and the coprecipitation of Br^- and K^+ with halite. *Journal of Sedimentary Petrology*, **57**: 928-937.

Nova Scotia Department of Natural Resources, 1979. Well history report, Nova Scotia Department of Mines & Energy-Devco P-6, Point Aconi Coalfield Area, Nova Scotia. H.B. Peach & Associates Limited.

Piper, A.M., (1944) A graphic procedure in the geochemical interpretation of water-analysis. *Transactions, American Geophysical Union*, **25**: 914-923.

Piper, J.W., and Aksu, A.E., (1992) Architecture of stacked Quaternary deltas correlated with global oxygen isotopic curve. *Geology*, **20**: 415-418.

Shimeld J.W., Martel T.M., Kennedy A., Gibling M.R., Williamson M.W., 1997, in preparation. Geophysical determination of formation water conductivity in the Sydney Basin, offshore Cape Breton, and implications for the regional hydrogeologic flow system.

Schlumberger Educational Services, 1991. Log Interpretation, Principles/Applications, Houston: p198.

Tucker M.E., 1981. *Sedimentary Petrology An Introduction* (ed. by Hallam, A.), Halsted Press, pp. 15 & 18.

Pettijohn F.J., Potter P.E., & Siever R., 1973. *Sand and Sandstone*, Springer-Verlag, Berlin, p. 617.

APPENDIX 1

Method for the Measurement of Alkalinity in Water Samples by the Cobas Method

1 Introduction

1.1 Alkalinity in water is its acid-neutralizing capacity. It is significant in many for treatments of natural water and waste waters. Because the alkalinity of many surface waters is primarily a function of carbonate, bicarbonate, and hydroxide content, it is taken as an indication of the concentration of these constituents.

2 Principle Method

2.1 There are many different ways to measure alkalinity. This method uses the Cobas Fara II Centrifugal Analyzer to determine alkalinity. The sample is placed in a sample cup and then the proper reagents are placed in the reagent trays. Then the test for alkalinity is programmed into the Cobas and the sample is run including standards and quality control samples. The concentration is calculated by the Cobas automatically.

3 Detection Limits and Method Validation

3.1 The minimum concentration that can be reported with 99% confidence range is 0.4 mg/L when using the 0 - 50 mg/L range.

Method 0 - 50 mg/L Alkalinity Low
0 - 250 mg/L Alkalinity High

Precision based on 10 replicates is 0.27 mg/L and accuracy is 99.2%.

4 Interferences

4.1 Not applicable

5 Sample Requirements

5.1 Samples can be collected in either glass or plastic bottles. They can be stored for up to 14 days refrigerated. There is no sample pretreatment required.

6 Equipment

6.1 Cobas Fara II Centrifugal Analyzer.
6.2 Sample cups and rotors needed for the Cobas Analyzer.

7 Reagents

7.1 Methyl Orange. Dissolve 144 mg of methyl orange in 800 mls of demineralized water in a 1 liter volumetric flask and then dilute to the mark. This solution should be stored in an amber bottle.
7.2 Stock Buffer. Dissolve 5.1 grams of potassium acid phthalate in 400 mls of demineralized water in a 500 ml volumetric flask. Then add 87.5 mls of 0.1 N HCL and dilute to 500 mls. The pH should be 3.1; if not, adjust with 1.0 N HCl.
7.3 Working Buffer. Dilute 10.0 mls of he stock buffer to 100 mls in a 100 ml volumetric flask with demineralized water.
7.4 Stock Standard (1000 mg/L as CaCO3). Dissolve 1.060 g of anhydrous sodium carbonate (oven dried at 250 degrees Celsius for 4 hours) in demineralized water in a 1 liter volumetric flasks and then dilute to the mark.
7.5 Calibration Standards. Serial dilutions are made of the stock standard to make concentrations of 10, 20, 30, 40 and 50 mg/L of CaCO3 for alkalinity low and 100 150, 250 mg/L of CaCO3 for alkalinity high. Keep refrigerated.

8 Test Procedures

8.1 Prepare standards and reagents as above.
8.2 Fill the standard positions in standard rack # 2 positions 41 - 52.
8.3 Fill reagents in Rack 5s2 section 1. Methyl orange in position 1 and the working buffer in position 2.
8.4 Program in the general parameters and the analysis parameters following the SOP for Programming the Operating of the Cobas Fara II Analyzer using the values located in appendix A of this method.
8.5 Refer to the SOP for the Operation of the Cobas Fara II for analysis of set of samples.

9 Calculation of Results

9.1 The Cobas Fara II analyzer will automatically calculate the alkalinity concentration of a sample by calculating a calibration curve with the standards and then calculating the concentration of the sample.

Method for the Measurement of Ammonia in Water Samples by the Cobas Method

1 Introduction and Scope

1.1 This method measures the amount of ammonia -NH3 in a water sample. It has a sensitivity of 10 ug NH3-N/L and is useful for up to 500 ug NH3-N/L

2 Principle Method

2.1 When using this method an intensely blue compound, indophenol, is formed by the

reactions of ammonia, hypochlorite and phenol. The intensity of the color is read on a spectrometer and a calibration curve is constructed. Unknowns are compared to the curve.

3 Detection Limits and Method Validation

3.1 The minimum concentration that can be reported with 99% confidence is 0.04 mg/L when using the 0 - 2 mg/L range.

Method Range 0 - 2.0 mg/L Ammonia Low
0 - 20.0 mg/L Ammonia High

Precision based on 10 replicates is 0.028 mg/L and accuracy is 89.9%

4 Interferences

4.1 Alkalinity ver 500 mg as CaCO3 /L, acidity over 100 mg as CaCO3/L and turbidity can interfere with the detection of ammonia. These interferences can be removed by preliminary distillation.

5 Sample Requirements

5.1 Samples can be collected in either glass or plastic bottles. It is preferable that ammonia be analyzed for as soon as possible, however, samples can be stored with refrigeration for up to 7 days.

6 Equipment

6.1 Cobas Fara II Centrifugal Analyzer
6.2 Sample cups and rotors needed for the Cobas Analyzer

7 Reagents

7.1 Complexing Reagent. Dissolve 50 grams of EDTA (disodium salt) and 6 pellets of NaOH (or more until solution is clear) in 1000 mls of demineralized water in a 1 liter volumetric flask.
7.2 Alkaline Phenol. Add 6.5 mls of 50 % (w/w) NaOH to approximately 5.0 ml demineralized water. Stir and cool. Slowly add 10.5 mls of 90% (w/w) phenol solution in a 100 ml volumetric flask and then dilute to the mark. Prepare daily.
7.3 Working Reagent. Mix 3.55 ml of alkaline phenol with 5.0 ml of the complexing reagent. Prepare daily.
7.4 Sodium Nitroprusside Solution. Dissolve 1/0 g sodium nitroprusside in 900 mls of demineralized water
7.5 Sodium Hypochlorite Solution (3.3% available chlorine). Dilute 65 mls of commercial bleach solution (5.1% w/v available chlorine) to 100 mls with demineralized water in a 100 ml volumetric flask.

7.6 Stock Ammonia Standard (1000 mg/L (N)). Dissolve 3.819 g of anhydrous ammonia chloride (dried at 105°C) with demineralized water in a 1 liter volumetric flask and then dilute to the mark. Keep refrigerated.
7.7 Calibration Standards. Serial dilutions of the stock ammonia standard are made to make concentrations of 0.05, 0.5, 1.0 and 2.0 mg/L (N) for ammonia low and 5, 10, 15, 20 mg/L (N) for ammonia high. Keep refrigerated.

8 Test Procedures

8.1 Prepare standards and reagents as above
8.2 Fill the standard positions in standard rack # 1 positions 11-21.
8.3 Fill reagents in Rack 5s1 section 1. The working reagent is in the primary position, sodium nitroprusside solution in position 1 and the sodium hypochlorite solution in position 2.
8.4 Program in the general parameters and the analysis parameters following the SOP for Programming and Operating of the Cobas Fara II Analyzer using the values located in appendix A of this method.
8.5 Refer to the SOP for the Operation of the Cobas Fara II for analysis of a set of samples.

9 Calculation of Results

9.1 The Cobas Fara II analyzer will automatically calculate the ammonia concentration of a sample by calculating a calibration curve with the standards and then calculating the concentration of the sample.

Method for the Measurement of Chloride in Water Samples

1 Introduction and Scope

1.1 Chloride in the form of chloride (Cl-) ion, is one of the major inorganic anions in water and wastewater. This method determines the concentration of the Cl- ion in potable water and wastewater.

2 Principle Method

2.1 The method is an automated Ferricyanide method. The thiocyanate ion is liberated from mercuric thiocyanate by the formation of soluble mercuric chloride. In the presence of ferric ion, free thiocyanate ions form a highly colored ferric thiocyanate, of which its intensity is proportional to the chloride concentration.

3 Detection Limits and Method Validation

3.1 The detection limit is 0.3 mg/L using the range of 0 - 100 mg/L with 99% confidence limit.

Method Range 0 - 100.0 mg/L Chloride Low
0 - 500.0 mg/L Chloride High
Precision based on 10 replicates is 0.17 and accuracy is 100.8%

4 Interferences

4.1 None significant

5 Sample Requirements

5.1 Samples can be collected in either glass or plastic bottles. No sample preservation or pretreatment is required.

6 Equipment

6.1 Cobas Fara II Centrifugal Analyzer
6.2 Sample cups and rotors needed for the Cobas Analyzer.

7 Reagents

7.1 Ferric Nitrate. Dissolve 202 g of ferric nitrate in approximately 200 ml of demineralized water in a 1 liter volumetric flask. Then add 21 ml of concentrated nitric acid and dilute to 1000 mls. Store in an amber bottle.
7.2 Mercuric Thiocyanate. Dissolve 4.17 g of mercuric thiocyanate in approximately 500 mls of methanol in a 1 liter volumetric flask and then dilute to the mark with methanol. Then the solution is filtered and is stored in an amber bottle.
7.3 Color Reagent. Mix equal volumes (15 ml) each of ferric nitrate and mercuric thiocyanate in a 100 ml volumetric flask and dilute to the mark with demineralized water.
7.4 Stock Standard (1000 mg/L as Cl). Dissolve 1.6482 g of sodium chloride (dried at 140°C) with demineralized water in a 1 liter volumetric flask and then dilute to the mark.
7.5 Calibration Standards. Serial dilutions are make of the stock standard to make concentrations of 10, 20 40, 60, 80 and 100 mg/L Cl for chloride low and 100, 200, 300, 400, and 500 mg/L Cl for chloride high. Keep standards refrigerated.

8 Test Procedures

8.1 Prepare standards and reagents as above
8.2 Fill the standard positions in standard rack #2 positions 53 - 65.
8.3 Fill reagents in Rack 5s2 section 3. The color reagent is in the primary position.
8.4 Program in the general parameters and the analysis parameters following the SOP for Programming and Operating of the Cobas Fara II Analyzer using the values located in appendix A of this method.
8.5 Refer to the SOP for the Operation of the Cobas Fara II for analysis of a set of samples.

9 Calculation of Results

9.1 The Cobas Fara II analyzer will automatically calculate the chloride concentration of a sample by calculating a calibration curve with the standards and then calculating the concentration of the sample.

Method for the Measurement of pH in Water Samples

1 Introduction and Scope

1.1 This method involves the electrometric measurement of pH by the use of a meter and reference electrode.

2 Principle of Method

2.1 The meter is calibrated with prepared buffer solutions with the pH of 4.00 and 7.00. The pH of a sample is then measured. PH is read directly from the meter

3 Detection Limits and Method Validation

3.1 Not applicable

4 Interferences

4.1 Temperature can affect pH measurements. PH of samples should be measured at room temperature (20 degrees C). If not, the temperature of a sample should be recorded at time of measurement.

5 Sample Requirements

5.1 Water samples can be received in either plastic or glass bottles. Minimum volume need is 50 mls. Samples should be analyzed immediately.

6 Equipment

6.1 pH meter - Jenway Model #3410/3420 with a temperature probe connected
6.2 Beckman Gel-Filled Combination Electrode
6.3 magnetic stirrer and stirring bar

7 Reagents

7.1 ACS-grad prepared pH 7.00 buffer solution
7.2 ACS-grade prepared pH 4.00 buffer solution
7.3 Demineralized water

8 Test Procedures

8.1 Calibration of meter
8.2 Sample analysis

Measurements are taken directly from the meter.

Method for the Measurement of Sulfate in Water Samples by the Cobas Method

1 Introduction and Scope

1.1 Sulfate (SO4) is widely distributed in nature and may be present in natural waters in concentrations ranging from a few to several thousand mg/L.

2 Principle of Method

2.1 Sulfate ion is precipitated in an acetic acid medium with barium chloride so as to form barium sulfate crystals of uniform size. Light absorbance of the BaSO4 suspension is measured by a photometer and the SO4 concentration is determined by comparison for the reading with a standard curve.

3 Detection Limits and Method Validation

3.1 The minimum concentration that can be reported with 99% confidence is 0.3 mg/L when using the 0 - 50.0 mg/L range

Method ranges 0 - 50.0 mg/L Sulfate low
0 - 200.0 mg/L Sulfate High

Precision based on 10 replicates is 0.23 mg/L and accuracy is 100.0%

4 Inferences

4.1 Color or suspended matter in large amounts will interfere. Some suspended matter may be removed by filtration, silica in excess of 500 mg/L will interfere, and in waters containing large quantities of organic matter it may not be possible to precipitate BaSO4 satisfactorily.

5 Sample Requirements

5.1 Samples can be collected in either glass or plastic bottles. Samples should be analyzed immediately.

6 Equipment

6.1 Cobas Fara II Centrifugal Analyzer.
6.2 Sample cups and rotors needed for the Cobas Analyzer

7 Reagents

7.1 Start Reagent. Dilute 16 ml of conditioning reagent and 1 m of 1000 mg/L SO4 solution to 100 ml with deionized water

7.2 Barium Chloride. Dissolve 7.0 g of BaCl2*2H2O Analar grade in 20 ml of deionized water. Make up to 50 ml with deionized water.

7.3 Conditioning Reagent. Mix 50 ml of glycerol with a solution containing 30 ml concentrated HCl, 300 ml

7.4 Stock Standard (1000 mg/L as SO4). Dissolve 1.479 g of anhydrous sodium sulfate (NaSO4) in deionized water and dilute to 1000 ml. Keep refrigerated

7.5 Calibration Standards. Dilute stock standard appropriately for standards 1, 5, 10, 20, 30, 40, 50 and 0, 25, 50, 75, 100, 150, 200 mg/L. Keep refrigerated.

8 Test Procedures

8.1 Prepare standards and reagents as above

8.2 Fill the standard positions in standard rack #1 positions 11 - 24

8.3 Fill reagents in Rack 5s1 section 4. Place the start reagent in position 1 and barium chloride in position 2.

8.4 Program in the general parameters and the analysis parameters following the SOP for Programming and Operating the Cobas Fara II Analyzer using the values located in appendix A of this method.

8.5 Refer to the SOP for the Operation of the Cobas Fara II for analysis of a set of samples.

Results automatically calculated by the Cobas Fara II Analyzer.

APPENDIX 2
Petrographic Descriptions

P6 - 1

General Mineralogy:

Quartz	70%
Lithic grains	15%
Clay minerals	13%
Carbonate	2%

Description:

Average Grain Size: 0.1 - 0.2 mm
Maturity: Grains are sub-angular to sub rounded, low sphericity
Sorting: Well sorted

Pore Spaces:

abundance - 8% of the slide is pore space
size - generally smaller than or equal to the average grain size (90% of the pores are smaller than the average grain size.)
shape - smaller pores are generally irregular. Larger pores tend to be more rectangular in shape.

Pore filling - 60% of the pores have been filled with kaolinite. All the pores larger than the average grain size have been filled with kaolinite.

Mica grains and clay minerals have been deformed. Silica has been deposited on the surface of many of the quartz crystals (Figure P6-1a). The previous grain boundary is defined by fine grained particles, most likely clay. Carbonate has filled the pore spaces at the edge of the thin section (Figure P6-1b). This is the only area of the thin section where carbonate is present.

A

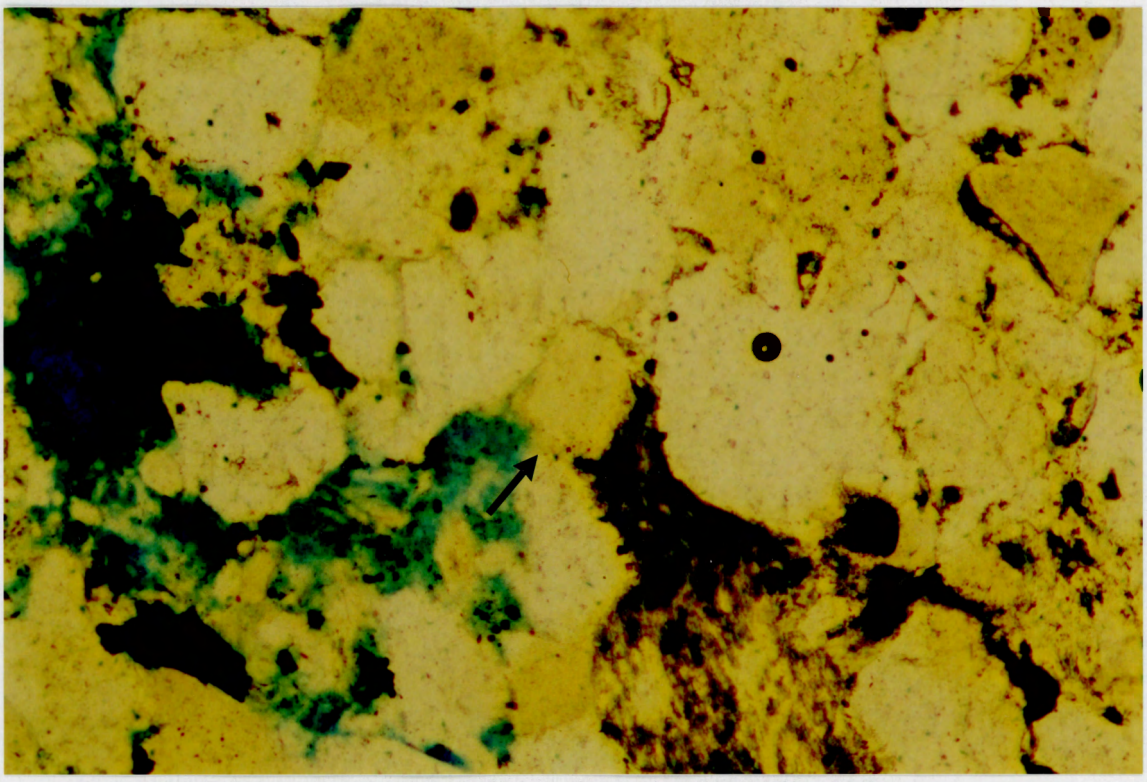

B

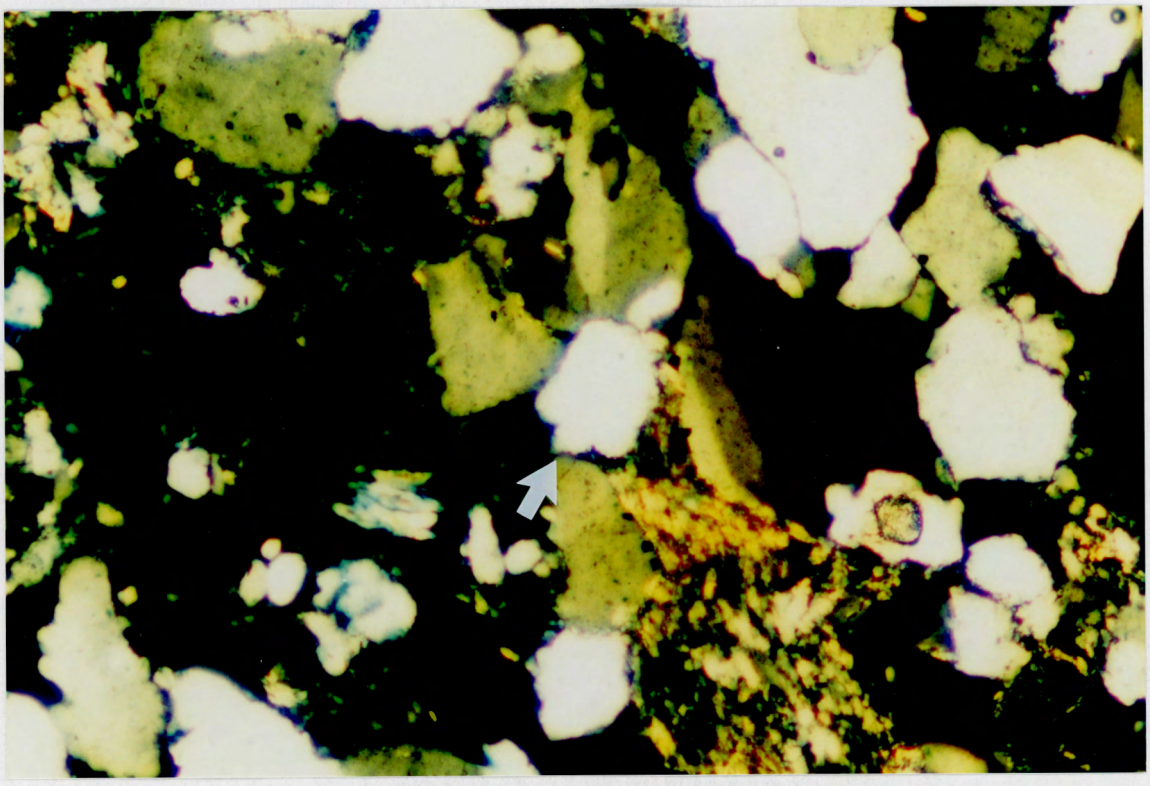

Figure P6-1a Silica deposition on the boundary of quartz grain (magnification 64 x actual size), (A) ppt, (B) cross polars

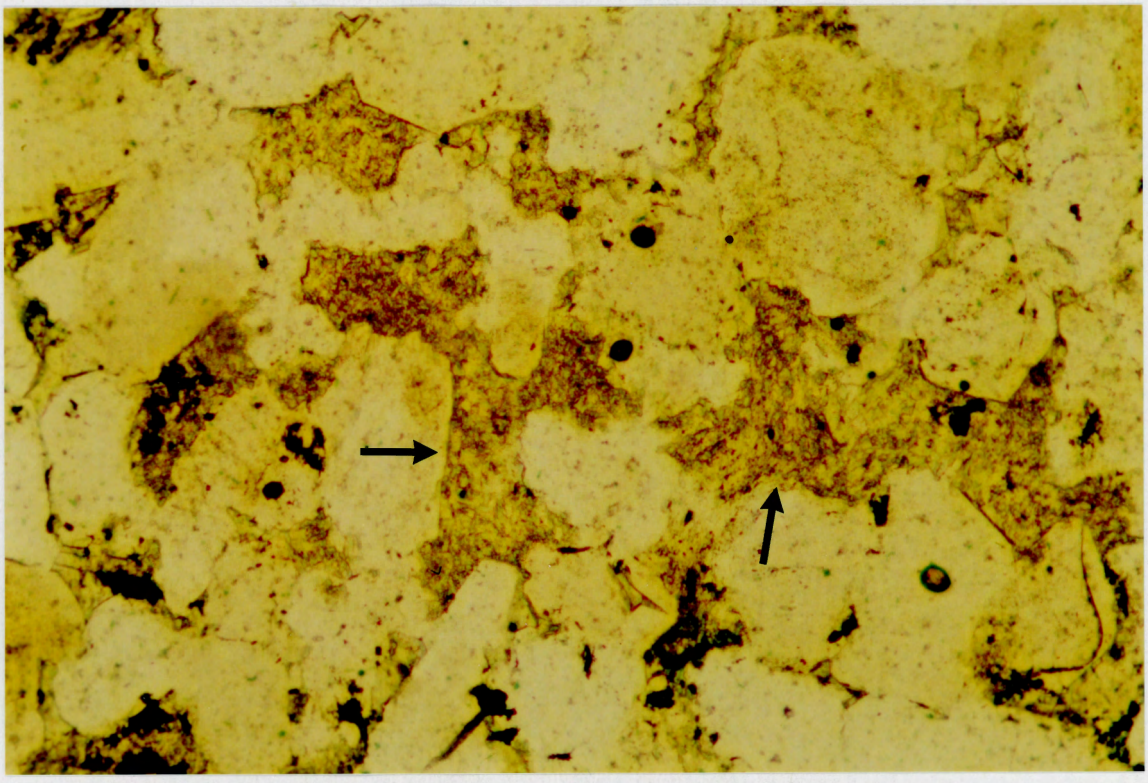

Figure P6-1b Pore filling carbonate in thin secion (magnification 64 x actual size).

P6 - 2

General Mineralogy:

Quartz	70%
Lithic Grains (including micaceous grains)	12%
Siderite	13%
Clay minerals	10%

Description:

Average Grain Size: 0.5 mm
Maturity: Sub-angular, low sphericity
Sorting: Poorly sorted

Pore Spaces:

abundance - 15% of the thin section
size - generally larger than or equal to the average grain size, 95% of the pores are larger than the average grain size.
shape - All of the pores are generally irregular in shape. Some of the pores have sharp boundaries.
Pore filling - 35% of the pores have been completely filled with kaolinite.

Grain size and pore spaces are larger than P6-1. Fine grained clay minerals have been deformed around many of the pores suggesting a secondary porosity.

There are two forms of carbonate present in this section. One has a "dog's tooth" habit the other carbonate occurs as larger crystals. Both carbonates have a brownish rusty coating on them. The dog's toothed carbonate is siderite (Appendix 3) but the composition of the larger carbonate is unknown. The brownish rusty coating suggests that it is also enriched in Fe.

The siderite crystals (up to 0.125 mm) in this thin section are euhedral and show good cleavage. The crystals have grown from the surface of previously existing grains into the open pores (Fig P6-2a). The crystals show compositional zoning in a backscattering electron image (Figure P6-1b). The lighter areas are more Fe-rich and the darker areas in the image (Appendix 3). There are clusters of smaller siderite

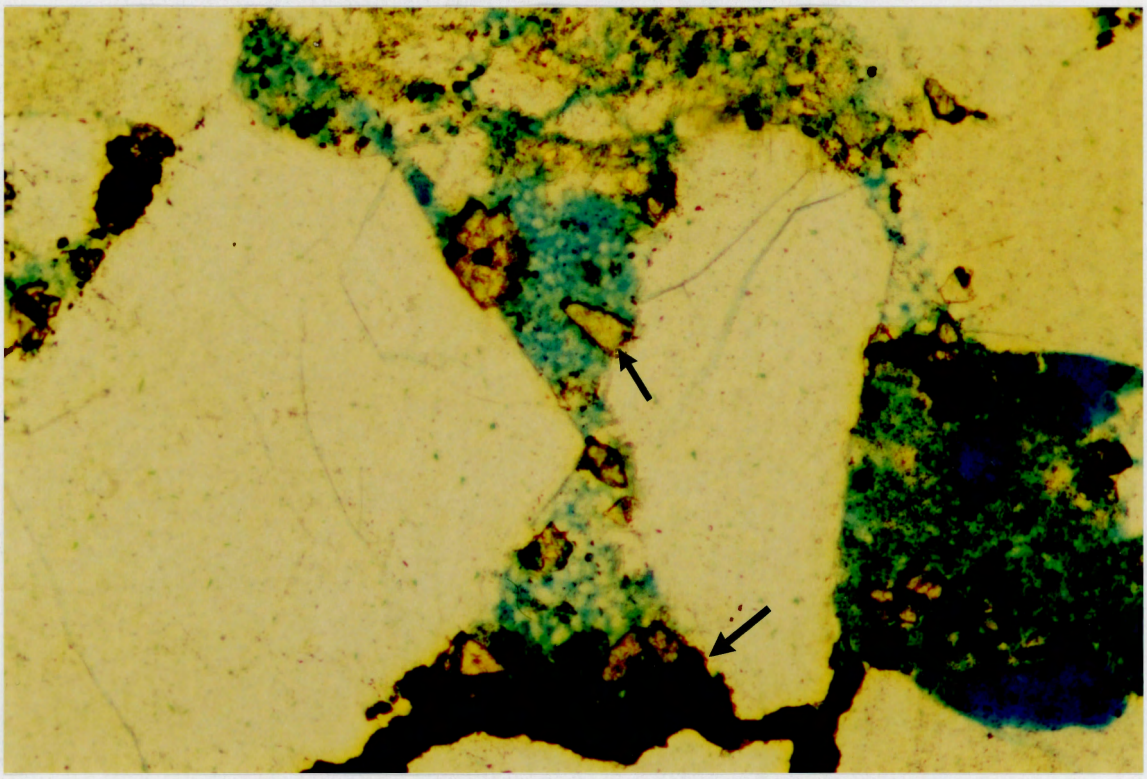

Figure P6-2a Small siderite clusters and larger euhedral siderite which grew from the crystal face of the quartz grains. The larger siderite grew off the cluster of siderite crystals. Kaolinite filled the pore spaces after the siderite (magnification 64 x actual size).

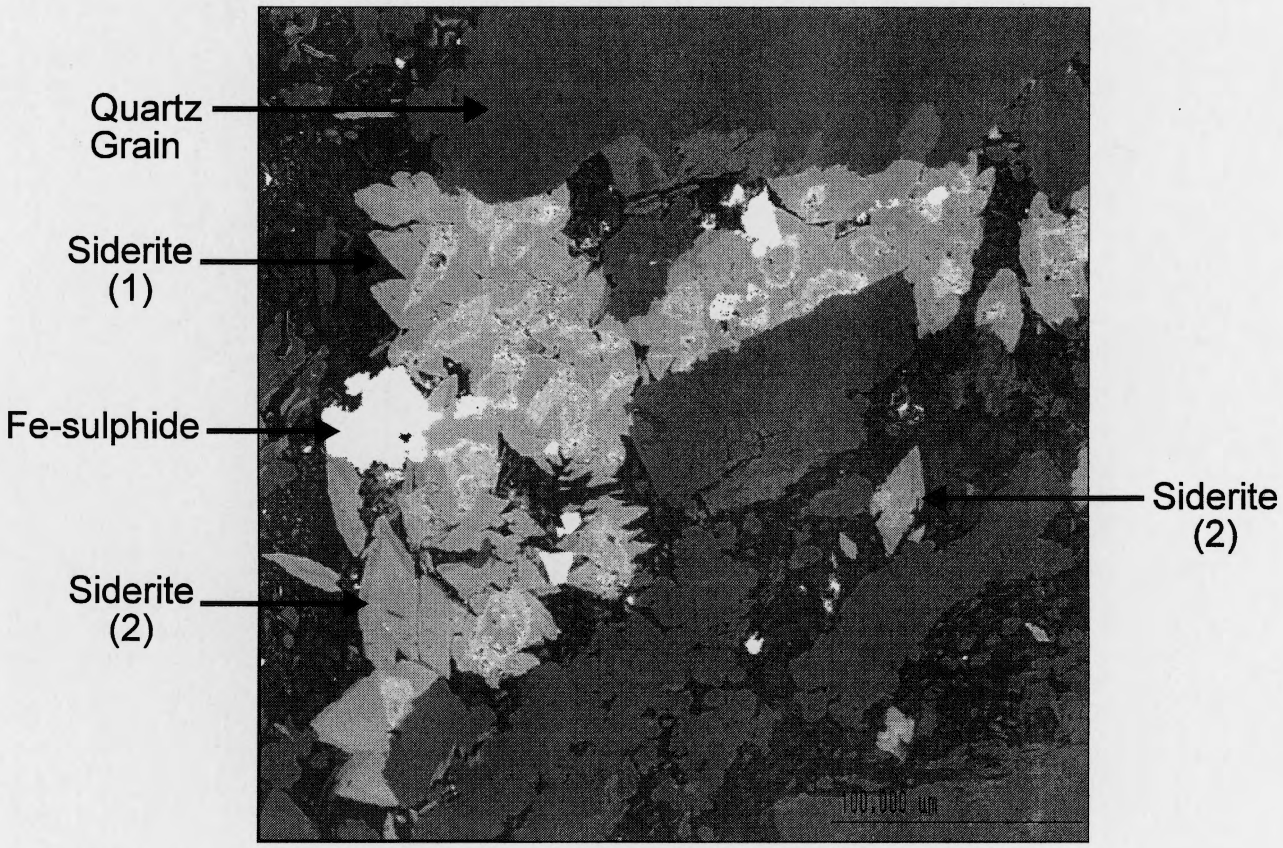

Figure P6-2b Backscattering electron image, Siderite (1) shows spatial zoning within a cluster of siderite crystals. Siderite (2) shows compositional zoning parallel to the crystal face. The lighter areas are more Fe-rich.

crystals throughout the thin section as well. These crystals are very small (<1mm) and are usually hard to differentiate from the brownish rusty coating. In some cases there are two layers of crystals and the top layer of crystals is partially dissolved.

The Fe-carbonate has grown over siderite crystals indicating the siderite grew first. Kaolinite then has filled in the pore after the Fe-calcite was deposited.

Quartz is the most abundant mineral in this thin section. There is no evidence to support growth of these crystals after deposition in this thin section. Many of the quartz crystals are fractured. There has not been any mineral growth or alteration on the surfaces of these fractures.

P6-3

General Mineralogy:

Quartz	70%
Lithic Grains (including micaceous grains)	15%
Siderite	3%
Clay minerals	5%
Carbonate	7%

Description:

Average Grain Size: 0.5 mm
Maturity: Sub-angular to Sub-rounded, low to moderate sphericity
Sorting: Moderately-well sorted (refer p.15 Tucker 1981)

Pore Spaces:

abundance - constitute approximately 15% of the slide
size - the majority of the pores are 0.4 mm (measuring longest dimension). At the top and bottom of the slide the pores size increases so that the average pores size is larger than the average grain size (0.5 mm).
shape - Pores are generally irregular in shape, the larger pores have very angular boundaries.

Pore filling - 50% of the pores have been completely filled with kaolinite

The majority of the pores are less than the average grain size. Clay minerals have been deformed around some pores (Figure P6-3a). The larger pores at the top and bottom of the slide do not appear to be formed by plucking when the thin section was made. They have been stained and some of the pores have been partially filled (up to 90%) with kaolinite.

Siderite grains occur as clusters (individual crystals <1 mm) or individually (>1 mm). Some of the siderite crystals around the pore boundaries are not perfectly euhedral. The grains appear to have been partially dissolved.

A larger Fe-carbonate has filled some pore spaces (anhedral) and occurs as individual crystals. The Fe-carbonate was deposited after the siderite crystals and before kaolinite filled the pore spaces (Figure P6-3b).

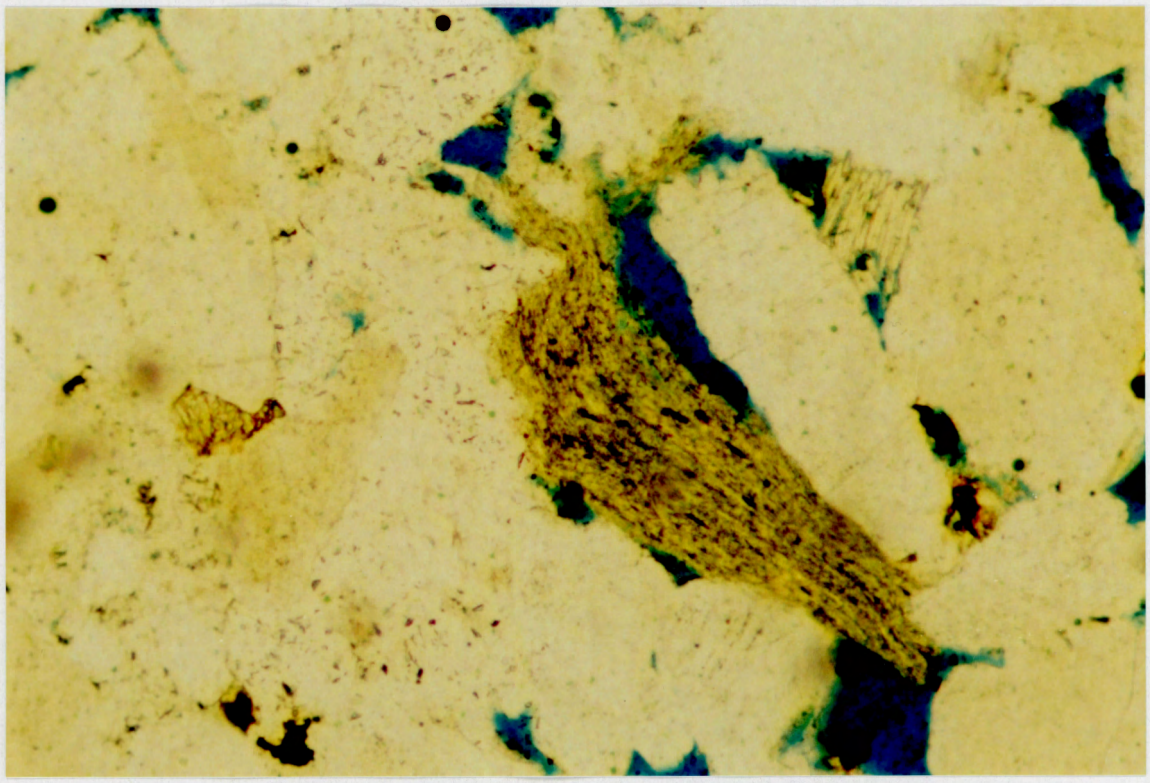

Figure P6-3a Clay mineral partially deformed around small pores space (magnification 32 x actual size.

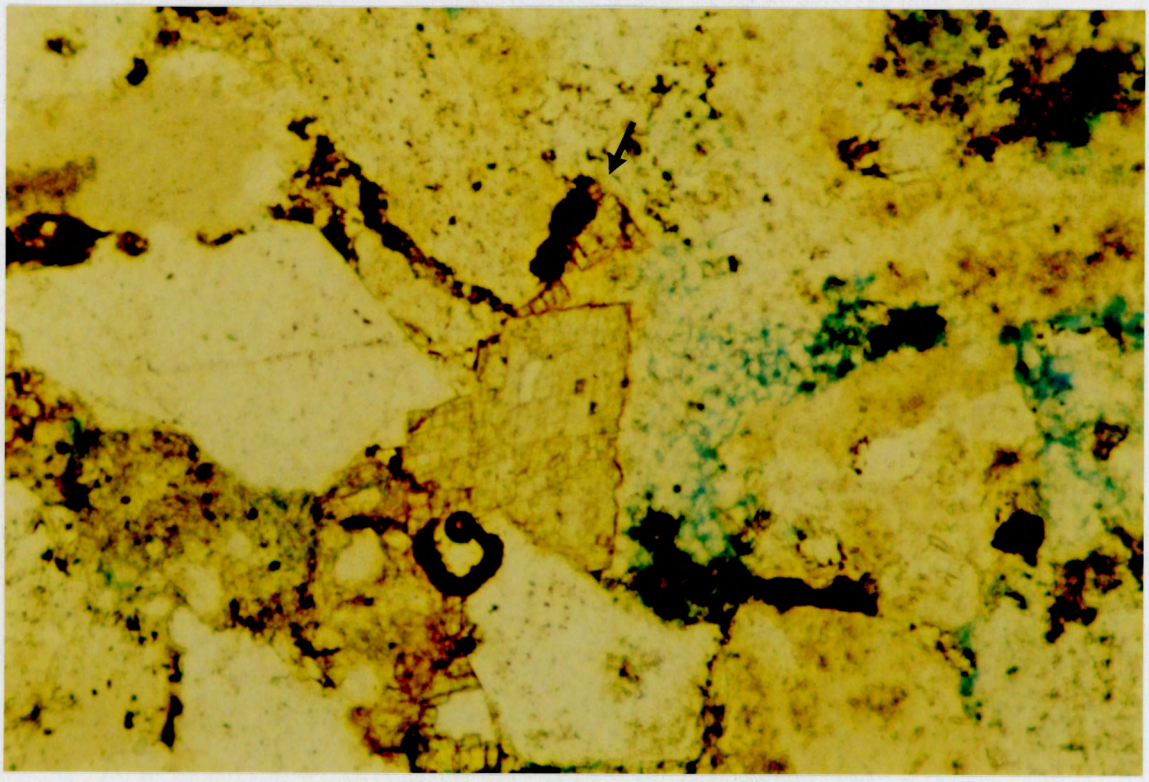

Figure P6-3b Siderite and Fe-carbonage have grown off the face of quartz crystals. The Fe-carbonate has also grown from the siderite crystlas. Kaolinite filled the pore space after carbonate growth, (magnification 64 x actual size).

P6-4

General Mineralogy:

Quartz	65%	
Lithic Grains (including minor biotite and chlorite)		18%
Clay Minerals	10%	
Siderite	5%	
Opaque Minerals	2%	

Description:

Average Grain Size: 0.5 mm
Maturity: Sub-angular to sub-rounded, low sphericity
Sorting: Poorly sorted

Pore Spaces:
abundance - constitute approximately 20% of the slide
size - 7% of the pores are larger than the average grain size.
shape - angular to sub angular. Some pores are rectangular
Pore filling - 25% of the pores are completely filled with kaolinite. The remaining 75% are only partially filled or have no kaolinite at all.

Some of the pores are very large (1.5 mm) and a connection between pores can be seen in thin section (Figure P6-4a).

Many of the quartz grains are fractured. There has been no mineral deposition or alteration on the surface of these fractures.

There is a band of opaque and clay material present approximately 1/3 down from the top of the thin section. Quartz crystals have been incorporated into the clay material (Figure P6-4b).

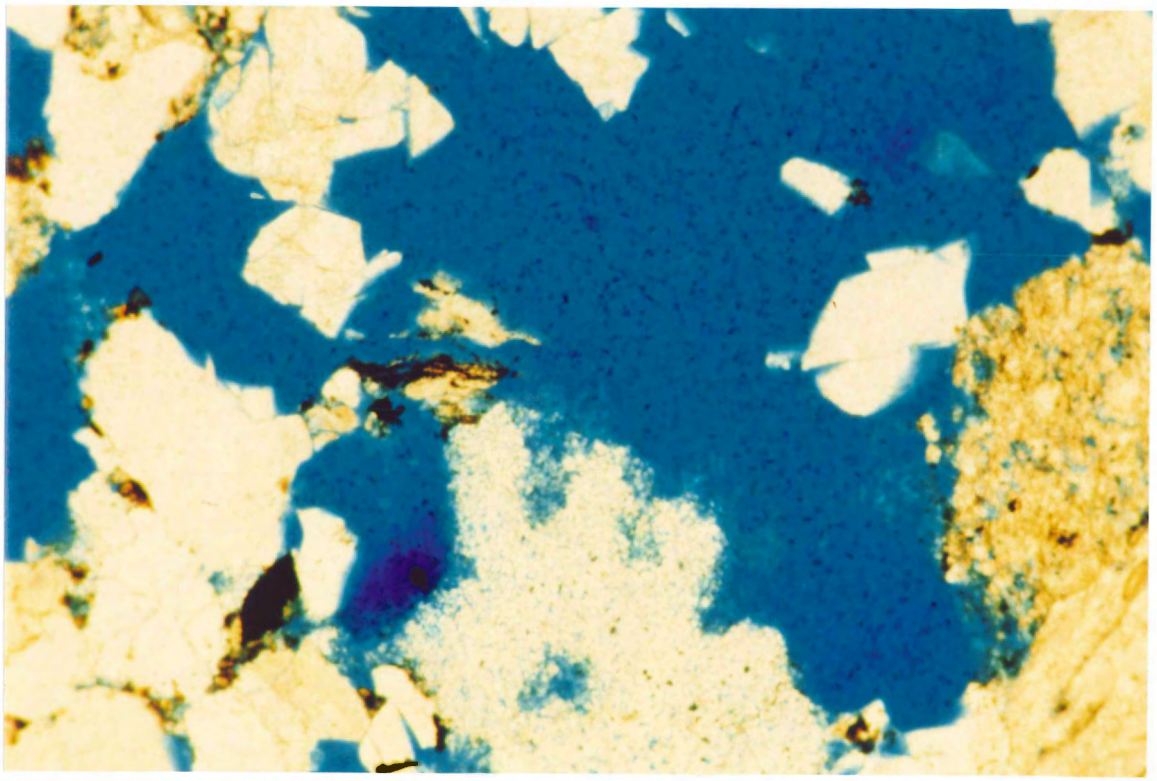

Figure P6-4a Large pore in thin section, pores show good connectiveness, (magnification 32 x actual size).

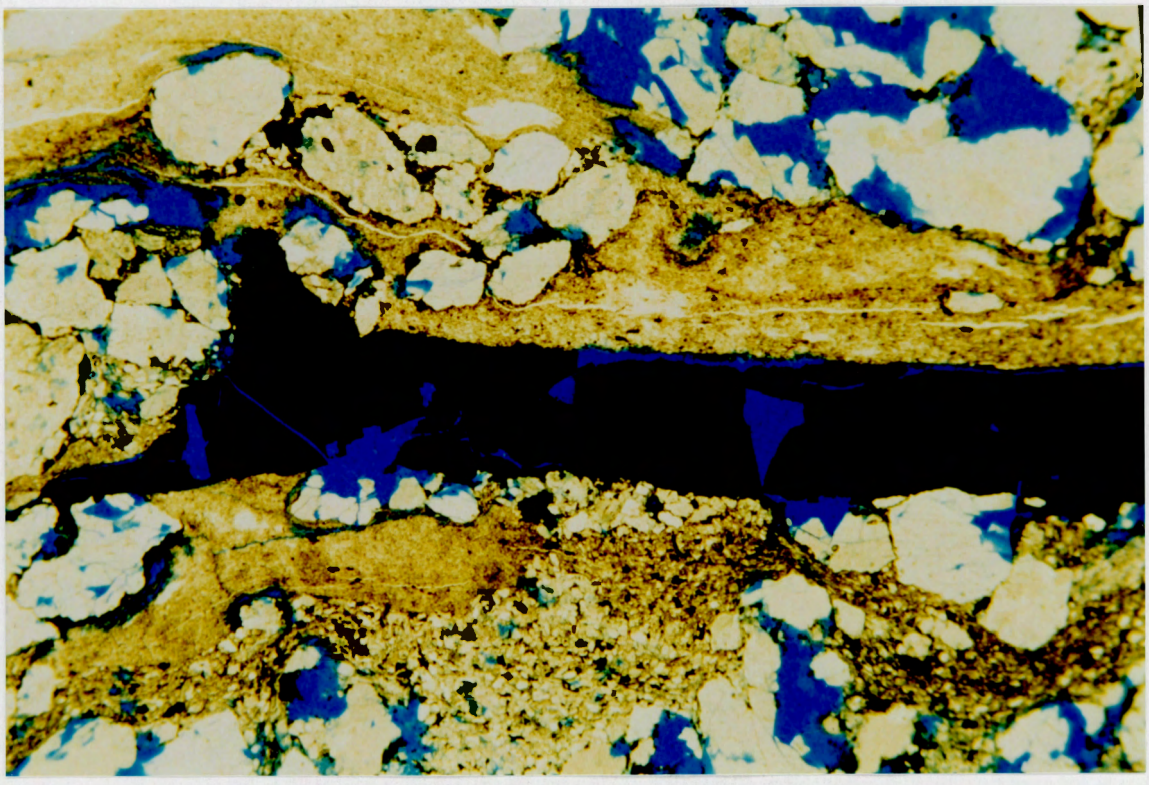

Figure P6-4b Opaque band in thin section P6-4 (magnification 12.6 x actual size).

Siderite crystals are present as cluster of small crystals. The crystals are generally small (< 0.1 mm) and in many cases cannot be differentiated from the brownish rusty alteration. These clusters of crystals surround grains and fill pores spaces and larger euhedral siderite crystals have grown after the smaller crystals (Figure P6-4c).

P6-5

General Mineralogy:

Quartz	65%
Lithic grains (including micaceous grains)	10%
Siderite/Carbonate	15%
Opaque	5%
Clay Minerals	5%

Description:

Average Grain Size: 0.54 mm
Maturity: Sub-rounded, low sphericity
Sorting: Poorly sorted

Pore Spaces:
abundance - Pores constitute approximately 15% of the slide
size - 0.35 mm, the average pore is smaller than the average grain size, but some pores are as large as 1.5 mm in length and as small as 0.1 - 0.2 mm.
shape - generally angular and somewhat spherical
Pore filling -.15% of the smaller pores have been completely filled, larger pores are rarely completely filled.

The slide consists predominately of quartz grains some of which are fractured. There has been no mineral deposition or alteration on the fracture boundaries.

There is a band 1/3 from the top of the slide (right way up) and extends across 2/3 of the thin section (Figure P6-5a). The band consists of an opaque mineral and clay material. There is an abrupt decrease in pore abundance in the proximity of the opaque band.

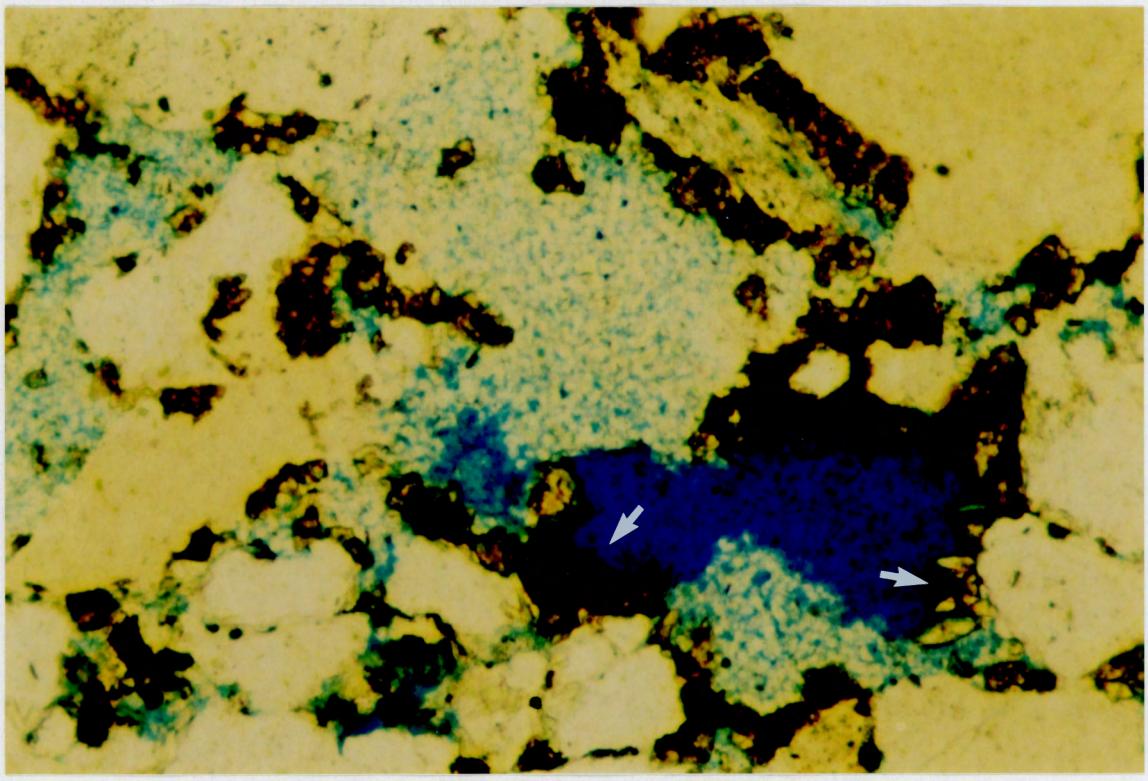

Figure P6-4c Siderite has grown off the crystal face of quartz grains, the pore was then filled with kaolinite, (magnification 64 x actual size).

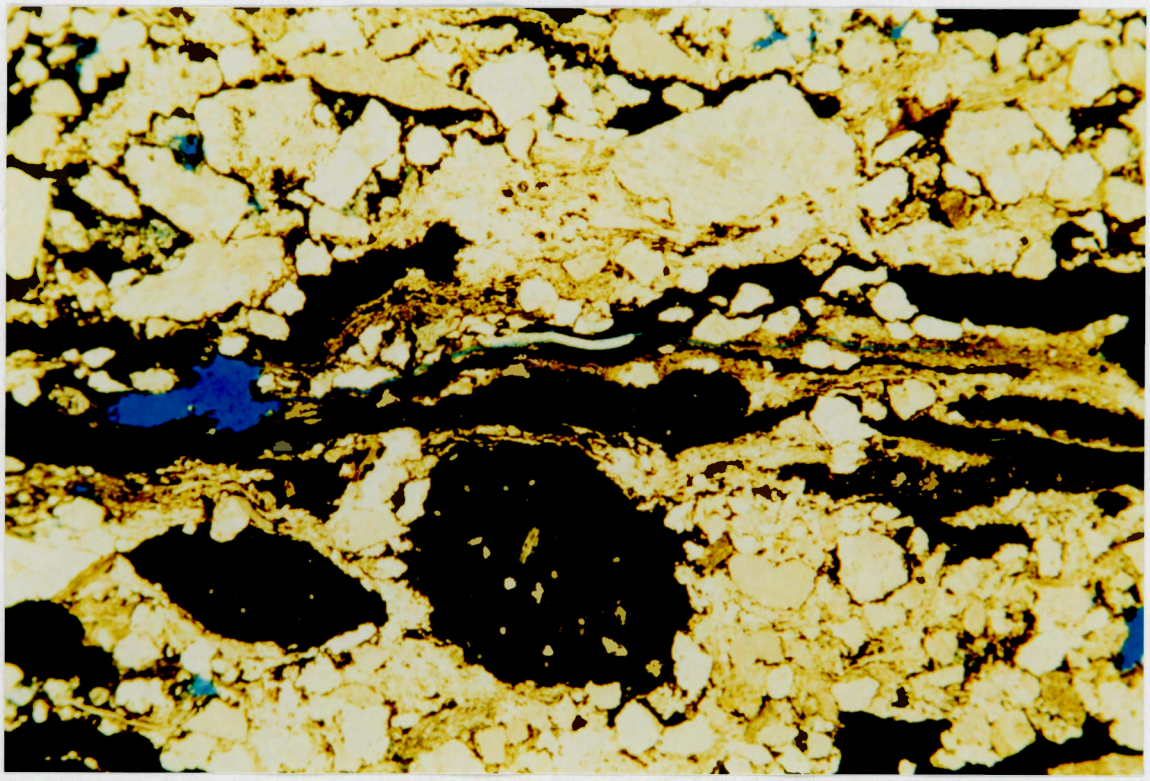

Figure P5-5a Band of opaque mineral(s) and clay material, (magnification 12.6 x actual size).

Siderite crystals have grown on grain boundaries appear to have been partially dissolved. Clusters of smaller (<1mm) siderite crystals have also filled pore spaces. All the siderite grains in thin section have a brownish rusty coating which masks the boundaries of the small crystals. Small siderite crystals increase in abundance with increasing proximity to the opaque band.

Larger carbonate (Fe-calcite) crystals fill pore spaces (<2%) and are present as individual crystals. These also have a brownish rusty coating. Grain size is variable.

P6-6

General Mineralogy

Quartz	70%
Lithic grains (including micaceous grains)	20%
Clay minerals	8%
Carbonate/dolomite	2%

Description:

Average Grain Size: 0.2 mm
Maturity: Grains are sub-rounded, moderate sphericity.
Sorting: Well sorted

Pore Spaces:
abundance - 15% of the slide is pore space
size - majority of pores (90%) are smaller than the average grain size
shape - pores are irregular in shape, not as angular as in previous slides
Pore filling - ~60% of the pores have been filled with kaolinite

The slide is comprised predominately of quartz grains and is very similar in grain size and sorting to P6-1. Over half of the pore spaces have been filled with kaolinite. There has been secondary silica growth on the surface of many of the quartz grains. This growth has occurred in the form of new crystal faces. In many cases clay minerals define the previous grain boundary.

Grains show a horizontal alignment. Siderite crystals occur as small clusters which fill pores (Figure P6-6a). These crystals contain less Mg (minor) than the siderite crystals in P6-2 (Appendix 3). In thin section Fe-carbonate grains have filled pore spaces in one area of the slide.

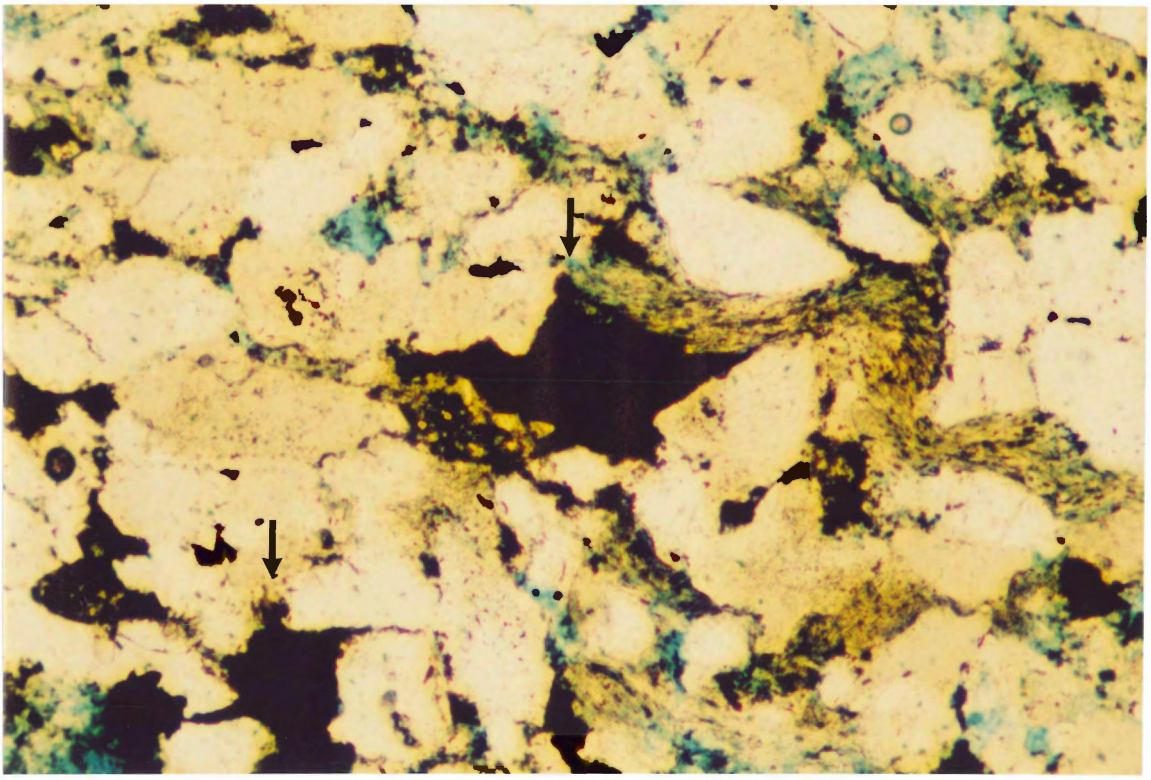

Figure P6-6a Small crystals of siderite have filled pore spaces, (magnification 64 x actual size).

APPENDIX 3
Microprobe Results

Standard	Element	Zaf	%Elmt	St. Dev	Atom. %		% Oxide	Formula
	Mg	0.968	12.871	0.076	24.417	MgO	21.342	0.488
	Ca	0.999	22.233	0.108	25.853		31.109	0.512
	O		17.347		50			1
	Total		52.451		100		52.451	1
P6-2 Analyses								
#1								
	Fe	1.092	32.435	0.244	33.151	FeO	41.727	0.663
	Mn	0.987	1.939	0.086	2.014	MnO	2.503	0.04
	Mg	0.723	5.126	0.065	12.037	MgO	8.5	0.241
	Ca	1.09	1.382	0.04	1.968	CaO	1.934	0.39
	Na	0.594	0.24	0.069	0.597	Na2O	0.324	0.12
	Si	0.883	0.125	0.028	0.254	SiO2	0.268	0.005
	O		14.009		49.978			1
	Total		55.257		100		55.257	1.001
#2								
	Fe	1.091	32.791	0.245	32.704	FeO	42.185	0.654
	Mn	0.986	2.172	0.087	2.202	MnO	2.805	0.044
	Mg	0.723	5.299	0.065	12.141	MgO	6.786	0.243
	Ca	1.089	1.205	0.039	1.675	CaO	1.686	0.033
	Na	0.594	0.291	0.069	0.706	Na2O	0.393	0.014
	Si	0.881	0.152	0.028	0.302	SiO2	0.326	0.006
	Al	0.731	0.115	0.035	0.237	Al2O3	0.217	0.005
	O		14.327		50.034			1
	Total		56.397		100		56.397	0.999
#3 (light area)								
	Fe	1.113	35.252	0.253	39.87	FeO	45.351	0.787
	Mn	1.006	3.281	0.097	3.772	MnO	4.236	0.074
	Mg	0.696	1.118	0.048	2.906	MgO	1.854	0.057
	Ca	1.115	1.202	0.039	1.894	CaO	1.682	0.037
	S	0.985	0.139	0.034	0.274	SO3	0.347	0.005
	Si	0.906	0.106	0.028	0.239	SiO2	0.228	0.005
	P	0.908	0.182	0.048	0.372	P2O5	0.418	0.007
	O		12.835		50.673			1
	Total		54.116		100		54.116	0.973
#4 (darker area)								
	Fe	1.078	38.347	0.267	27.67	FeO	49.333	0.476
	Mn	0.974	2.529	0.094	1.855	MnO	3.266	0.032
	Mg	0.733	2.323	0.053	3.851	MgO	3.852	0.066
	Ca	1.063	0.363	0.036	0.365	CaO	0.507	0.006
	S	0.982	6.468	0.063	8.13	SO3	16.151	0.14
	O		23.079		58.13			1
	Total		73.109		100		73.109	0.72

	Element	Zaf	%Elmt	St. Dev	Atom. %		% Oxide	Formula
#5 (dark area)								
	Fe	1.101	32.543	0.245	33.916	FeO	41.866	0.679
	Mn	0.995	4.228	0.104	4.48	MnO	5.46	0.09
	mg	0.715	3.916	0.06	9.375	MgO	6.493	0.188
	Ca	1.101	1.013	0.037	1.472	CaO	1.418	0.029
	Na	0.584	0.262	0.068	0.663	Na2O	0.353	0.013
	Si	0.891	0.084	0.028	0.173	SiO2	0.179	0.003
	O		13.722		49.921			1
	Total		55.768		100		55.768	1.003
#6								
	Fe	1.085	28.439	0.233	27.319	FeO	36.586	0.537
	Mn	0.981	5.341	0.112	5.216	MnO	6.896	0.102
	Mg	0.739	5.954	0.067	13.14	MgO	9.873	0.258
	Ca	1.082	0.65	0.035	0.87	CaO	0.909	0.017
	K	1.127	0.103	0.029	0.142	K2O	0.125	0.003
	Si	0.881	0.73	0.031	1.395	SiO2	1.563	0.027
	Al	0.736	0.505	0.039	1.005	SiO2	0.955	0.02
	O		15.184		50.913	Al2O3		1
	Total		56.906		100		56.906	0.964
P6-6 Analyses #1								
	Fe	1.123	40.627	0.267	44.86	FeO	52.265	0.892
	Mn	1.014	2.088	0.085	2.344	MnO	2.696	0.047
	Mg	0.685	0.329	0.042	0.834	MgO	0.545	0.017
	Ca	1.123	0.358	0.034	0.552	CaO	0.502	0.011
	Na	0.553	0.226	0.035	0.605	Na2O	0.304	0.012
	S	0.989	0.16	0.028	0.309	SO3	0.401	0.006
	Si	0.906	0.103		0.227	SiO2	0.221	0.005
	O		13.043		50.271			1
	Total		56.933		100		56.933	0.989
#2								
	Fe	1.117	36.994	0.258	40.248	FeO	47.592	0.795
	Mn	1.009	4.048	0.104	4.477	MnO	5.227	0.088
	Mg	0.694	0.652	0.044	1.63	MgO	1.081	0.032
	ca	1.118	0.925	0.037	1.402	CaO	1.294	0.028
	Na	0.562	0.218	0.062	0.577	Na2O	0.294	0.011
	S	0.988	0.17	0.035	0.322	SO3	0.424	0.006
	Sl	0.909	0.088	0.028	0.191	SiO2	0.188	0.004
	P	0.911	0.257	0.048	0.504	P2O5	0.588	0.01
			13.337		50.651			1
	Total		56.689		100			0.974

	Element	Zaf	%Elmt	St. Dev	Atom. %		% Oxide	Formula
#3(lighter area)								
	Fe	1.121	38.938	0.262	43.297	FeO	50.093	0.857
	Mn	1.013	3.422	0.099	3.868	MnO	4.419	0.077
	Mg	0.689	0.284	0.042	0.725	MgO	0.47	0.014
	Ca	1.122	0.56	0.035	0.868	CaO	0.784	0.017
	S	0.989	0.189	0.035	0.365	SO3	0.471	0.007
	Si	0.908	0.154	0.028	0.341	SiO2	0.33	0.007
	O		13.02		50.536			1
	Total		56.657		100		56.567	0.979
#4								
	Fe	1.116	38.725	0.264	40.023	FeO	49.82	0.788
	Mn	1.008	3.798	0.102	3.99	MnO	4.904	0.079
	Mg	0.695	0.78	0.045	1.852	MgO	1.293	0.036
	Ca		0.568	0.035	0.818	caO	0.764	0.016
	Na			0.064	0.734	Na2O	0.394	0.014
	S		0.233	0.036	0.419	SO3	0.581	0.008
	Si	0.907	0.181	0.029	0.327	SiO2	0.388	0.007
	Ti	1.101	0.194	0.053	0.234	TiO2	0.324	0.005
	Al	0.755	0.115	0.033	0.247	Al2O3	0.218	0.005
	P	0.909	0.187	0.049	0.349	P2O5	0.429	0.007
	Cl	1.141	0.123	0.028	0.2	Cl	0.123	0.004
	O		14.071		50.762			1
			59.268		100		59.268	0.97